TABLE OF CONTENTS

MATERIALS AND METHODS

DNA-origami Design and Assembly

The DNA structures were designed in caDNAno[1] (**Figure S1–S3, S24, S27, S31, S37, S42, S48**). Staple strands without chemical modifications were purchased from Integrated DNA Technologies, Inc. within 96-well plates and with concentrations normalized to 100 μM. Staple strands with fluorescent modifications were purchased in dry powder form from Integrated DNA Technologies, Inc. with HPLC purification. Scaffold strands p7308 and p8064 are variants of M13mp18 single-stranded DNA and produced using phages and *E.coli* strains as described before[2–4]. p3024, the pBlueScript-derived scaffold was prepared with JM109 cells and VCSM13 helper phages (Agilent Technologies) using a single-stranded phagemid rescue protocol recommended by the manufacturer.

The force clamps (**Figure 1a–c** and **S1–S3**) were assembled from p7308 scaffold strand (40 nM), a pool of core staple strands (200 nM each) and a pool of spring subset staple strands (tunes force clamp to specific tension[5], 400 nM each) in 1× TE buffer (5 mM Tris•HCl, 1 mM EDTA, pH 8.0) containing 20 mM $MgCl_2$, using a nonlinear thermal annealing ramp as described[5]. Force clamps with self-cleaving deoxyribozymes (**Figure 1d**) were assembled from a modified p7308 scaffold with two deoxyribozyme inserts (**Table S3**) under the same conditions as the other force clamp structures.

The semicircles with excess scaffold loops (**Figure 2a** and **S24**) were assembled from p3024 scaffold strand (50 nM), a pool of core staple strands (300 nM each) and a pool of handle staple strands (600 nM each; highlighted in red in caDNAno blueprint) in 1× TE buffer containing 12 mM $MgCl_2$, using a 36-hour annealing program (80−65 °C, -1 °C/5 min; 64−24 °C, -1 °C/50 min; 15 °C hold).

The circle structures with outer handle extensions for Cy5 anti-handle probes (**Figure 2b** and **S27**) were assembled from p8064 scaffold strand (50 nM) and a pool of staple strands (300 nM each) in 1× TE buffer containing 10 mM $MgCl_2$, using a 36-hour annealing program (80−65 °C, -1 °C/5 min; 64−24 °C, -1 °C/50 min; 15 °C hold).

The structures featuring a rod and three circles (three-circles-on-a-rod, **Figure 2c** and **S31**) were assembled from p7308 scaffold strand (40 nM) and a pool of staple strands (240 nM each) in 1× TE buffer containing 12 mM $MgCl_2$, using a 36-hour annealing program (80−65 °C, -1 °C/5 min; 64−24 °C, -1 °C/50 min; 15 °C hold).

The rotaxane structures (**Figure 3** and **S37**) were assembled from p8064 scaffold strand (40 nM) and a pool of staple strands (240 nM each) in 1× TE buffer containing 12 mM $MgCl_2$, using a 36-hour annealing program (80−65 °C, -1 °C/5 min; 64−24 °C, -1 °C/50 min; 15 °C hold).

The elastic beam structures (**Figure 4** and **S42**) were assembled from p8064 scaffold strand (40 nM) and a pool of staple strands (320 nM each) in 1× TE buffer containing 8 mM $MgCl_2$, using a 36-hour annealing program (80−65 °C, -1 °C/5 min; 64−24 °C, -1 °C/50 min; 15 °C hold).

The rod-through-square structure[6] used for Cas12a cleavage in Octyl β-D-glucopyranoside (OG, **Figure S54**) were assembled from p7308 scaffold strand (50 nM) and a pool of staple strands (400 nM each) in 1× TE buffer containing 12.5 mM $MgCl_2$, using a 36-hour annealing program (80−65 °C, -1 °C/5 min; 64−24 °C, -1 °C/50 min; 15 °C hold).

The folded structures were purified by rate-zonal centrifugation.[7] Typically, 1 mL of assembly product were concentrated to 200 μl using Amicon Ultra-0.5 mL Centrifugal Filters (EMD Millipore) with 30-kD nominal molecular weight limit (NMWL), loaded on top of a 15−45% (v/v) quasi-linear glycerol gradient in a polycarbonate centrifuge tube (13×51 mm, Beckman Coulter Inc.), and spun at 50 krpm on a Beckman SW-55-Ti rotor for 120 min (semicircle and rod-through-square structures) or 60 min (the rest of structures). The contents of the tube were fractionated from top to bottom (200 μL per fraction). Generally, 5 μL of

each fraction was loaded onto a 1.5% agarose gel containing 0.5 μg/mL ethidium bromide (EtBr) and run in 0.5× TBE (45 mM Tris-Base, 45 mM boric acid, and 1 mM EDTA), 10 mM $MgCl_2$ for 2 hours at 5 V/cm. After image analysis on a Typhoon FLA 9500 imager (GE Healthcare), the fractions containing well-formed monomeric DNA origami were combined and concentrated using Amicon Ultra-0.5 mL Centrifugal Filters with 30-kD NMWL. Origami concentrations were determined using a NanoDrop 2000 (ThermoFisher). The concentrated monomers were stored in 1× TE buffer, 10 mM $MgCl_2$ at -20 °C.

For labeling and protecting ssDNA segments of DNA-origami structures, a pre-hybridization step was added before Cas12a cleavage assays. Cy5-labeled ssDNA probes (probe:scaffold = 10:1) were allowed to hybridize to force clamp structures at 37 °C for 1 hour. Cy5 anti-handles (anti-handle:circle = 67:1) were allowed to hybridize to the eight identical handles on the circle structure at room temperature overnight. Protecting oligonucleotides (oligo:scaffold = 8:1) for single-stranded scaffold segments were allowed to bind to the tethers between the rod and circle at room temperature overnight.

Calculation of ssDNA Tendon Force

Guided by the examples of prior prestressed DNA origami tensegrity structures[5,8], we used the following Python (v 2.7.10) script to estimate the tension on stretched ssDNA segments in our force clamp, three-circles-on-a-rod, rotaxane, and rod-through-square structures by changing variable "N" to the number of stretched scaffold ssDNA bases used in our designs and "Length_in_m" to the length of the stretched scaffold ssDNA in our structures.

```
from __future__ import division
import math

Lk = 1.5E-9 # Kuhn length (m)
l = 0.63E-9 # contour length (m/base)
K = 800E-9 # stretching modulus (N)
kb = 1.38E-23 #Boltzmann constant (J/K)
T = 297 # Temperature (K)
N = 276 # ssDNA length (base); change to value used in each design
Lc = l*N

Length_in_m = 43E-9 # length of tensioned ssDNA (meters); change to value used in
each design

# Freely-Jointed Chain Model predicts end-to-end distance of a ssDNA as a function of
its tension force
def x(f):
    return Lc*(1/math.tanh(f*Lk/(kb*T))-kb*T/(f*Lk))*(1+f/K)

#Calculate end-to-end distance of a ssDNA with tension force from 0.1 pN to 19.9 pN,
in 0.1 pN increment.
#Save the result to a list called all_length
#Find the force that gives value closest to Length_in_m (ssDNA length in m)
all_length = []
for n in range (1,200):
    all_length.append(x(n*1E-13))

#print all_length

force = min(range(len(all_length)), key=lambda i: abs(all_length[i-1]-
(Length_in_m)))*1E-13
print (force)
```

Elastic Beam Bending Angle Prediction

The energies stored in the 6-helix bundle elastic beams at different bending angles and that in tensioned ssDNA scaffold tethers were calculated. The theoretical equilibrium bending angles[9] for the elastic beams before enzymatic cleavage of ssDNA springs were then determined by minimizing the total energy.

Calculations for 6-helix Bundle Arc without ssDNA Tethers

The energy stored in the 6-helix bundle elastic beam (arc) was calculated according to the toy model[10]. Briefly, it was calculated by a sum of bend, and stretch/compression contributions stored in each base pair in the arc, using the following functions:

$$E_{6\text{-}helix\ bundle\ arc} = \sum_{i=0}^{5}\left[\frac{1}{2}\cdot S\cdot n_i\cdot\frac{(d_i-d_{eq})^2}{d_{eq}}+\frac{1}{2}\cdot B\cdot n_i\cdot\frac{d_{eq}}{(r_0+\delta_i)^2}+\frac{1}{2}\cdot D\cdot\Phi_i\cdot\left(\frac{d_i}{d_{eq}}-1\right)\right]$$

$$d_i = \frac{n_0}{n_i}\cdot d_0\cdot\left(\frac{\delta_i}{r_0}+1\right)$$

$$\Phi_i = 2\cdot\pi\cdot\frac{N-n_i}{10.5}$$

where S, B, and D denote the stretch, bending, and twist-stretch-coupling moduli of DNA, with a set of values (S = 660 pN, B = 230 pN·nm^2, D = 0 pN·nm) calculated *via* Young's modulus.

The following Python (v 3.7.3 with SciPy[11]) script calculates the energy stored in the arc (without ssDNA tethers) as a function of a range of bending angles, resulting in the equilibrium bending angle at 121°.

```
from numpy import pi, sqrt

# All constants are listed below

D = 2.25E-9 # Diameter of dsDNA (m)
Lds = 0.335E-9 # length of dsDNA (m/base)
kb = 1.38E-23 #Boltzmann constant (J/K)
T = 297 # Temperature(K)
S = 660E-12 # Stretch moduli of DNA helix (N)
B = 230E-30 # Bending moduli of DNA helix (N*m2)


# All adjustable parameters are listed below

Nds = 6 # number of helices in the arc
Nbp = 168 # number of bp in the arc without insertion or deletion
L_arc = Nbp*Lds # length of the arc
bp1 = 14 # bp(n) is the number of bp inserted or deleted from each outer or inner
layer of helices
delta_coefficient = 1.125E-9 # each DNA helix is modeled as a 2.25 nm wide rod

n = [0 for i in range(Nds)] # n is the number of bp installed in helices
n[0] = Nbp + bp1
n[1] = Nbp + bp1
n[2] = Nbp - bp1
n[3] = Nbp - bp1
n[4] = Nbp
```

```
n[5] = Nbp

delta = [0 for i in range(Nds)] # distance of a helix from the bending axis (nm)
delta[0]  = sqrt(3.0)
delta[1]  = sqrt(3.0)
delta[2]  = -sqrt(3.0)
delta[3]  = -sqrt(3.0)
delta[4]  = 0
delta[5]  = 0

for i in range(Nds):
        delta[i] *= delta_coefficient


# Calculate the energy stored in the arc to find the bending angle with the energy
minimum

helix_total_energy = []
for angle_in_degrees in range(1,180):
        angle_in_radians = angle_in_degrees/180.0*pi
        rref = L_arc/angle_in_radians
        helix_stretch_energy = 0
        helix_bending_energy = 0
        for i in range(Nds):
                d = (float(Nbp)/n[i])*float(Lds)*(delta[i]/rref + 1)
                helix_stretch_energy += 0.5*S*n[i]*((d-Lds)**2)/Lds
                helix_bending_energy += 0.5*B*n[i]*Lds/((rref + delta[i])**2)
        helix_total_energy.append(helix_stretch_energy + helix_bending_energy)
bending_angle = (helix_total_energy.index(min(helix_total_energy))+1)
print("The bending angle of the arc is", bending_angle)
```

Calculations for 6-helix Bundle Arc with ssDNA Tethers

Before enzymatic cleavage of the ssDNA tethers, the total energy stored in the prestressed elastic beam structure with 4 stretched, ssDNA tethers was calculated as the sum of energy stored in the central, curved 168-bp 6-helix bundle elastic beam (arc) and the four ssDNA tethers, three of which are 157-nt long and one of which is 471-nt long.

The internal tension force of the ssDNA scaffold tethers was estimated based on the worm-like-chain (WLC) model[12] as

$$\frac{F \cdot L_{pss}}{k_b \cdot T} = \frac{1}{4 \cdot \left(1 - \frac{x}{L_C} + \frac{F}{K}\right)^2} - \frac{1}{4} + \frac{x}{L_C} - \frac{F}{K}$$

where F is the internal tension, L_{pss} is the persistence length of ssDNA, k_b is the Boltzmann constant, T is the temperature (298 K), x is the extension of the ssDNA tethers, L_C is the contour length of the ssDNA tethers, and K is the elastic modulus.

The energy stored in the ssDNA scaffold tethers was calculated by

$$E_{ssDNA}(\Delta x) = \sum_i \int_0^{\Delta x} F(x)\, dx$$

where the index i iterates over all the ssDNA tethers.

We calculated the total energy as a function of the bending angle (θ) of the arc. Using the geometrical relationship shown in **Box S1**, the end-to-end distance (d) of the ssDNA tethers can be calculated as

$$d = 2 \cdot \left(R - \sqrt{3} \cdot r\right) \cdot \sin\frac{\theta}{2}$$

$$R = \frac{L_{arc}}{\theta}$$

where R denotes the radius of the 6-helix-bundle arc, r denotes the radius of dsDNA helix, θ denotes the bending angle of the 6-helix-bundle arc, and L_{arc} denotes the length of the 6-helix bundle arc.

Box S1. Calculation of end-to-end distance of the ssDNA tethers against the bending angle of the 6-helix bundle arc. The ends of the ssDNA tethers are labeled as red dots. The ssDNA tethers are not shown.

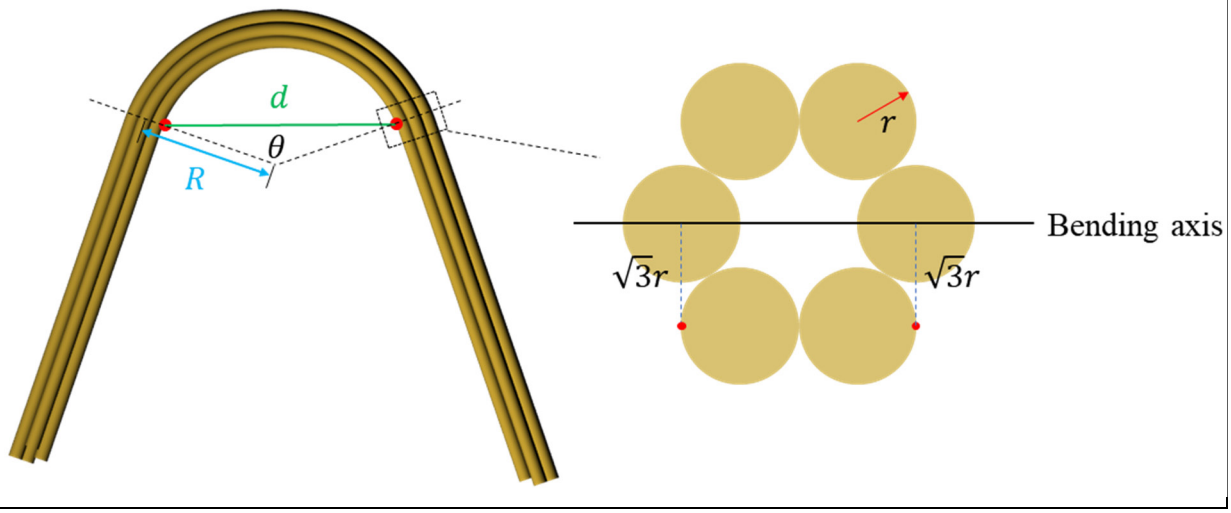

The total energy of the elastic beam with ssDNA tethers can be calculated as

$$E_{total} = E_{arc} + E_{ssDNA\ tether}$$

This calculation was processed using the following Python (v 3.7.3 with SciPy) script.

```
from numpy import sin, pi, sqrt
from scipy.integrate import quad


# All constants are listed below

D = 2.25E-9 # Diameter of dsDNA (m)
Lss = 0.63E-9 # Contour length of ssDNA (m/base)
Lds = 0.335E-9 # length of dsDNA (m/base)
kb = 1.38E-23 #Boltzmann constant (J/K)
T = 297 # Temperature(K)
Lpss = 0.75E-9 # persistence length of ssDNA (m)
S = 660E-12 # Stretch moduli of DNA helix (N)
B = 230E-30 # Bending moduli of DNA helix (N*m2)
K = 50E-12 # Elastic modulus of ssDNA (N)
```

```
# All adjustable parameters are listed below

N1 = 157 # number of nucleotides in ssDNA tether type 1
N1ss = 3 # number of ssDNA tether type 1
N2 = 471 # number of nucleotides in ssDNA tether type 2
N2ss = 1 # number of ssDNA tether type 2
Nds = 6 # number of helices in the arc
Nbp = 168 # number of bp in the arc without insertion or deletion
L_arc = Nbp*Lds # length of the arc
L_tether_max = N1*Lss # maximum length of ssDNA tethers
theta_step = 1 # increasing step of bending angle of the arc (in degree)
bp1 = 14 # bp(n) is the number of bp inserted or deleted from each outer or inner
layer of helices
delta_coefficient = 1.125E-9 # each DNA helix is modeled as a 2.25 nm wide rod

n = [0 for i in range(Nds)] # n is the number of bp installed in helices
n[0] = Nbp + bp1
n[1] = Nbp + bp1
n[2] = Nbp - bp1
n[3] = Nbp - bp1
n[4] = Nbp
n[5] = Nbp

delta = [0 for i in range(Nds)] # distance of a helix from the bending axis (nm)
delta[0]  = sqrt(3.0)
delta[1]  = sqrt(3.0)
delta[2]  = -sqrt(3.0)
delta[3]  = -sqrt(3.0)
delta[4]  = 0
delta[5]  = 0

for i in range(Nds):
        delta[i] *= delta_coefficient


# Worm-Like Chain Model predicts the force and energy stored in a ssDNA tether as a
function of its end-to-end distance “x” and number of bases “N”

def delta_F(f,x,N):
    return(f*Lpss/(kb*T)+f/K+0.25-x/(N*Lss)-(1/(4*((1-x/(N*Lss)+f/K)**2))))

def F(x,N):
    all_delta_F = []
    for n in range (1,10000):
        all_delta_F.append(delta_F(n*1E-15,x,N))
    force = (min(range(len(all_delta_F)), key=lambda i: abs(all_delta_F[i]))+1)*1E-15
    return(force)


# Stretching energy stored in ssDNA tethers

def Energy_tether(x,N):
    return(quad(F,0,x,args=(N))[0])
```

```
# Calculate the end-to-end distance of ssDNA tethers as a function of bending angle
theta of the arc

def L_tether(theta):
    return(2*(L_arc/theta-sqrt(3.0)/2*D)*sin(theta/2))


# Calculate the bending angle of the arc without ssDNA tethers

helix_total_energy = []
for angle_in_degrees in range(1,180):
        angle_in_radians = angle_in_degrees/180.0*pi
        rref = L_arc/angle_in_radians
        helix_stretch_energy = 0
        helix_bending_energy = 0
        for i in range(Nds):
                d = (float(Nbp)/n[i])*float(Lds)*(delta[i]/rref + 1)
                helix_stretch_energy += 0.5*S*n[i]*((d-Lds)**2)/Lds
                helix_bending_energy += 0.5*B*n[i]*Lds/((rref + delta[i])**2)
        helix_total_energy.append(helix_stretch_energy + helix_bending_energy)
bending_angle = (helix_total_energy.index(min(helix_total_energy))+1)
print("The bending angle of the arc without ssDNA tethers is",bending_angle)


# Calculate the total energy stored in the arc and ssDNA tethers to find the bending
angle with the energy minimum

theta_all = []
L_tether_all = []
force1_all = []
force2_all = []
total_energy_all = []
theta = bending_angle # Starting from the bending angle of the arc without ssDNA
tethers
while(theta < 180):
    if(L_tether(theta/180*pi) > N1*Lss):
        theta += theta_step
    else:
        rref = L_arc/(theta/180*pi)
        beam_stretch_energy = 0
        beam_bending_energy = 0
        for i in range(Nds):
            d = (float(Nbp)/n[i])*float(Lds)*(delta[i]/rref + 1)
            beam_stretch_energy += 0.5*S*n[i]*((d-Lds)**2)/Lds
            beam_bending_energy += 0.5*B*n[i]*Lds/((rref + delta[i])**2)
        total_energy = beam_stretch_energy + beam_bending_energy +
N1ss*Energy_tether(L_tether((theta/180*pi)),N1) +
N2ss*Energy_tether(L_tether((theta/180*pi)),N2)
        theta_all.append(theta)
        L_tether_all.append(L_tether(theta/180*pi))
        force1_all.append(F(L_tether(theta/180*pi),N1))
        force2_all.append(F(L_tether(theta/180*pi),N2))
        total_energy_all.append(total_energy)
        theta += theta_step
```

```
index = total_energy_all.index(min(total_energy_all))
print("The minimum energy point has the bending angle of", theta_all[index], "degree,
the ssDNA tether length of",\
      L_tether_all[index]*1.0E9, "nm, with", N1, "nt in the ssDNA tethers, the force
in the ssDNA tethers of",\
      force1_all[index]*1.0E12, "pN; with", N2, "nt in the ssDNA tether, the force in
the ssDNA tether of",\
      force2_all[index]*1.0E12, "pN, the total energy of", total_energy_all[index],
"J.")
```

Calculations for 6-helix Bundle Arc with 6-helix Bundle Bar

The total energy stored in an elastic beam with arms held by a pre-folded, 6-helix-bundle, 84-bp-long bar is calculated as the sum of three terms: (1) the energy stored in the curved 168-bp 6-helix bundle arc, (2) that stored in the eight, 5-nt-long ssDNA springs at both ends of the tethering 6-helix bundle bar, and (3) stretching energy stored in the bar. This calculation was processed using the following Python (v 3.7.3 with SciPy) script.

```
from numpy import sin, pi, sqrt
from scipy.integrate import quad


# All constants are listed below

D = 2.25E-9 # Diameter of dsDNA (m)
Lss = 0.63E-9 # Contour length of ssDNA (m/base)
Lds = 0.335E-9 # length of dsDNA (m/base)
kb = 1.38E-23 #Boltzmann constant (J/K)
T = 297 # Temperature(K)
Lpss = 0.75E-9 # persistence length of ssDNA (m)
S = 660E-12 # Stretch moduli of DNA helix (N)
B = 230E-30 # Bending moduli of DNA helix (N*m2)
K = 50E-12 # Elastic modulus of ssDNA (N)


# All adjustable parameters are listed below

N = 5 # number of nucleotides in the ssDNA springs
Nss = 8 # number of the ssDNA springs
Nds = 6 # number of helices in the arc
Nbp = 168 # number of bp in the arc without insertion or deletion
Nbp_bar = 84 # number of bp of 6-helix bundle bar in the tether
L_arc = Nbp*Lds # length of the arc
L_bar = Nbp_bar*Lds # length of 6-helix bundle bar in the tether under the
unstretched condition
L_spring_max = N*Lss # maximum length of the ssDNA springs
theta_step = 1 # increasing step of bending angle of the arc (in degree)
bp1 = 14 # bp(n) is the number of bp inserted or deleted from each outer or inner
layer of helices
delta_coefficient = 1.125E-9 # each DNA helix is modeled as a 2.25 nm wide rod

n = [0 for i in range(Nds)] # n is the number of bp installed in helices
n[0] = Nbp + bp1
n[1] = Nbp + bp1
```

```
n[2] = Nbp - bp1
n[3] = Nbp - bp1
n[4] = Nbp
n[5] = Nbp

delta = [0 for i in range(Nds)] # distance of a helix from the bending axis (nm)
delta[0]  = sqrt(3.0)
delta[1]  = sqrt(3.0)
delta[2]  = -sqrt(3.0)
delta[3]  = -sqrt(3.0)
delta[4]  = 0
delta[5]  = 0

for i in range(Nds):
        delta[i] *= delta_coefficient


# Worm-Like Chain Model predicts the force and energy stored in a ssDNA tether as a
function of its end-to-end distance “x”

def delta_F(f,x):
    return(f*Lpss/(kb*T)+f/K+0.25-x/(N*Lss)-(1/(4*((1-x/(N*Lss)+f/K)**2))))

def F(x):
    all_delta_F = []
    for n in range (1,200):
        all_delta_F.append(delta_F(n*1E-13,x))
    force = (min(range(len(all_delta_F)), key=lambda i: abs(all_delta_F[i]))+1)*1E-13
    # print(all_delta_F)
    return(force)


# Stretching energy stored in ssDNA springs

def Energy_spring(x):
    return(quad(F,0,x)[0])


# Calculate the end-to-end distance of the tether as a function of bending angle
theta of the arc

def L_tether(theta):
    return(2*(L_arc/theta-sqrt(3.0)/2*D)*sin(theta/2))


# Calculate the stretching energy stored in the 6-helix bundle bar

def Energy_bar(d_bp):   # d_bp is the average distance of a stretched base pair in
the bar (m/base)
    return(0.5*S*Nbp_bar*6*(d_bp-Lds)**2/Lds)


# Find the minimum energy stored in the tether (the bar and ssDNA springs) against a
given end-to-end tether distance. Return the minimum energy and the force in ssDNA
springs
```

```
def Min_energy_tether(L):   # L is the end-to-end distance of the tether
    d_bp = Lds   # define the starting average distance of a stretched base pair in
the bar
    delta_d_bp = Lds/100.0   # define the increasing step distance of the stretched
base pair in the bar
    force_spring_all = []
    total_energy_tether_all = []
    while(d_bp*Nbp_bar < L):
        if(L-d_bp*Nbp_bar >= 2*L_spring_max):
            d_bp += delta_d_bp
        else:
            total_energy_tether = Energy_bar(d_bp) + Nss*Energy_spring((L-
d_bp*Nbp_bar)/2.0)
            force_spring_all.append(F((L-d_bp*Nbp_bar)/2.0))
            total_energy_tether_all.append(total_energy_tether)
            d_bp += delta_d_bp
    index = total_energy_tether_all.index(min(total_energy_tether_all))
    return((total_energy_tether_all[index],force_spring_all[index]))


# Calculate the bending angle of the arc without ssDNA tethers

helix_total_energy = []
for angle_in_degrees in range(1,180):
        angle_in_radians = angle_in_degrees/180.0*pi
        rref = L_arc/angle_in_radians
        helix_stretch_energy = 0
        helix_bending_energy = 0
        for i in range(Nds):
                d = (float(Nbp)/n[i])*float(Lds)*(delta[i]/rref + 1)
                helix_stretch_energy += 0.5*S*n[i]*((d-Lds)**2)/Lds
                helix_bending_energy += 0.5*B*n[i]*Lds/((rref + delta[i])**2)
        helix_total_energy.append(helix_stretch_energy + helix_bending_energy)
bending_angle = (helix_total_energy.index(min(helix_total_energy))+1)
print("The bending angle of the arc without the tether is",bending_angle)


# Calculate the total energy stored in the arc, the bar, and ssDNA springs as a
function of different bending angles of the arc to find the bending angle with the
energy minimum

theta_all = []
L_tether_all = []
force_all = []
total_energy_all = []
theta = bending_angle # Starting from the bending angle of the arc without the tether
while(L_tether(theta/180*pi) > L_bar):
    rref = L_arc/(theta/180*pi)
    beam_stretch_energy = 0
    beam_bending_energy = 0
    for i in range(Nds):
        d = (float(Nbp)/n[i])*float(Lds)*(delta[i]/rref + 1)
        beam_stretch_energy += 0.5*S*n[i]*((d-Lds)**2)/Lds
        beam_bending_energy += 0.5*B*n[i]*Lds/((rref + delta[i])**2)
```

```
    total_energy = beam_stretch_energy + beam_bending_energy +
Min_energy_tether(L_tether(theta/180*pi))[0]
    theta_all.append(theta)
    L_tether_all.append(L_tether(theta/180*pi))
    force_all.append(Min_energy_tether(L_tether(theta/180*pi))[1])
    total_energy_all.append(total_energy)
    theta += theta_step
index = total_energy_all.index(min(total_energy_all))
print("The minimum energy point has the bending angle of", theta_all[index], "degree,
the tether length of", \
      L_tether_all[index]*1.0E9, "nm, with", N, "nt in the ssDNA springs, the force
in ssDNA springs of", \
      force_all[index]*1.0E12, "pN, and the total energy of",
total_energy_all[index], "J.")
```

According to Boltzmann distribution, probability density P(z) of each bending angle can be calculated as

$$P(z) = \frac{e^{-\frac{E(z)}{k_b \cdot T}}}{\sum_j e^{-\frac{E(j)}{k_b \cdot T}}}$$

where *j* iterates over all bending angles.

The bending angle distribution of the three different versions of elastic beams is shown in **Box S2**.

Box S2. Predicted bending angle distribution of the three different versions of the elastic beams.

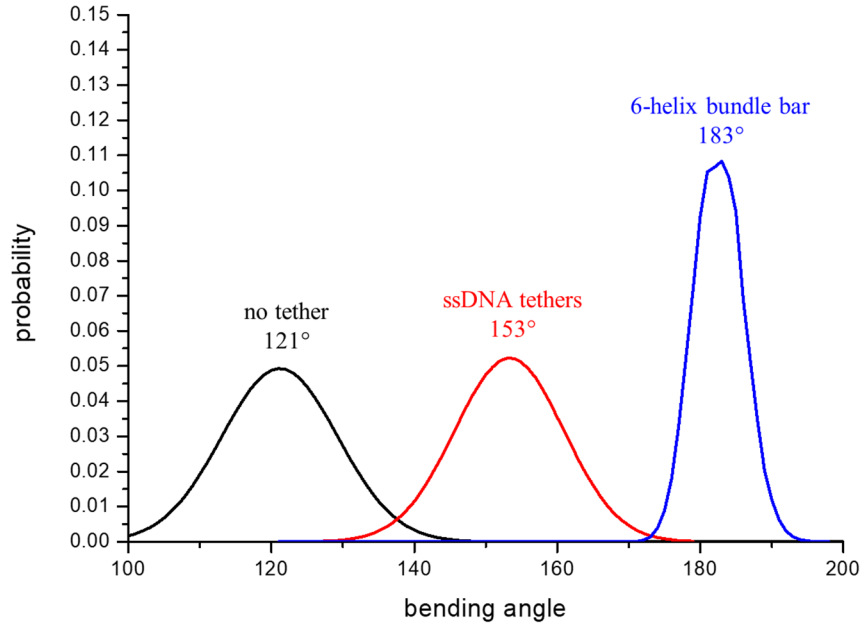

Transmission Electron Microscopy

For negative-stain TEM, a drop of the sample (5 µL) was deposited on a glow discharged formvar/carbon-coated copper grid (Electron Microscopy Sciences), incubated for 1 min, and blotted away. The grid was first rinsed twice with 1× TE buffer containing 10 mM $MgCl_2$, then washed briefly and stained for 1 min with 2% (w/v) uranyl formate. Images were acquired on a JEOL JEM-1400Plus microscope (acceleration voltage: 80 kV) with a bottom-mount 4k×3k CCD camera (Advanced Microscopy Technologies).

Nuclease Preparation and Cleavage

Nuclease P1 was pre-diluted in 1× NEBuffer 1.1; both were purchased from New England Biolabs. S1 (Promega Corporation) and mung bean (New England Biolabs) nucleases were pre-diluted in their respectively manufacturer-provided 1× reaction buffers.

dsDNA activator and crRNA's DNA template sequences (Integrated DNA Technologies; sequence information in **Table S1**) were annealed into duplexes in nuclease-free water by heating at 95 °C for 10 min, followed by gradual cooling to 85 °C (-2 °C/min) and then to 12 °C (-0.365 °C/min). crRNA for Cas12a was *in vitro* transcribed using HiScribe™ T7 High Yield RNA Synthesis Kit (New England Biolabs). Resulting RNA was extracted using phenol:chloroform:isoamyl alcohol (25:24:1) and precipitated using ethanol pre-chilled at -20 °C. The pellet was dissolved in RNAse free water, heated to 95 °C for 5 min to denature secondary structures, and then flash-frozen on ice for storage. The crRNA was characterized by 12% denaturing polyacrylamide gel electrophoresis (PAGE) in 1× TBE buffer (**Box S3**).

Box S3. PAGE characterization of in vitro transcribed crRNA (41 nt) and an RNA control (35 nt).

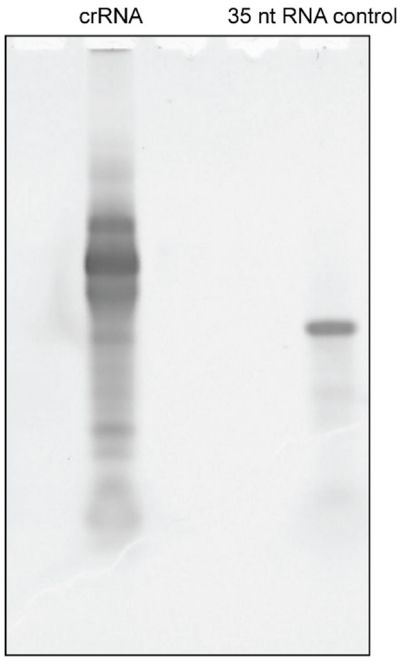

To generate the trans-activated Cas12a complex, 28 nM Cas12a (New England Biolabs: EnGen Lba Cas12a) was pre-assembled with 28 nM crRNA and 333 nM dsDNA activator (in excess) in 1× NEBuffer 2.1 (New England Biolabs) at 37 °C for 10 min. Unless otherwise noted, Cas12a digestions were carried out at 37 °C. DNA-origami structure (in 1× TE buffer, 10 mM $MgCl_2$) to nuclease volume and concentration ratios in each nuclease digestion assay can be found in **Table S2**.

Preparation of Custom Scaffold with Deoxyribozyme Sequences

M13-derived p7308 was replicated *via* polymerase chain reaction (PCR) using primers containing one deoxyribozyme split sequence (Integrated DNA Technologies, Inc., **Table S3**). 70 ng of linear PCR products were circularized with KLD Enzyme Mix (New England Biolabs) and transformed into JM109 competent cells. Transformants were spread on Luria-Bertani (LB) plates and incubated at 37 °C overnight. Six plaques were picked, and each inoculated in 10 ml 2× YT medium. Double-stranded plasmids were harvested with the Plasmid Miniprep Kit (Qiagen) and verified by sequencing.

BsaI recognition site sequence (**Table S3**) was then inserted into the plasmid through PCR. A second deoxyribozyme sequence and the complementary sequence to the Cy5-labeled ssDNA probe (Integrated DNA Technologies, Inc., **Table S3**) were also inserted into the plasmid (plasmid:oligo molar ratio = 1:3) with the Golden Gate Assembly Kit (New England Biolabs). 5 µl of the product was transformed into JM109 competent cells, and the resulting culture was inoculated in 2× YT medium overnight growth at 37 °C/220 rpm. Bacteria cells were pelleted by centrifugation for 15 min at 5000 rcf and phage particles in supernatant were harvested. 40 g PEG-8000 and 30 g NaCl were added to the supernatant with stirring, and the mixture was centrifuged for 30 min at 5500 rcf. The pellet was resuspended with 10 mL of buffer containing 10 mM Tris (pH 8), 1 mM EDTA. Residual bacteria cells were pelleted and removed through centrifugation for 10 min at 16000 rcf. Finally, single-stranded scaffold was rescued from phage supernatant through alkaline lysis[3].

Deoxyribozyme Self-cleavage Assay

After assembly and glycerol gradient purification, the buffer of force clamp structures was exchanged with 50 mM HEPES (pH 7.0), 100 mM NaCl, 10 mM $MgCl_2$ using Amicon Ultra-0.5 mL Centrifugal Filters with 30-kD NMWL. 50 µl of10 nM force clamp was incubated with 3 µl of 1.6 µM Cy5-labeled ssDNA probes at 37 °C for 60 min and then distributed equally into nine 0.6 mL tubes (5.4 µl per tube). The mixture, as well as the Zn^{2+} reaction buffer (50 mM HEPES pH 7.0, 100 mM NaCl, 10 mM $MgCl_2$, 4 mM $ZnCl_2$), was preheated to 37 °C. 5.4 µl of the reaction buffer was then added into eight of the nine origami mixture tubes (one tube kept as control) and the reaction tubes were kept at 37 °C. The reaction was quenched with 1.08 µl 33 mM EDTA and cleaved products were analyzed with 1.5% AGE.

Before conducting cleavage assays in free DNA strands each containing two deoxyribozyme sequences (Integrated DNA Technologies, Inc., **Table S3**), 55 µl of 0.5 µM deoxyribozyme ssDNA was annealed with Cy5-labeled ssDNA probes (deoxyribozyme strand: probe molar ratio = 1.1: 1). 5 µl solution was reserved as a control, while the remaining mixture was incubated with an equal volume of the Zn^{2+} reaction buffer at 37 °C. At each time point, 10 µl solution was quenched with 1 µl 33 mM EDTA. The resulting cleaved products were analyzed using 12% non-denaturing PAGE in 1× TBE buffer.

Gel Purification

Samples were loaded in a 1.5% agarose gel (0.5× TBE, 10 mM $MgCl_2$) with 0.5 µg/mL EtBr and a 1 kb DNA ladder (New England Biolabs), then run for 3 hours at 5 V/cm in 0.5× TBE and 10 mM $MgCl_2$ running buffer. After image analysis on a Typhoon FLA 9500 imager (GE Healthcare), bands of interest were excised using a razor and spun in Freeze 'N Squeeze DNA gel extraction columns (Bio-Rad Laboratories).

Image Data Analysis

Gel images were obtained using a Typhoon FLA 9500 imager (GE Healthcare). Densitometry was carried out using the "Gels" tool in ImageJ[13] (version 1.52b). Using the integrated intensity values of DNA-origami bands, the amount of Cy5-labeled ssDNA probe released from the force clamps in each nuclease digestion reaction was quantified:

$$\text{Percent Cy5-labeled ssDNA release} = \left(1 - \frac{Cy5_{nuclease-treated\ sample}}{EtBr_{nuclease-treated\ sample}} \div \frac{Cy5_{undigested\ control}}{EtBr_{\ undigested\ control}}\right) \times 100\%$$

For yield estimations, band intensities were normalized by the molecular weight of the corresponding structure of each gel band.

Macrocycle positions were traced and measured using the "Segmented Line" tool in ImageJ[13] (**Figure S40**). Pre-stressed beam angles were measured using the "Angle" tool in ImageJ[13]; samples used were not gel-purified to eliminate the possible effects of purification on bending angles (**Figure S44**).

Plots and statistics were generated using GraphPad Prism (v 8.3.0). The Mann–Whitney U test was used compare populations of rotaxane and elastic beam structures as the distributions of the macrocycle and bending angles are not normal.

SUPPLEMENTAL FIGURES

Figure S1. CaDNAno design of the 2 pN force clamp. Green: core staples. Red: staples specific to 2 pN version of force clamp. Mageneta: 5’ Cy5-labelled ssDNA probe. Staple extensions on termini of helices each consists of four thymines to prevent stacking interactions.

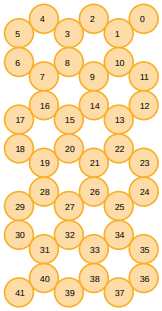

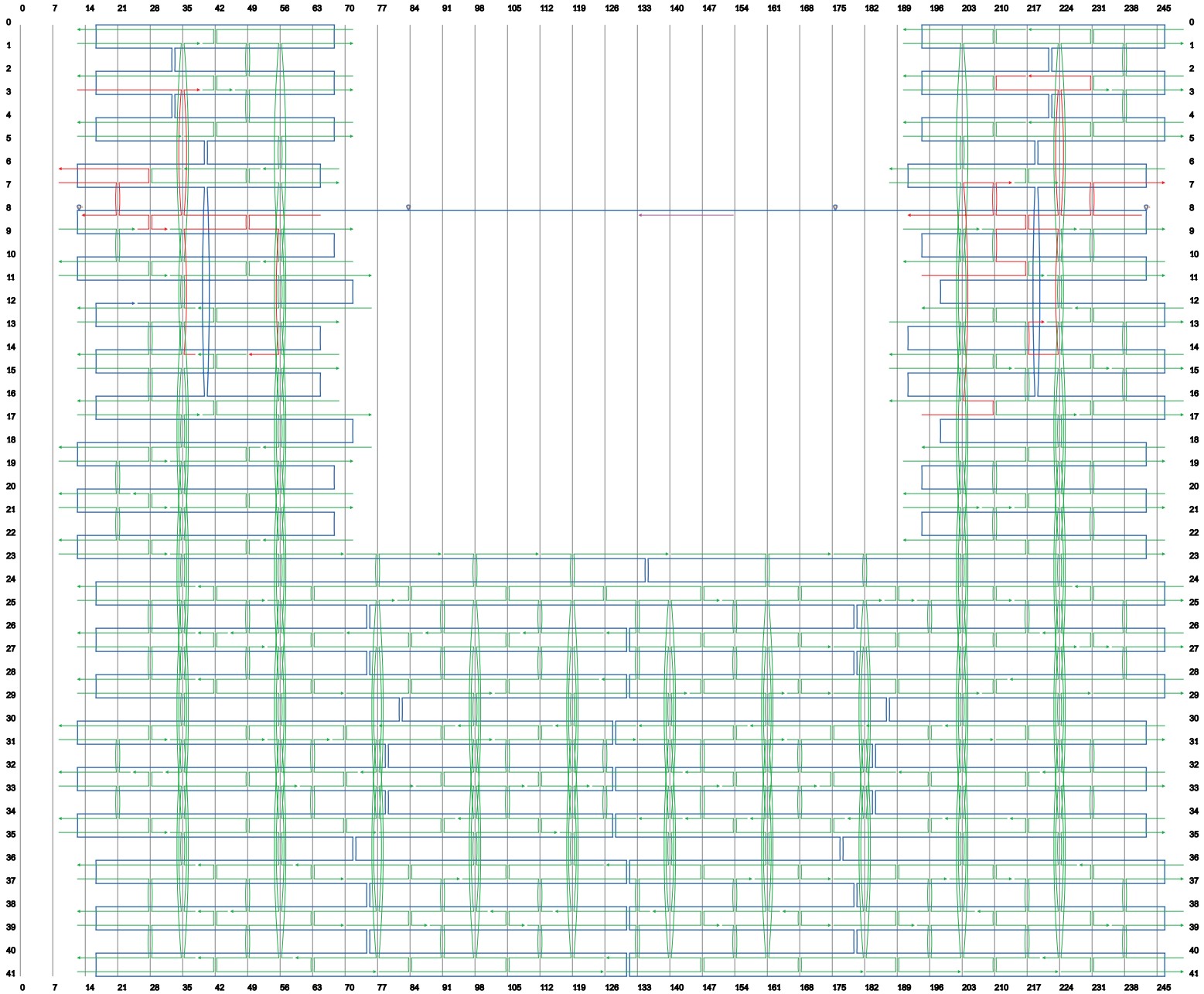

Figure S2. CaDNAno design of the 6 pN force clamp. Green: core staples. Red: staples specific to 6 pN version of force clamp. Mageneta: 5’ Cy5-labelled ssDNA probe. Staple extensions on termini of helices each consists of four thymines to prevent stacking interactions.

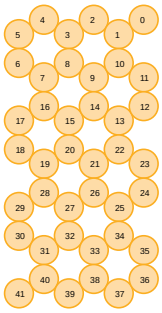

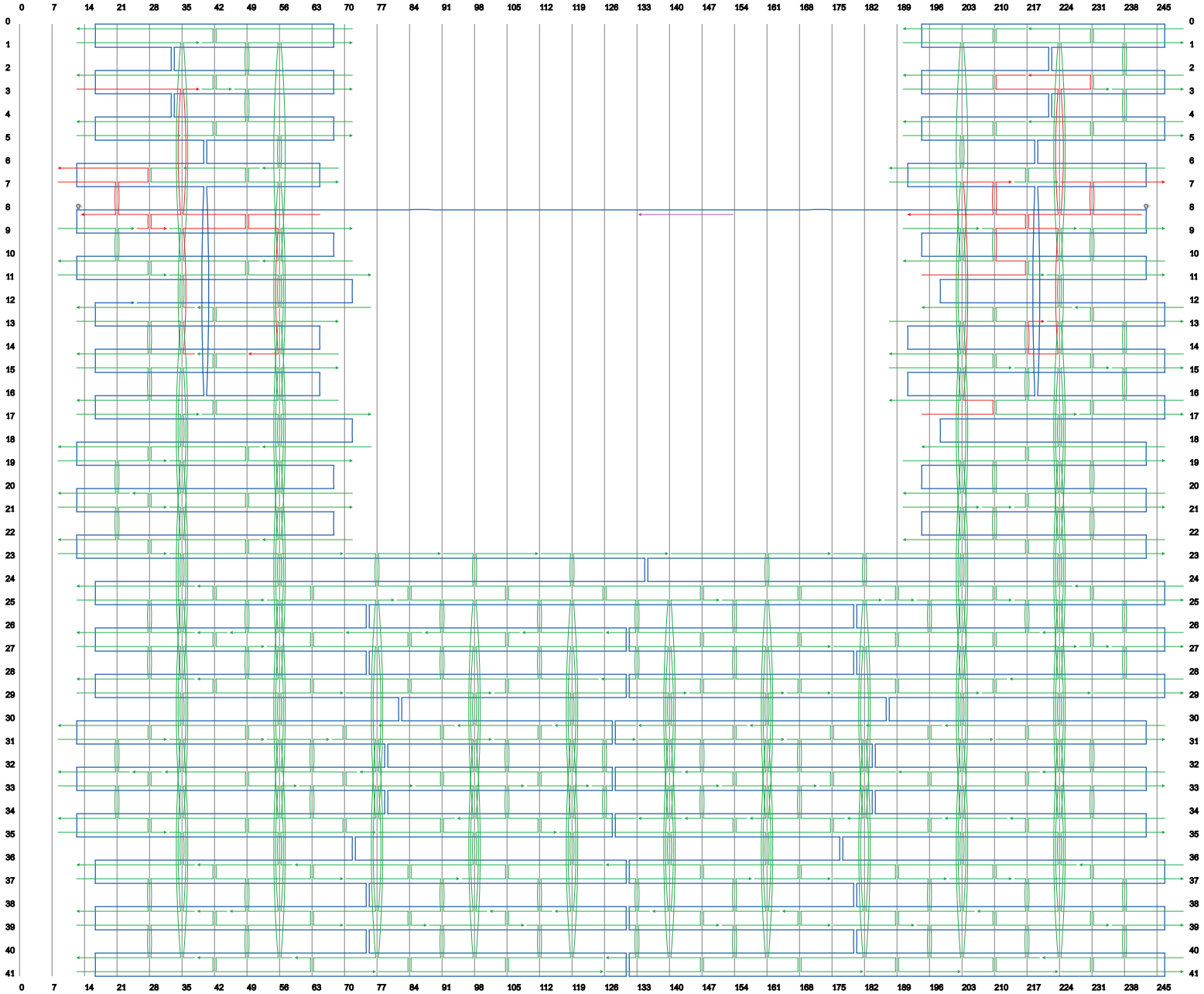

Figure S3. CaDNAno design of the 12 pN force clamp. Green: core staples. Red: staples specific to 12 pN version of force clamp. Mageneta: 5’ Cy5-labelled ssDNA probe. Staple extensions on termini of helices each consists of four thymines to prevent stacking interactions.

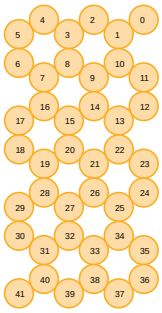

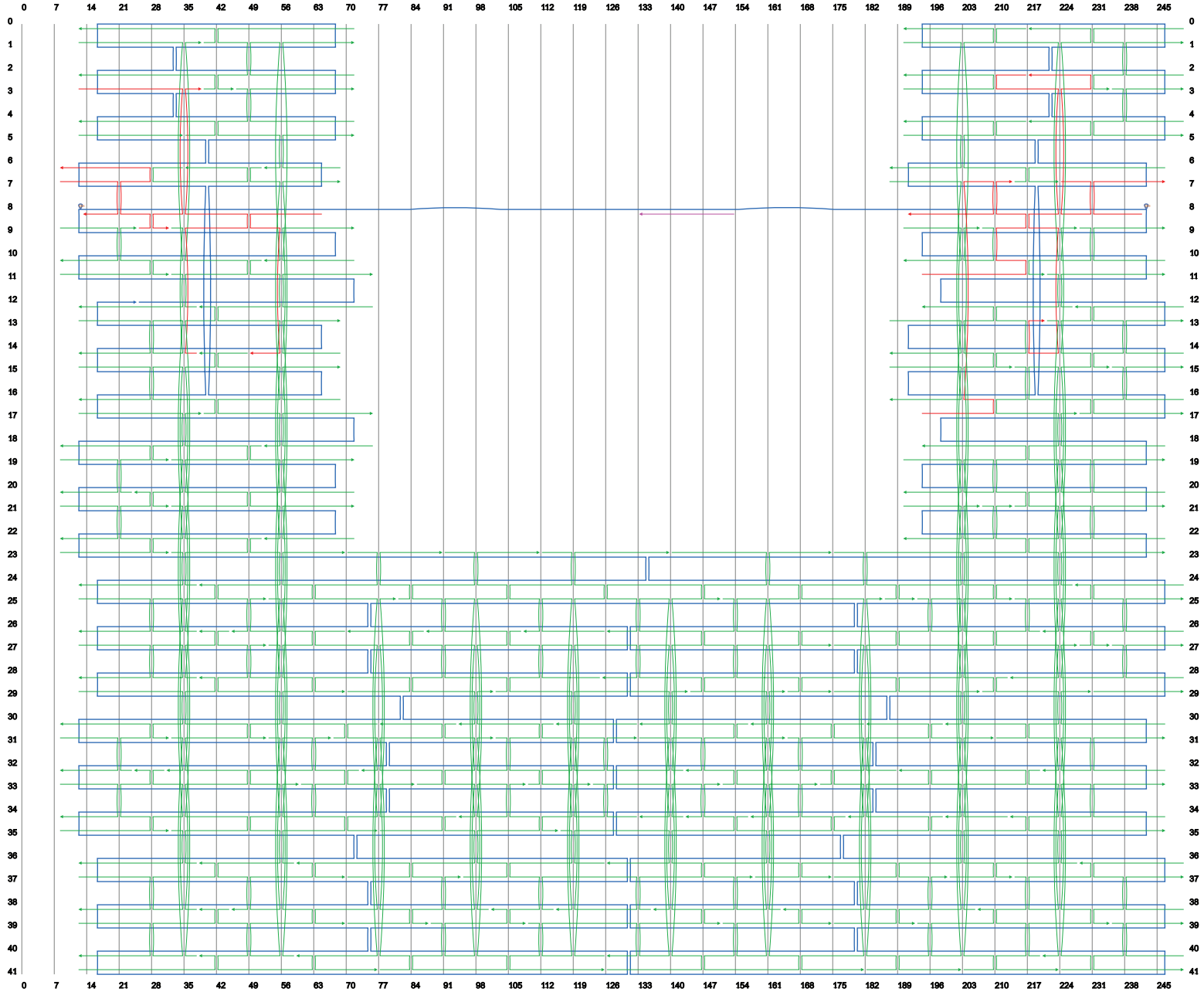

Figure S4. More electron micrographs showing gel-purified 2 pN force clamps. Scale bar: 100 nm.

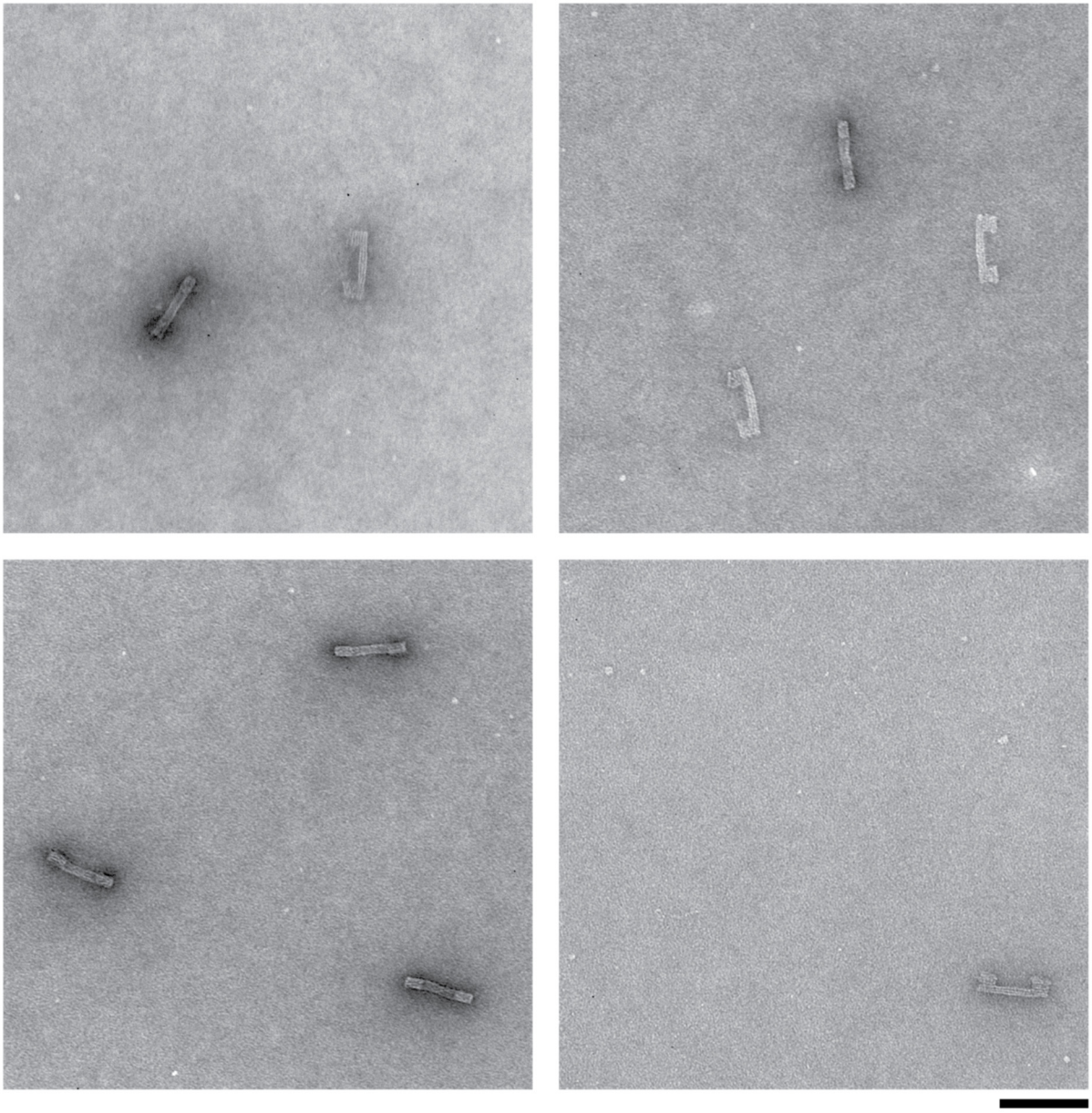

Figure S5. More electron micrographs showing 2 pN force clamps, gel-purified after 30 min of Cas12a treatment. Scale bar: 100 nm.

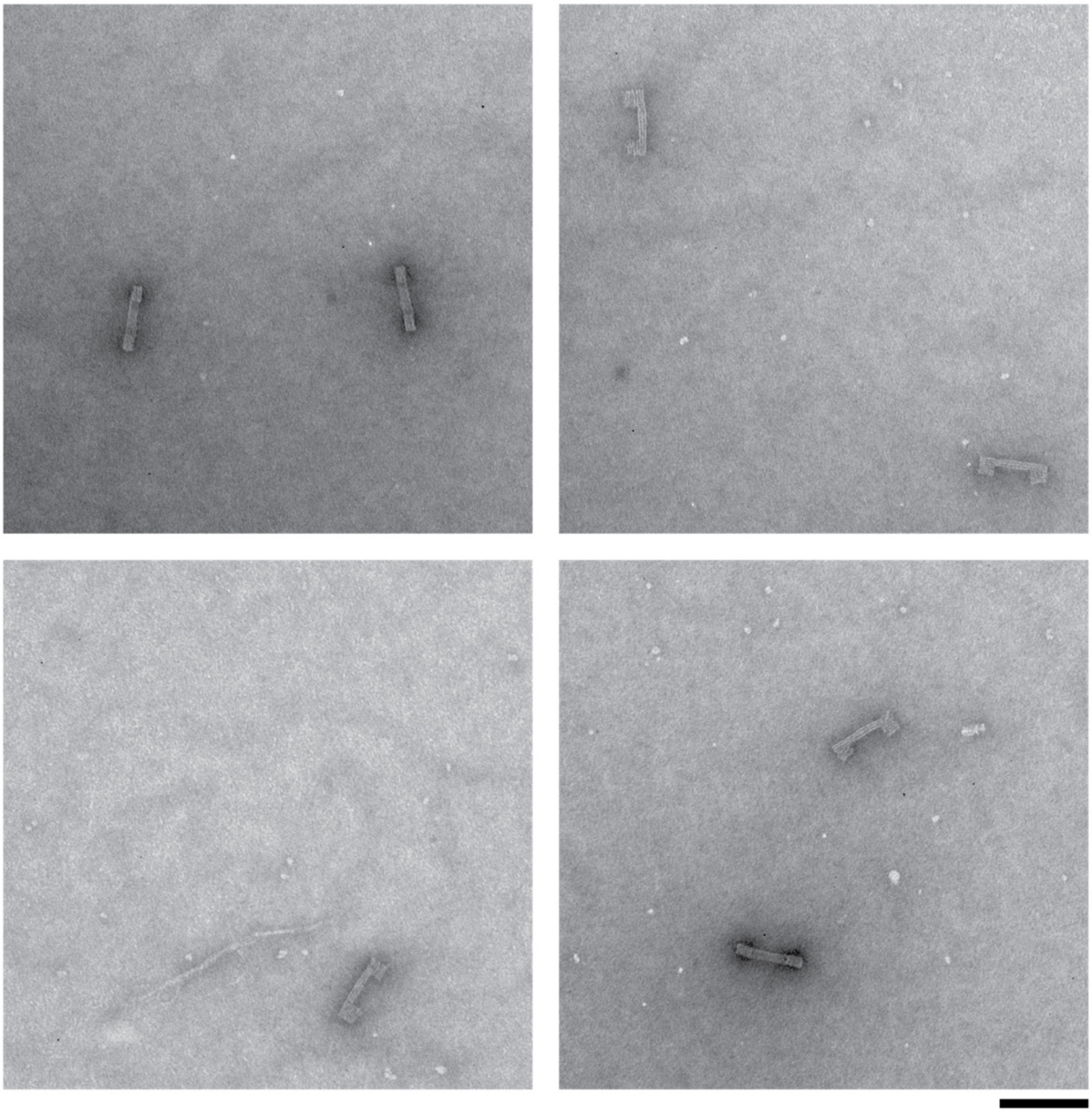

Figure S6. More electron micrographs showing 2 pN force clamps, gel-purified after 30 min of nuclease P1 treatment. Scale bar: 100 nm.

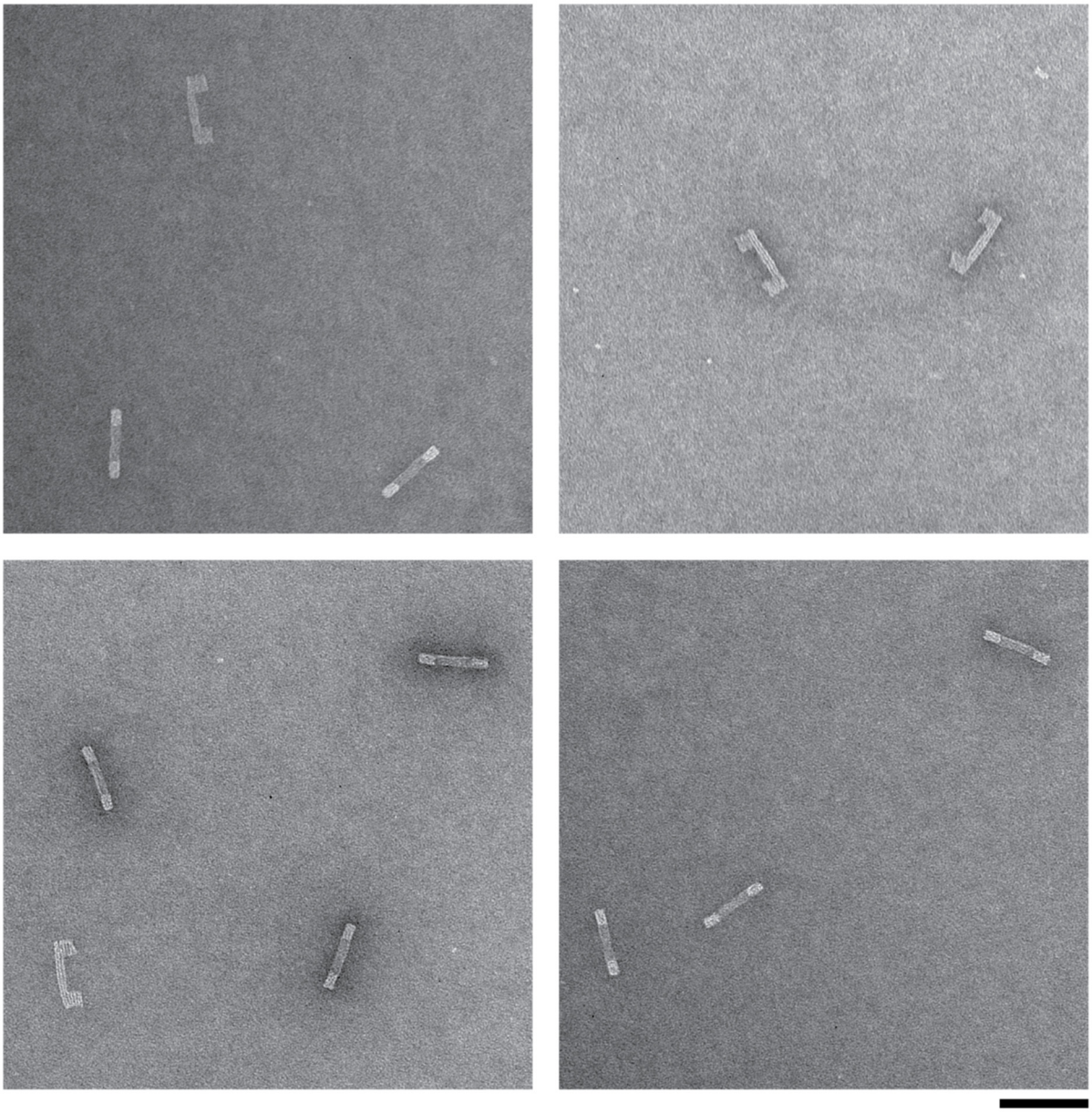

Figure S7. More electron micrographs showing 2 pN force clamps, gel-purified after 30 min of nuclease S1 treatment. Scale bar: 100 nm.

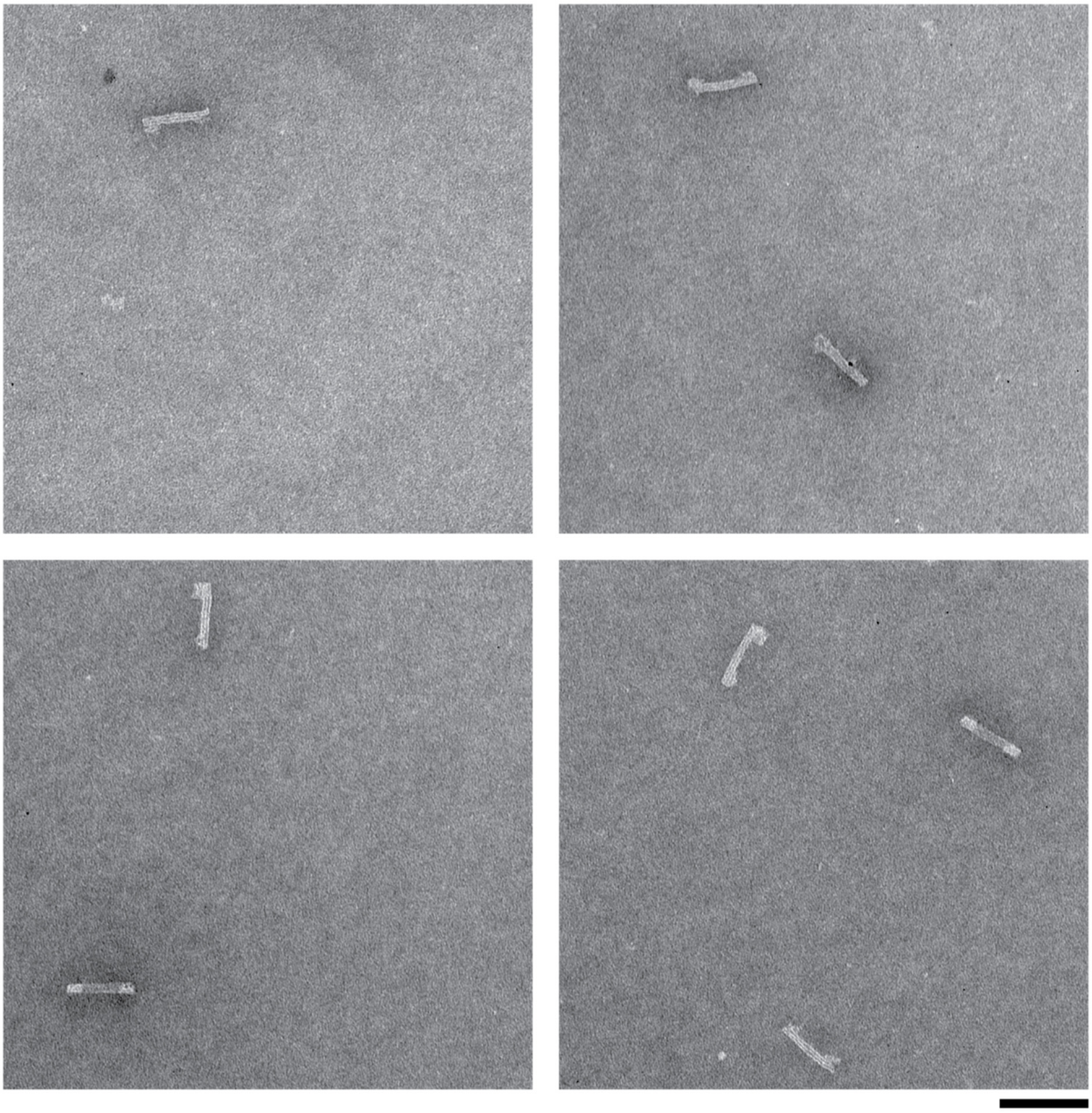

Figure S8. More electron micrographs showing 2 pN force clamps, gel-purified after 30 min of mung bean nuclease treatment. Scale bar: 100 nm.

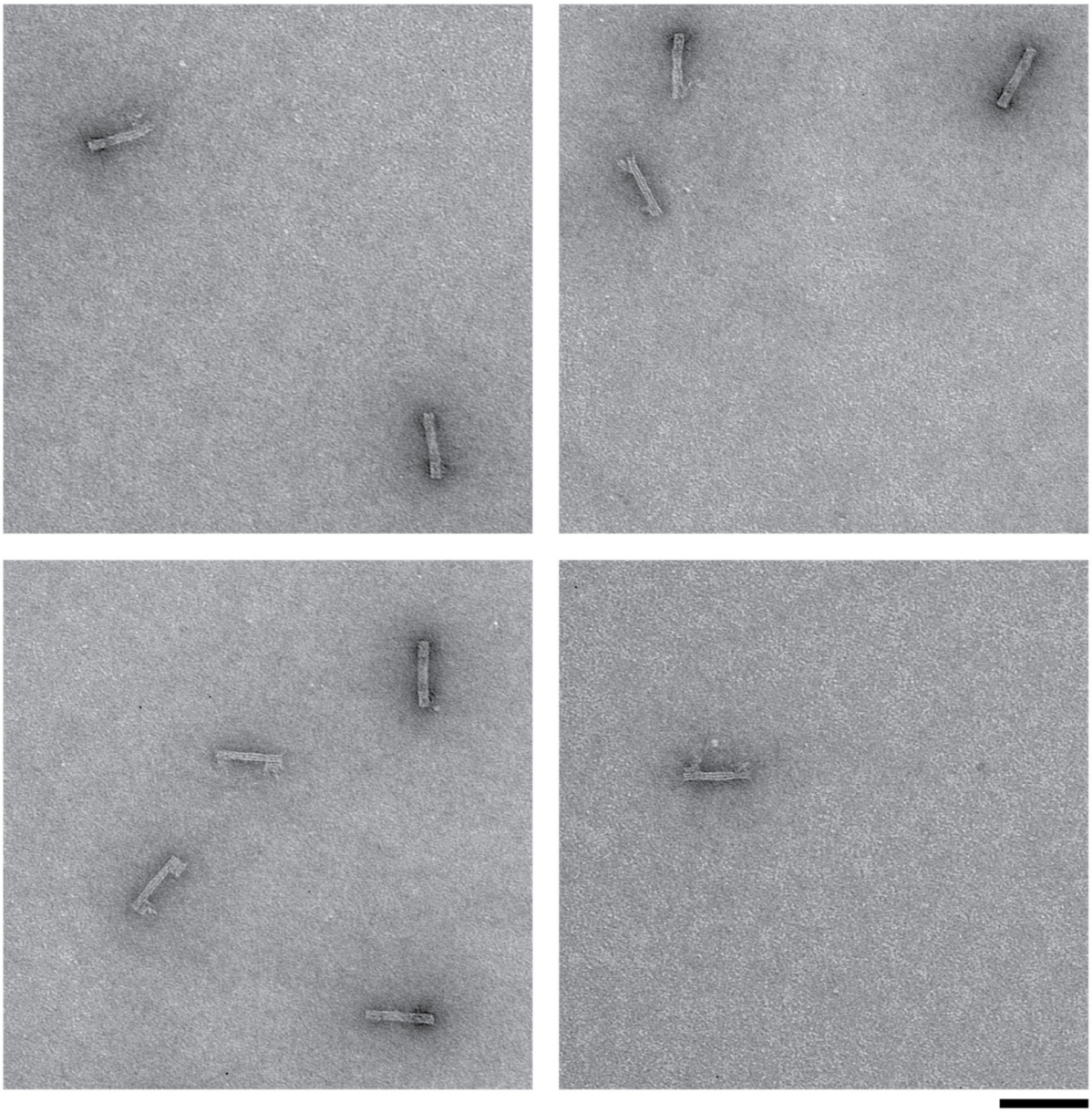

Figure S9. The AGE result from trial 1 of Cas12a digested 2 pN force clamps. Prior to the Cas12a cleavage assay, force clamps were pre-hybridized with Cy5-labeled ssDNA probes (Materials and Methods: DNA-origami Design and Assembly). Excess free Cy5-labeled ssDNA probes were not removed and present in the subsequent cleavage reaction mixture. Consequently, the cleavage reaction was measured by a loss of the Cy5-labeled ssDNA probes from the force clamps instead of a gain of fluorescence signals in solution from released Cy5-labeled ssDNA probes. The same applies to Figure S10–S13. M: 1 kb DNA ladder.

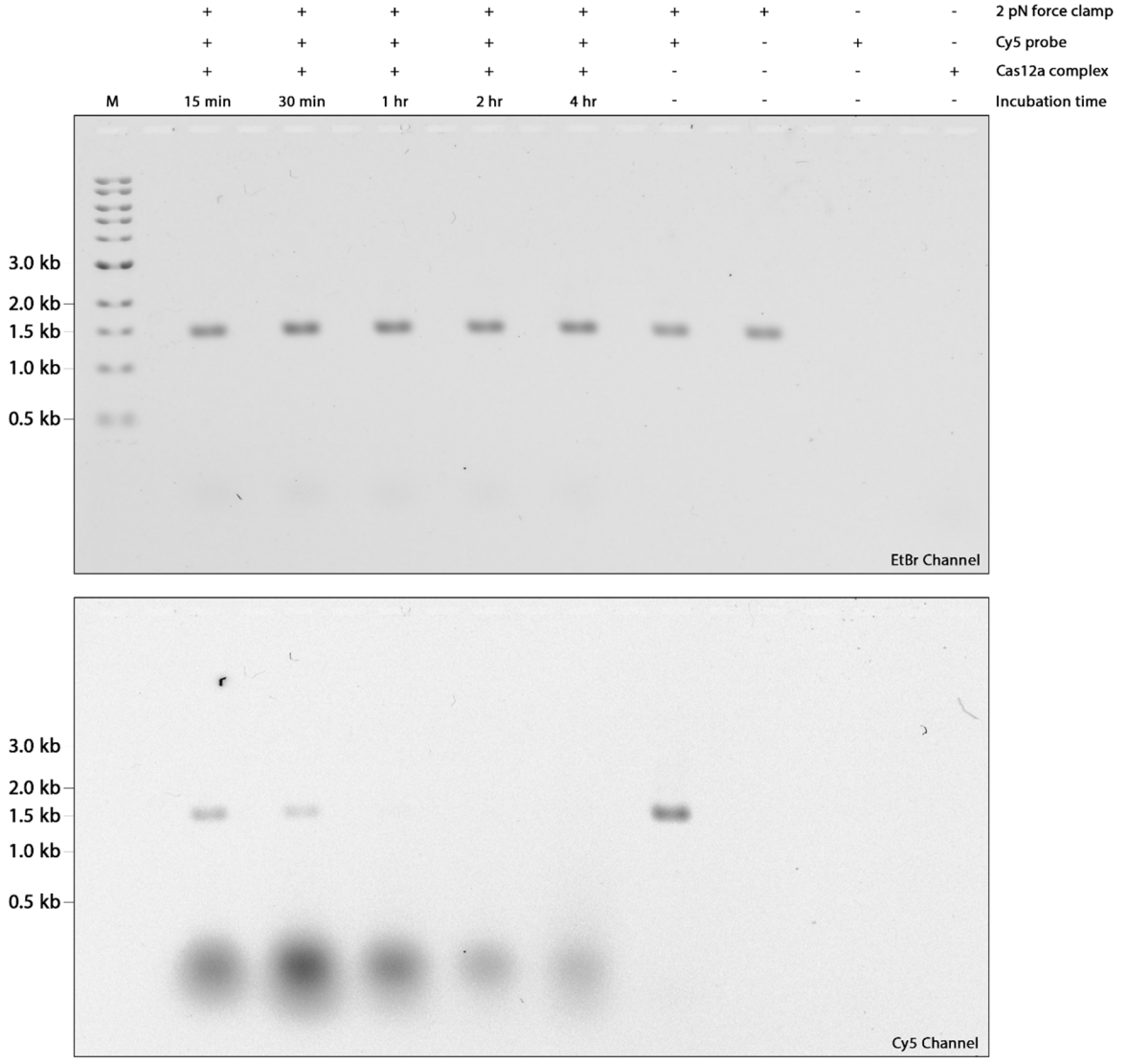

Figure S10. The AGE result from trial 1 of Cas12a digested 6 pN force clamps. M: 1 kb DNA ladder.

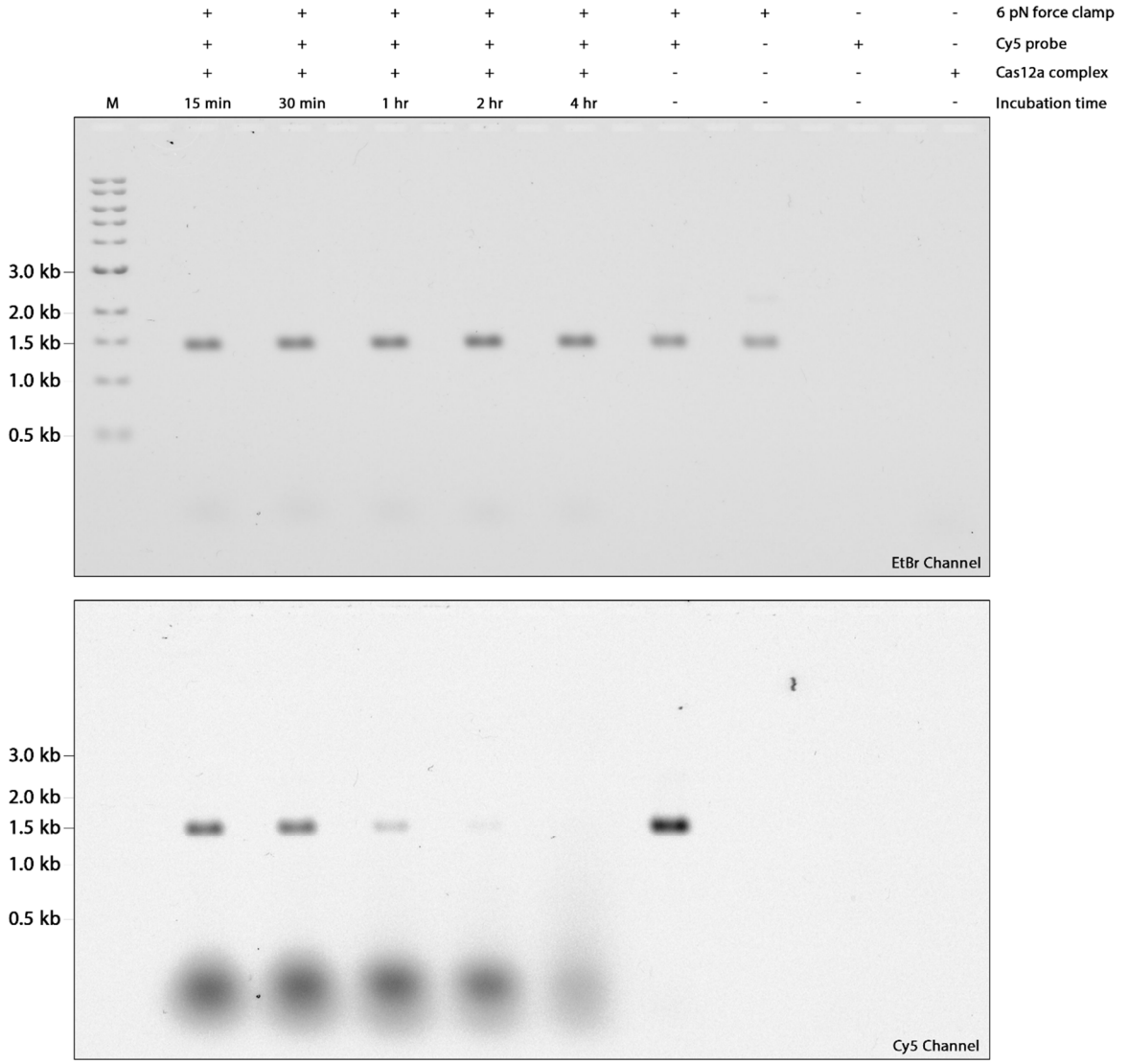

Figure S11. The AGE result from trial 1 of Cas12a digested 12 pN force clamps. M: 1 kb DNA ladder.

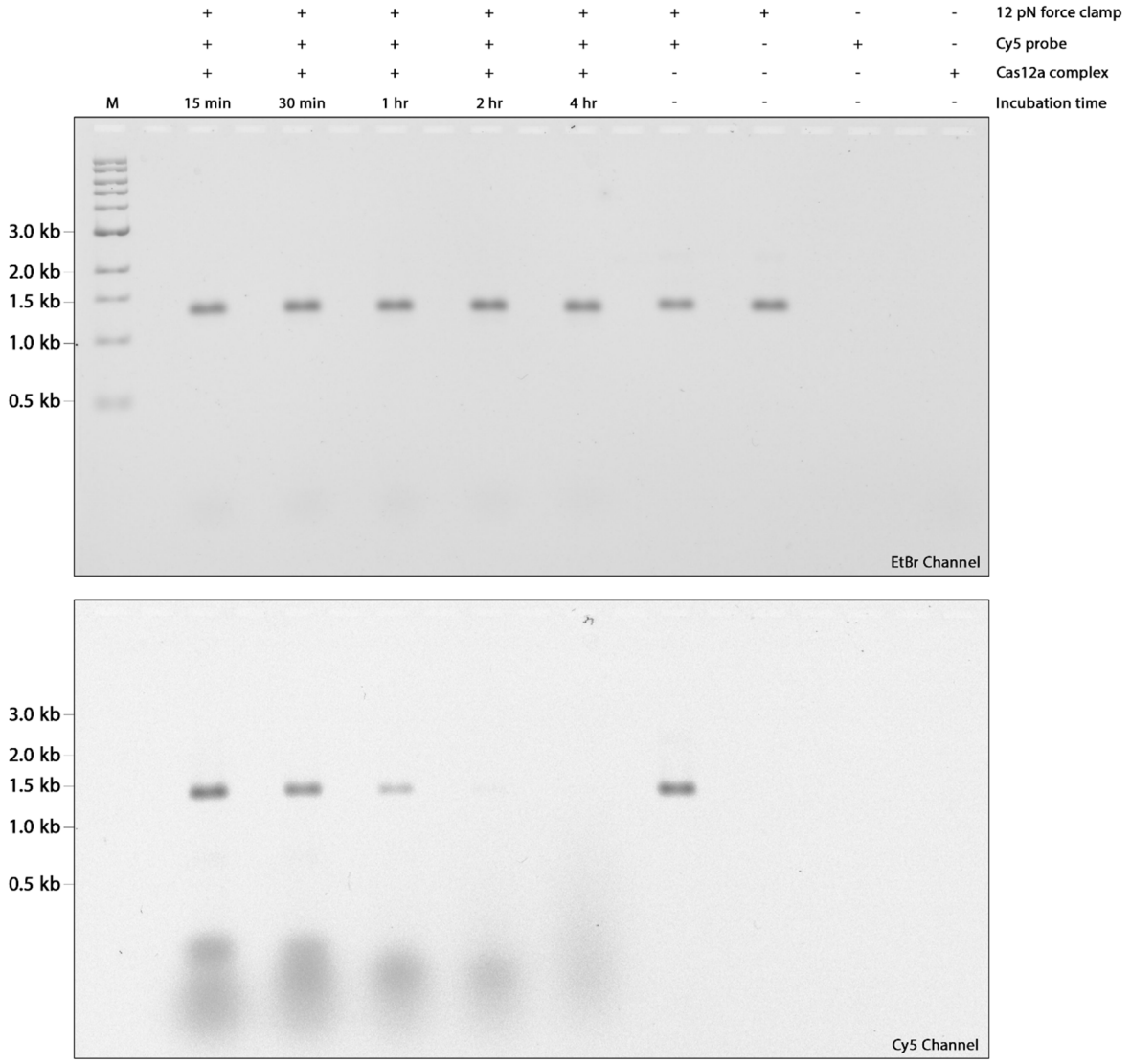

Figure S12. The AGE result from trial 2 of Cas12a digested force clamps. M: 1 kb DNA ladder.

Figure S13. The AGE result from trial 3 of Cas12a digested force clamps. M: 1 kb DNA ladder.

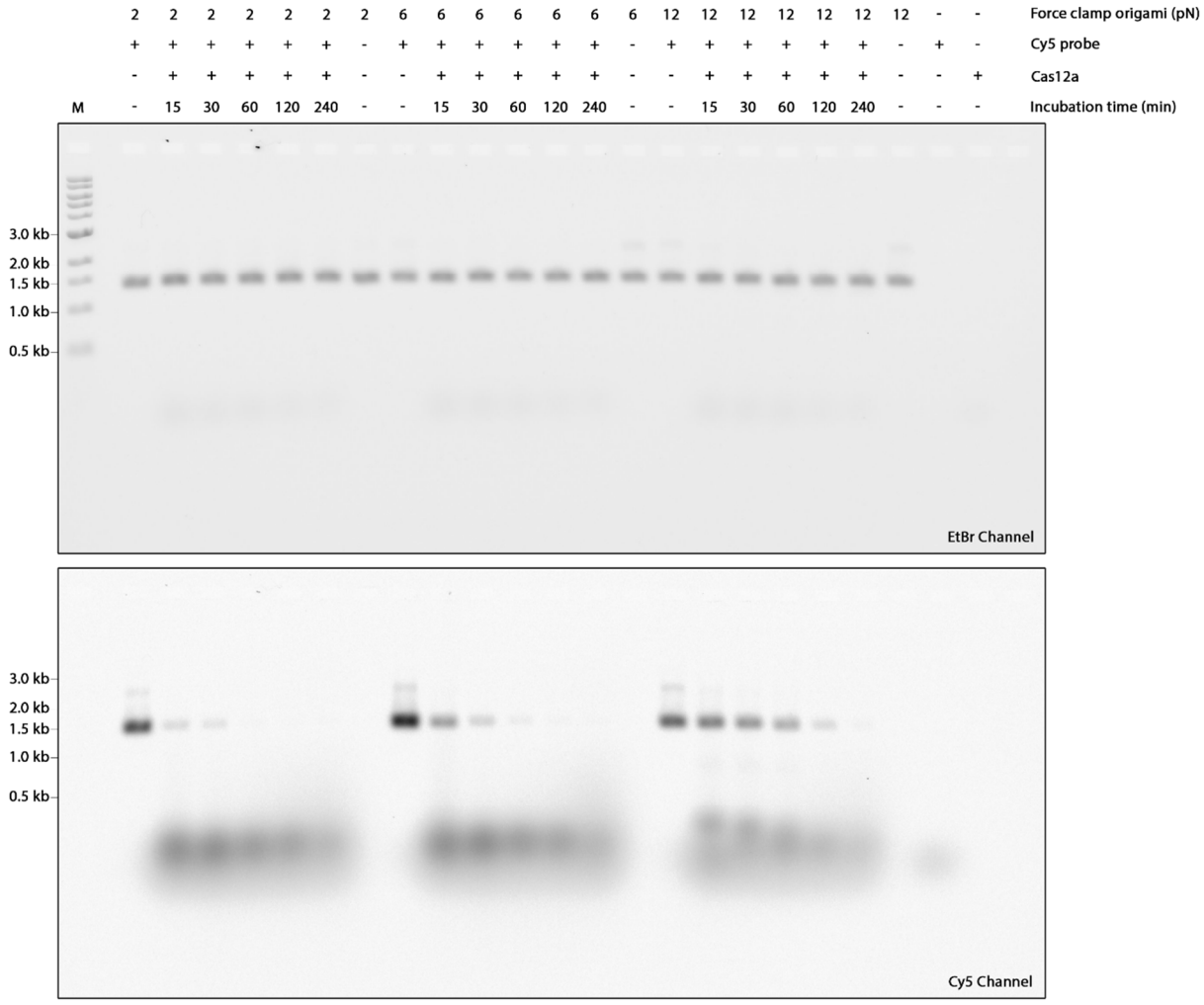

Figure S14. Electron micrographs showing 2 pN force clamps after four hours of Cas12a treatment. Sample was not purified. Scale bar: 100 nm.

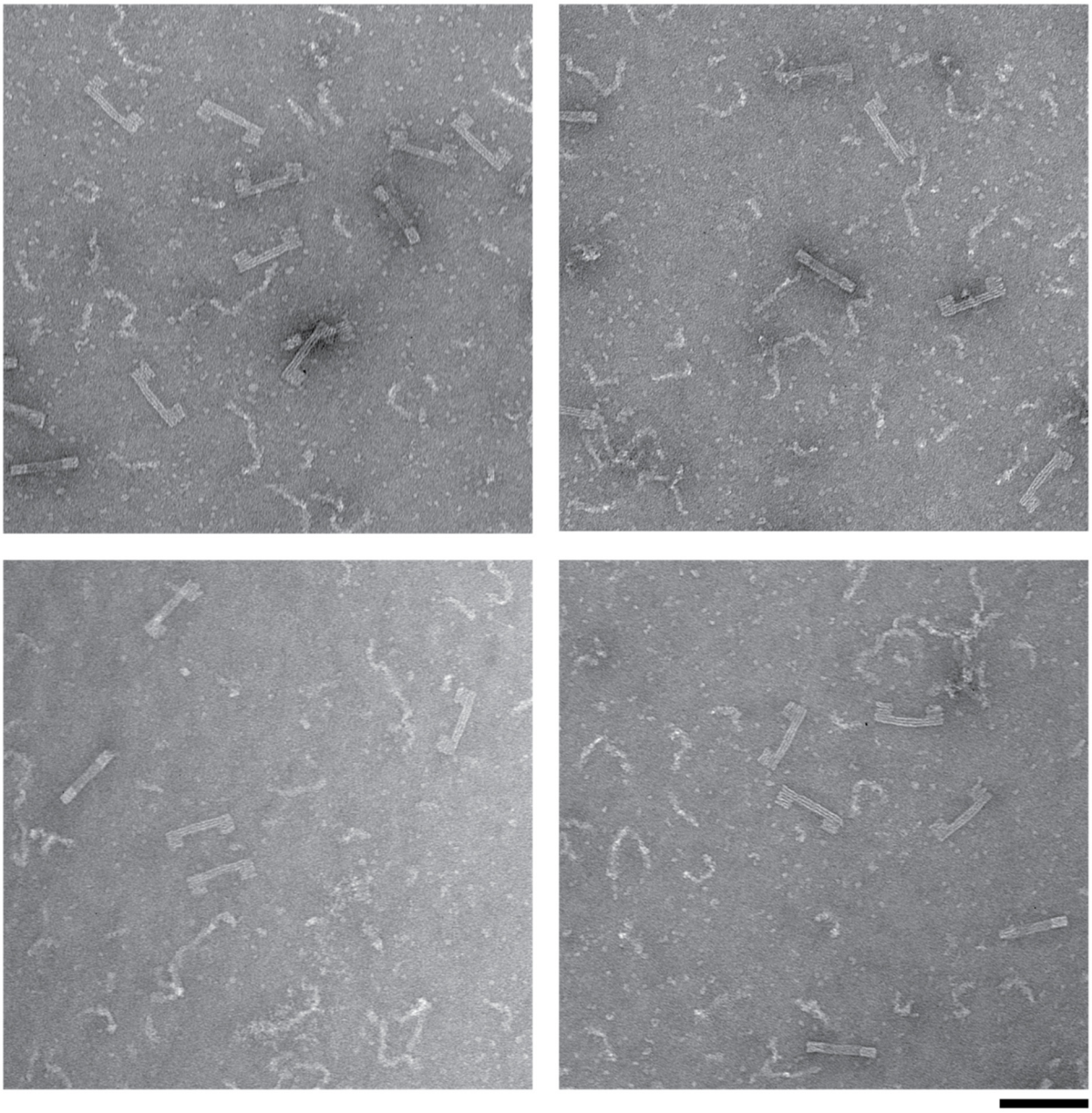

Figure S15. Electron micrographs showing 6 pN force clamps after four hours of Cas12a treatment. The sample was not purified. Scale bar: 100 nm.

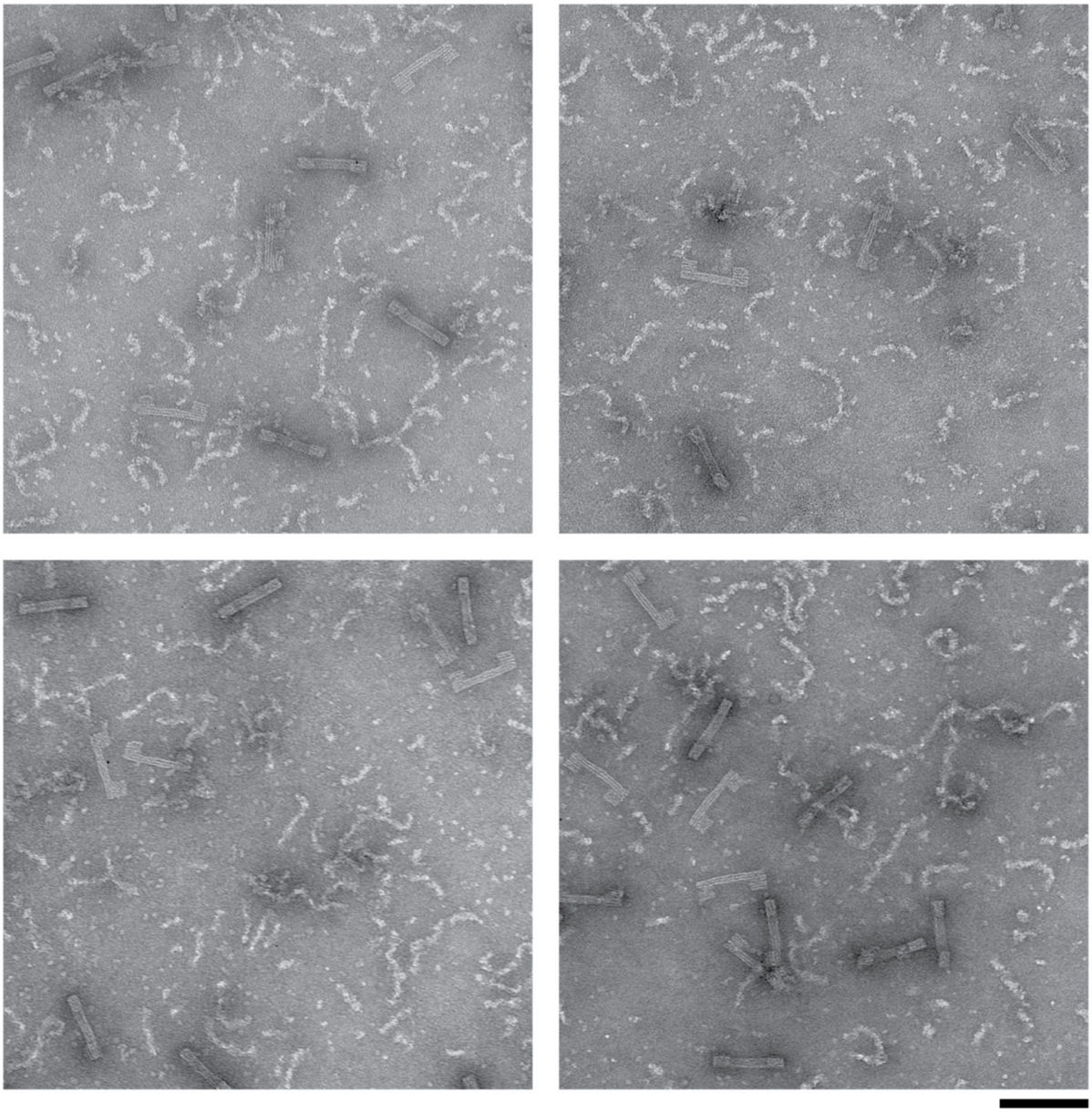

Figure S16. Electron micrographs showing 12 pN force clamps after four hours of Cas12a treatment. The sample was not purified. Scale bar: 100 nm.

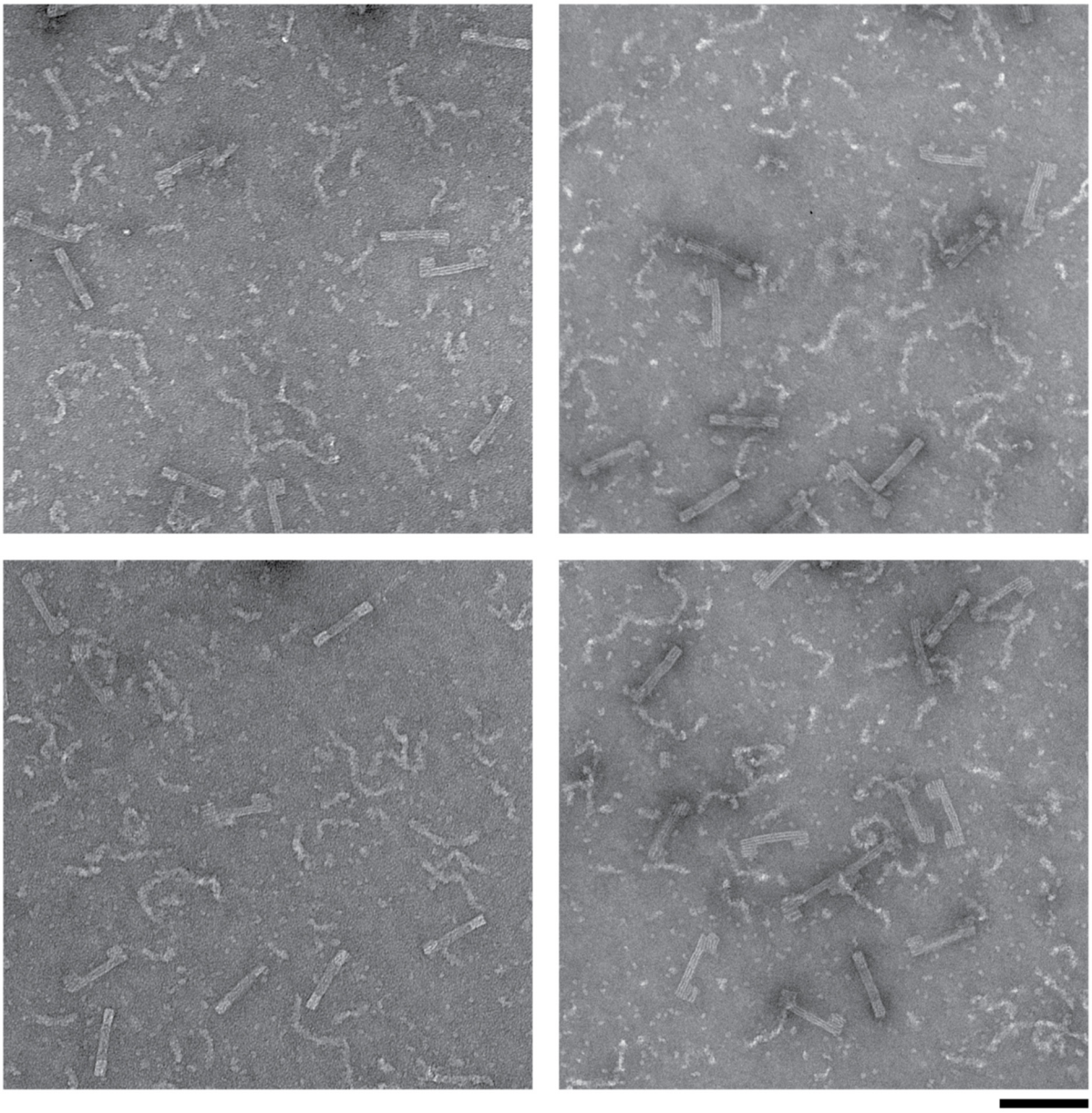

Figure S17. AGE characterization of 12 pN force clamps digested by Cas12a and P1 nucleases for 30 min at 37 °C. M: 1 kb DNA ladder.

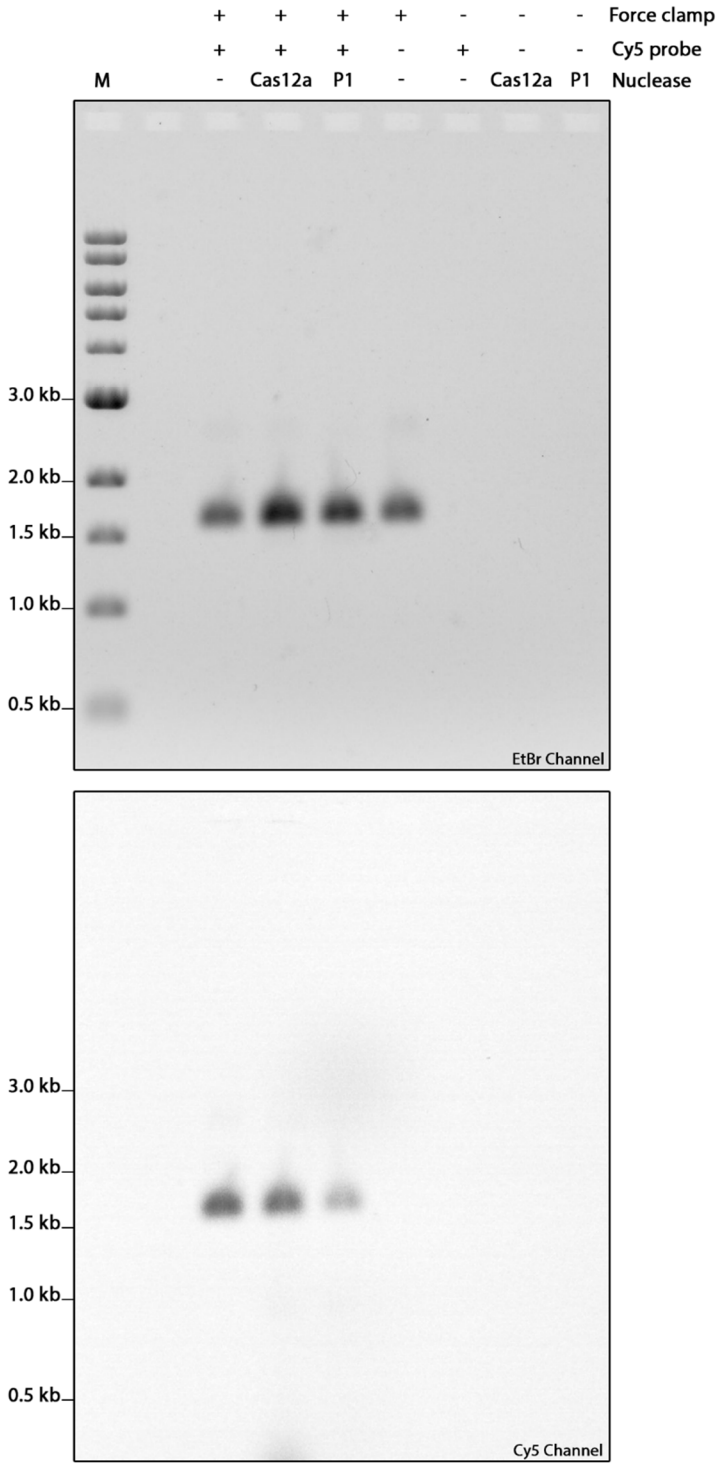

Figure S18. Electron micrographs showing gel-purified 12 pN force clamps. Scale bar: 100 nm.

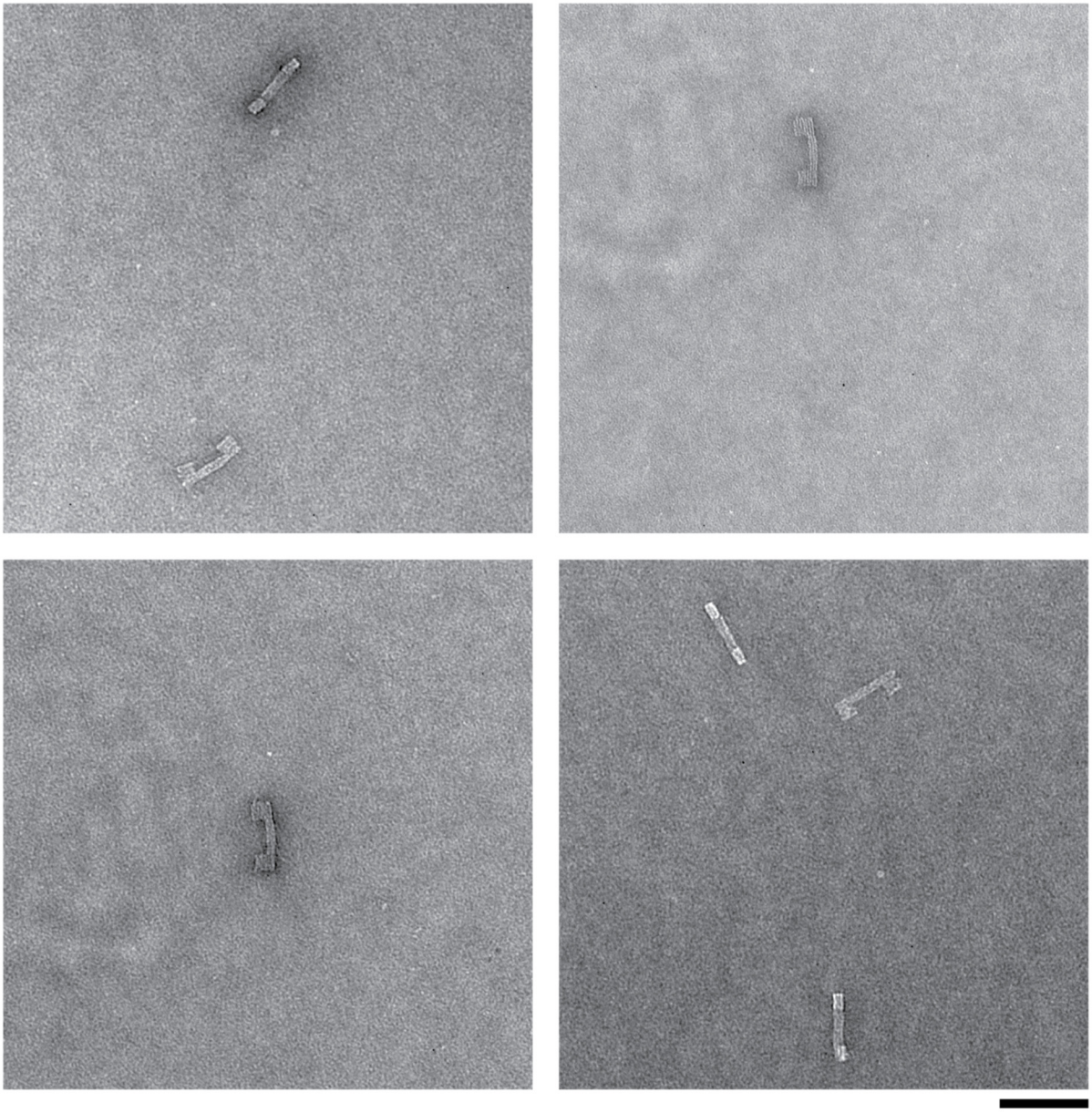

Figure S19. Electron micrographs showing 12 pN force clamps, gel-purified after 30 min of Cas12a treatment. Scale bar: 100 nm.

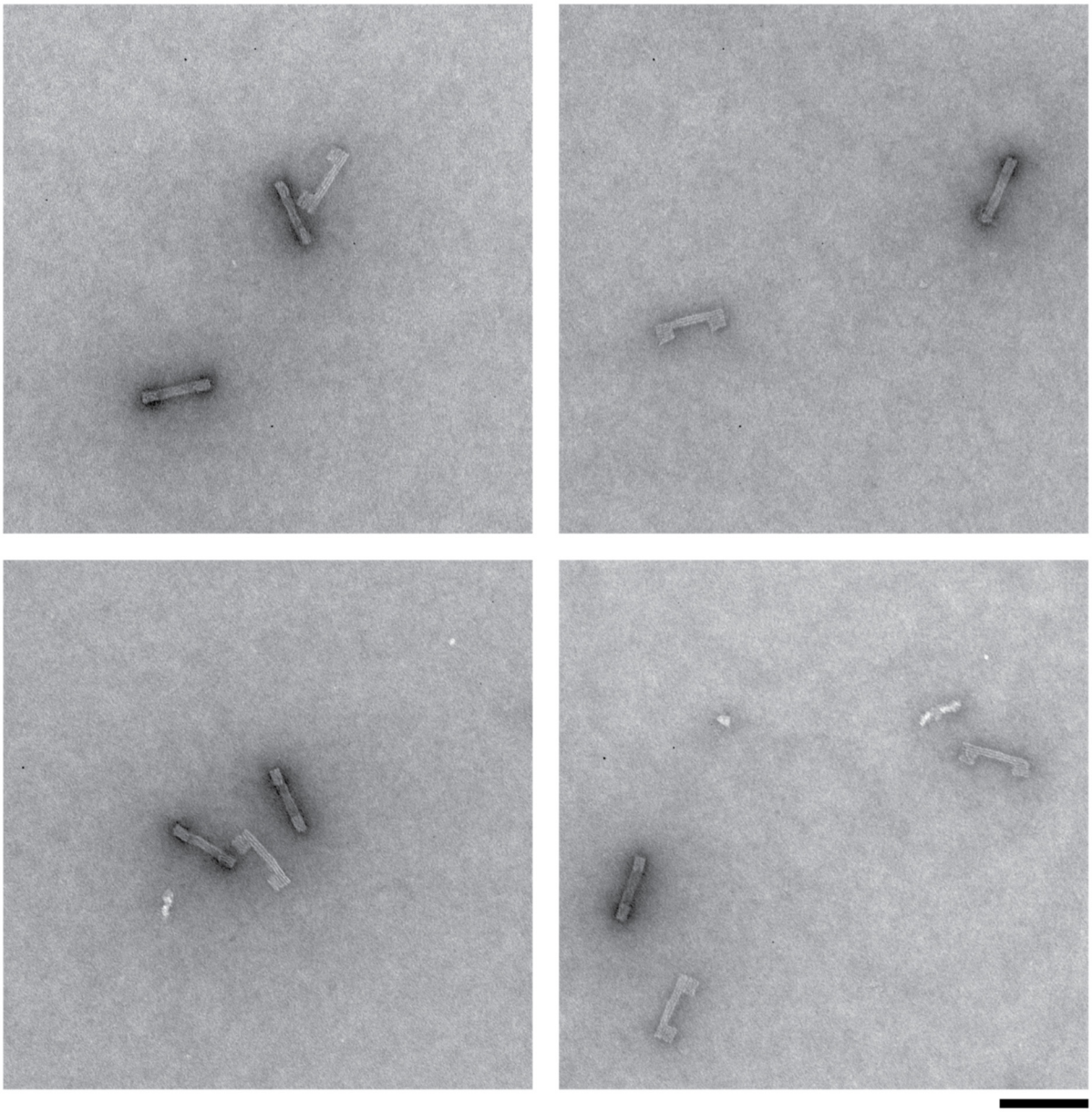

Figure S20. Electron micrographs showing 12 pN force clamps, gel-purified after 30 min of nuclease P1 treatment. Scale bar: 100 nm.

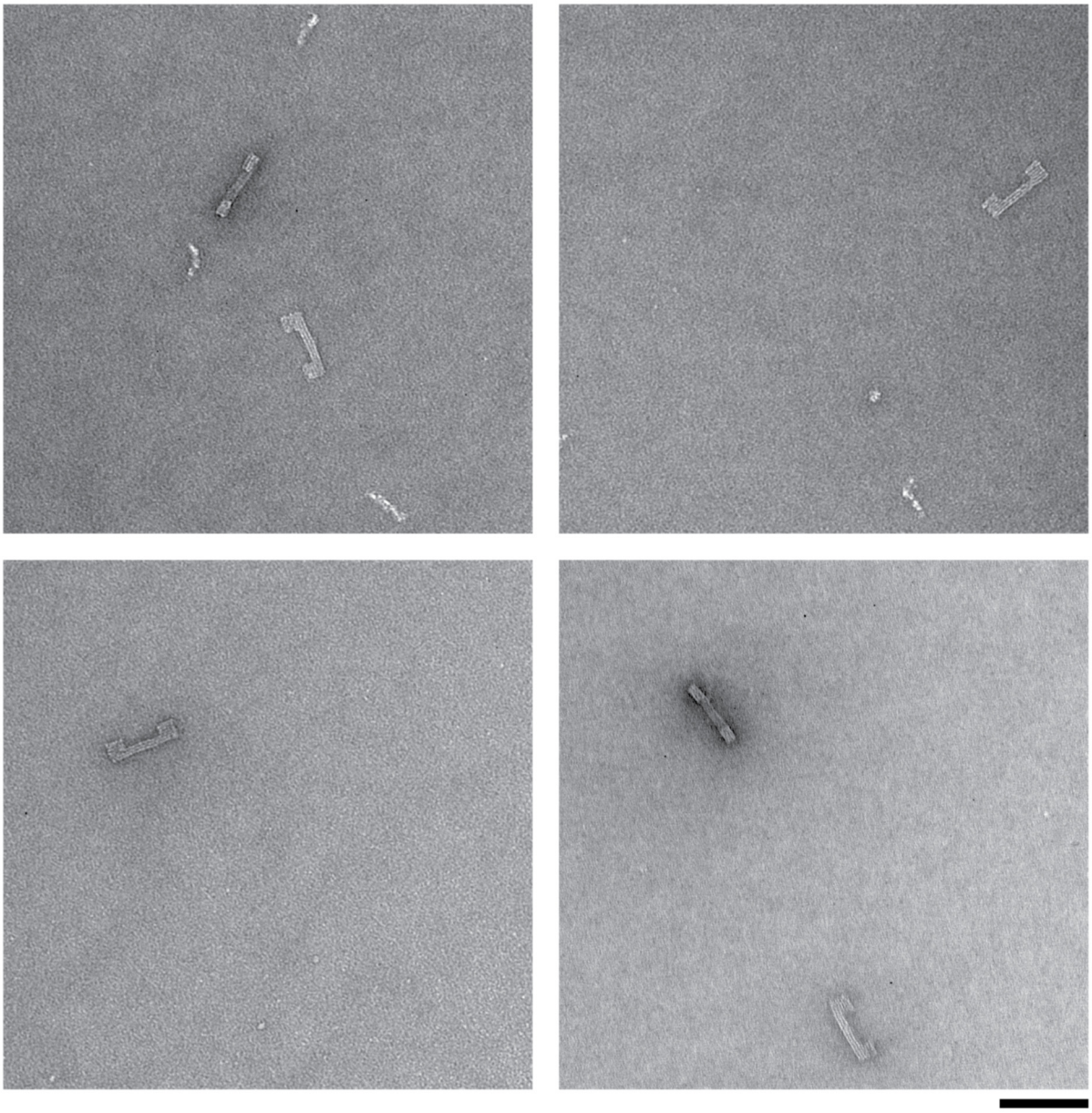

Figure S21. Non-denaturing PAGE data (gel imaged in Cy5 channel) showing the self-cleavage kinetics of a DNA oligonucleotide containing two deoxyribozyme sequences. The schematics show the Zn^{2+}-induced cleavage of both deoxyribozymes, separating the Cy5 (red star)-labeled segment from the 5'- and 3'- segments.

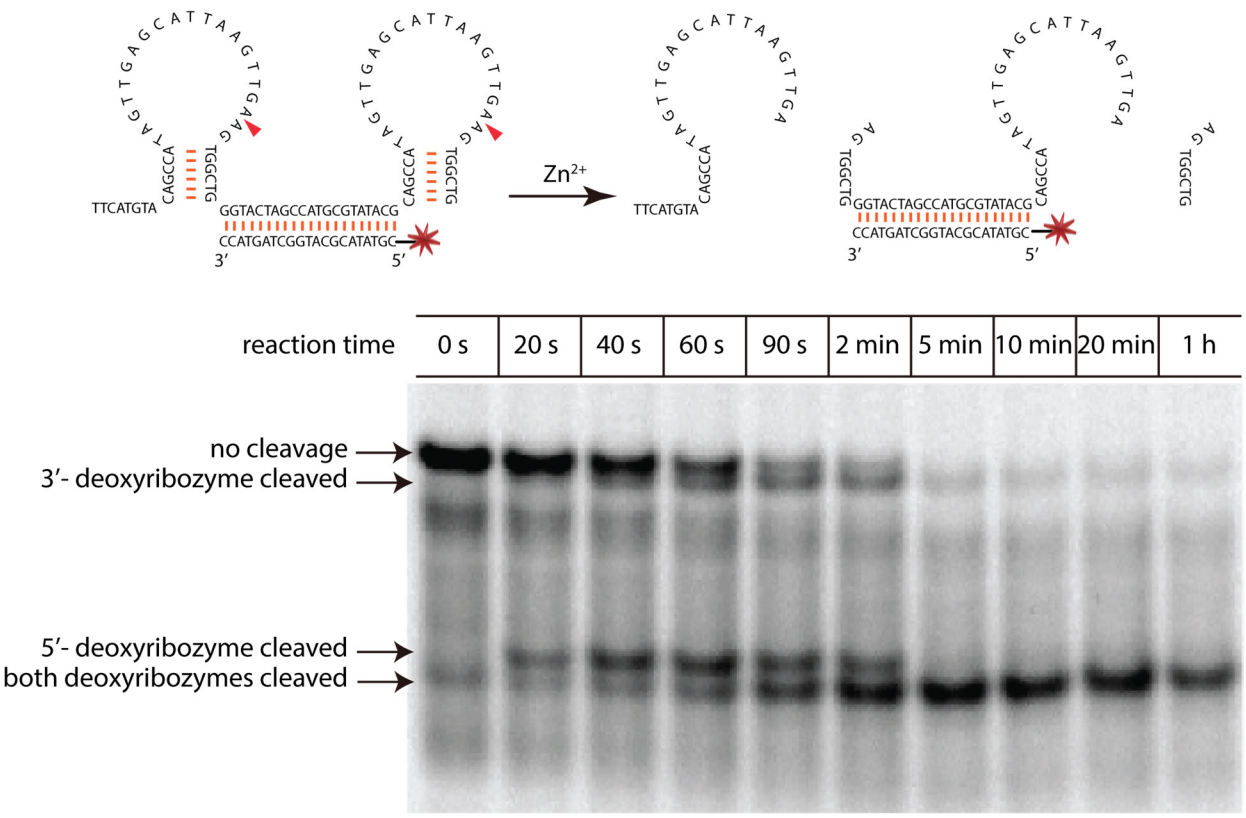

Figure S22. AGE characterization of deoxyribozyme self-cleavage under different tensions. Top and middle sets: same gel imaged in Cy5 and EtBr channels respectively. Bottom set: false-color composite of the Cy5 (red channel) and EtBr (green channel) sets. In each set, three strips from top to bottom contain 2pN, 6pN and 12pN force clamp origami structures, respectively. Each lane shows different cleavage time points.

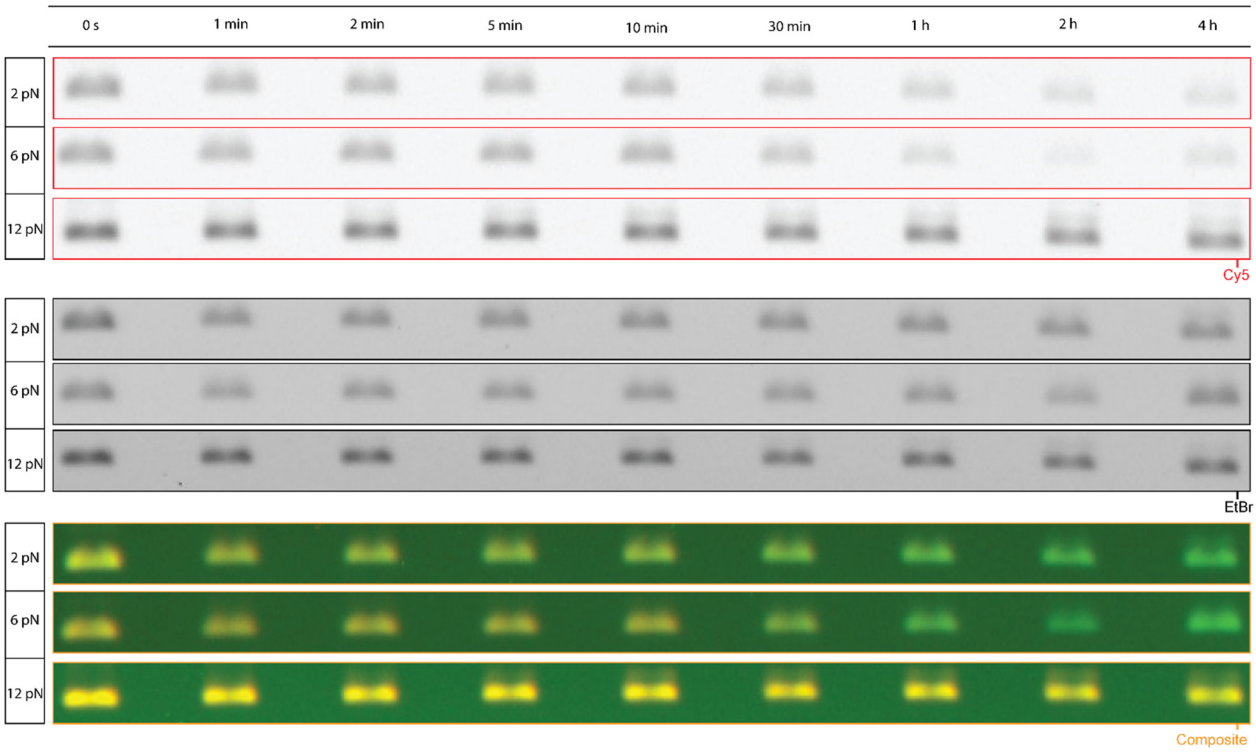

Figure S23. Electron micrographs of force clamp structures containing deoxyribozymes. Top row: before cleavage. Bottom row: after cleavage. Scale bar: main images 100 nm; insets (red boxes) 50 nm.

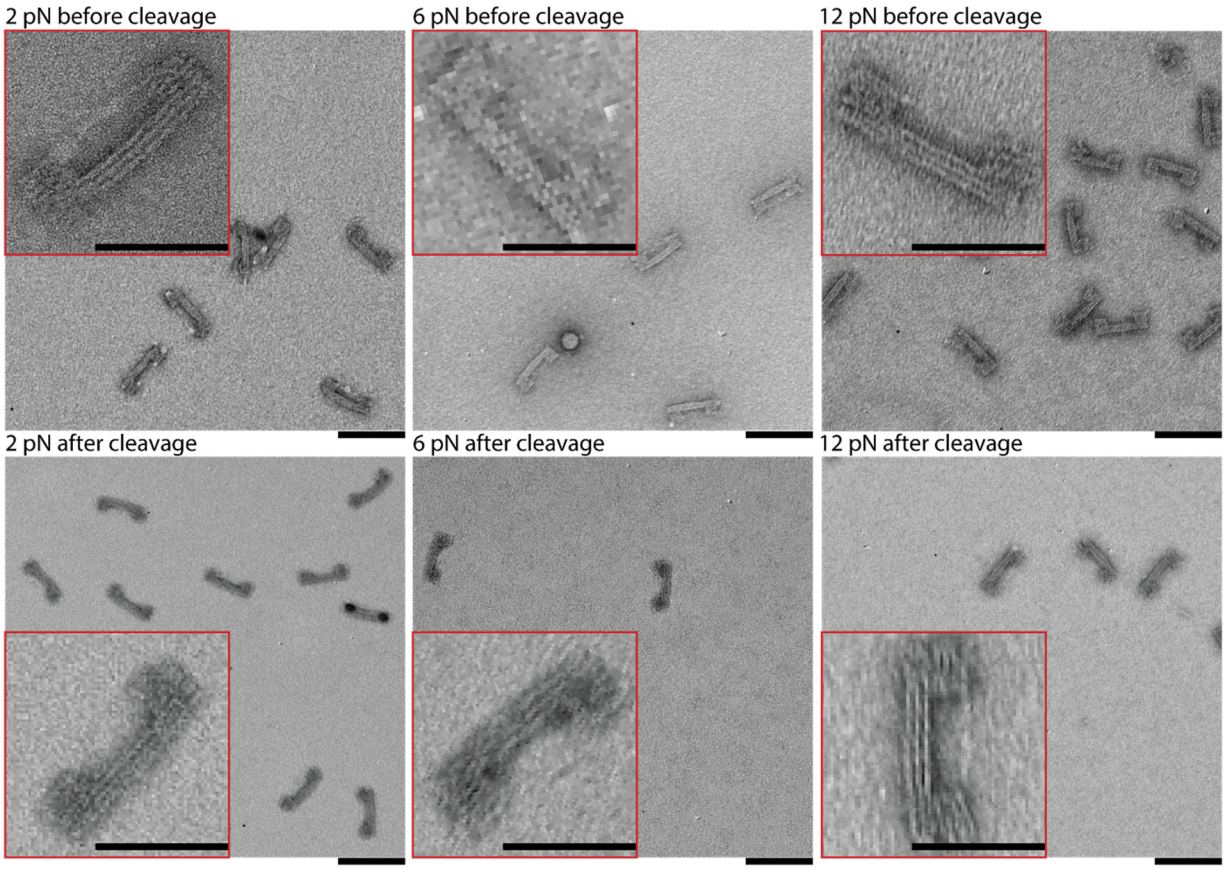

Figure S24. CaDNAno design of the semicircle. Green: core staples. Red: staples with handles (unutilized in this study).

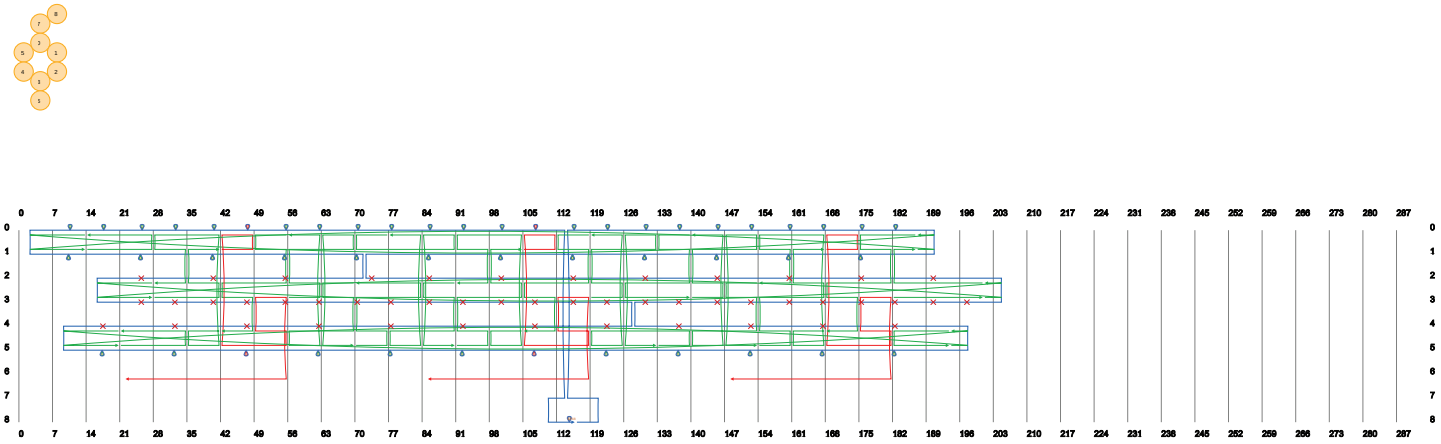

Figure S25. More electron micrographs showing gel-purified semicircles.

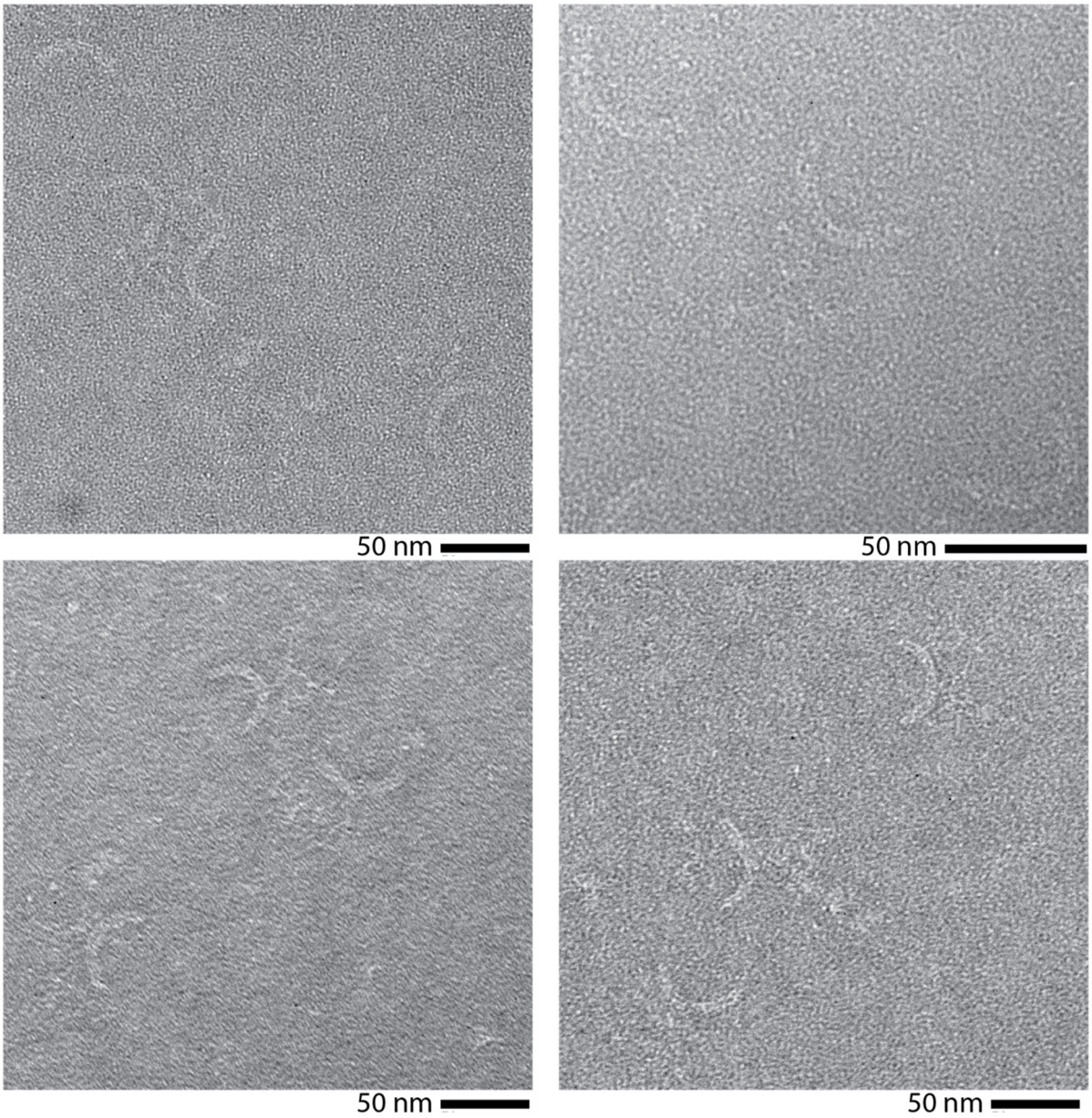

Figure S26. More electron micrographs showing semicircles, gel-purified after 30 min of Cas12a digestion.

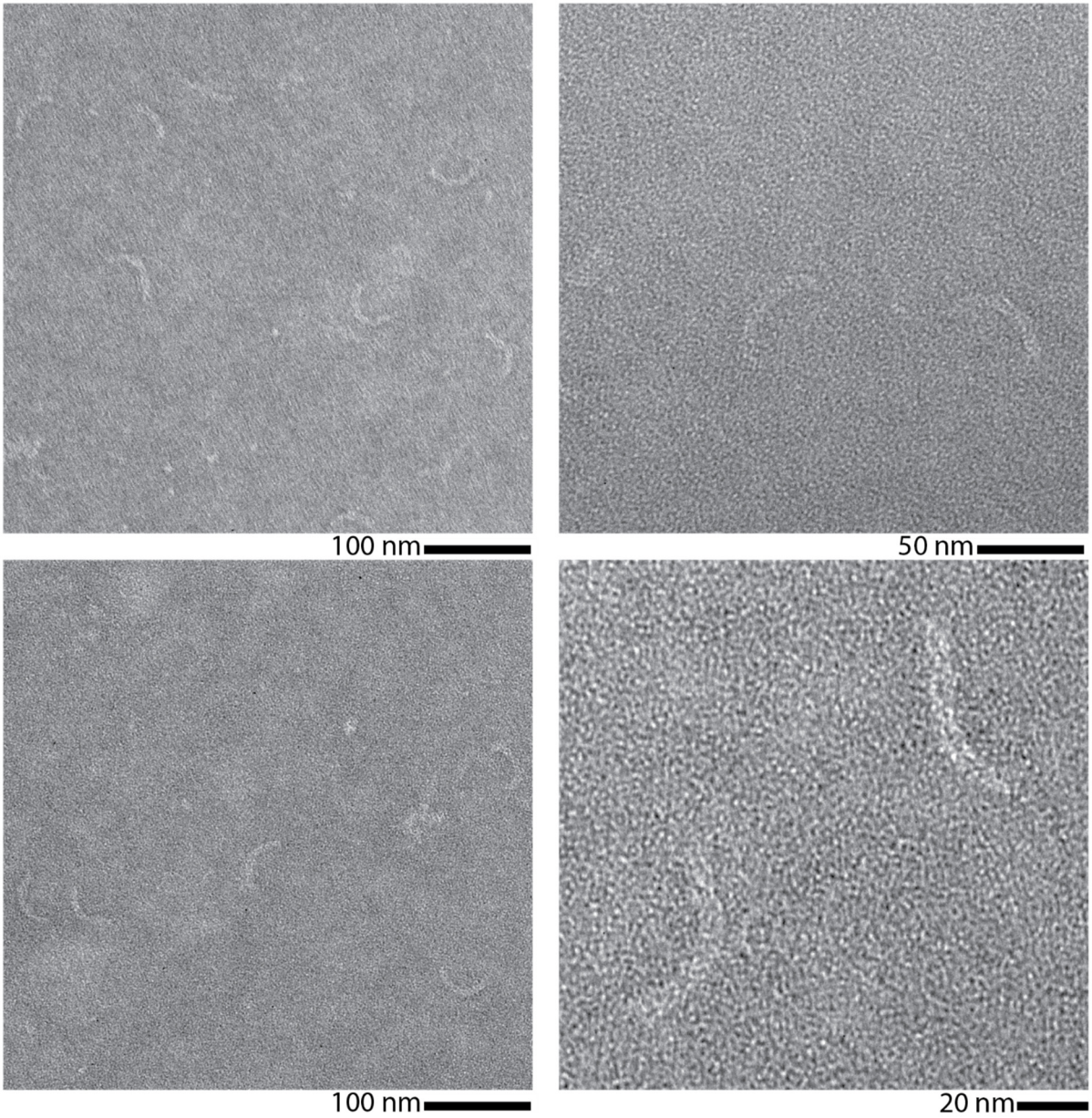

Figure S27. CaDNAno design of the circle with eight handle extensions. Green: core staples. Red: staples with handles (not drawn) extending out from Helix 0.

Corresponding anti-handle sequence to the handle extensions: 5'-TAGATGGAGTGTGGTGTGAAG/Cy5/-3'

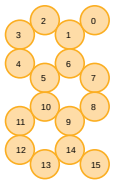

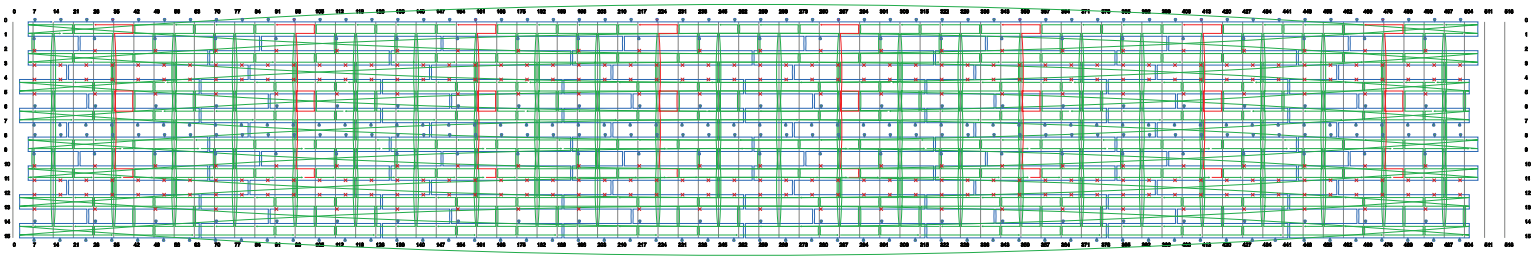

Figure S28. Electron micrographs showing gel-purified circles with ssDNA handles hybridized with Cy5-labeled anti-handles.

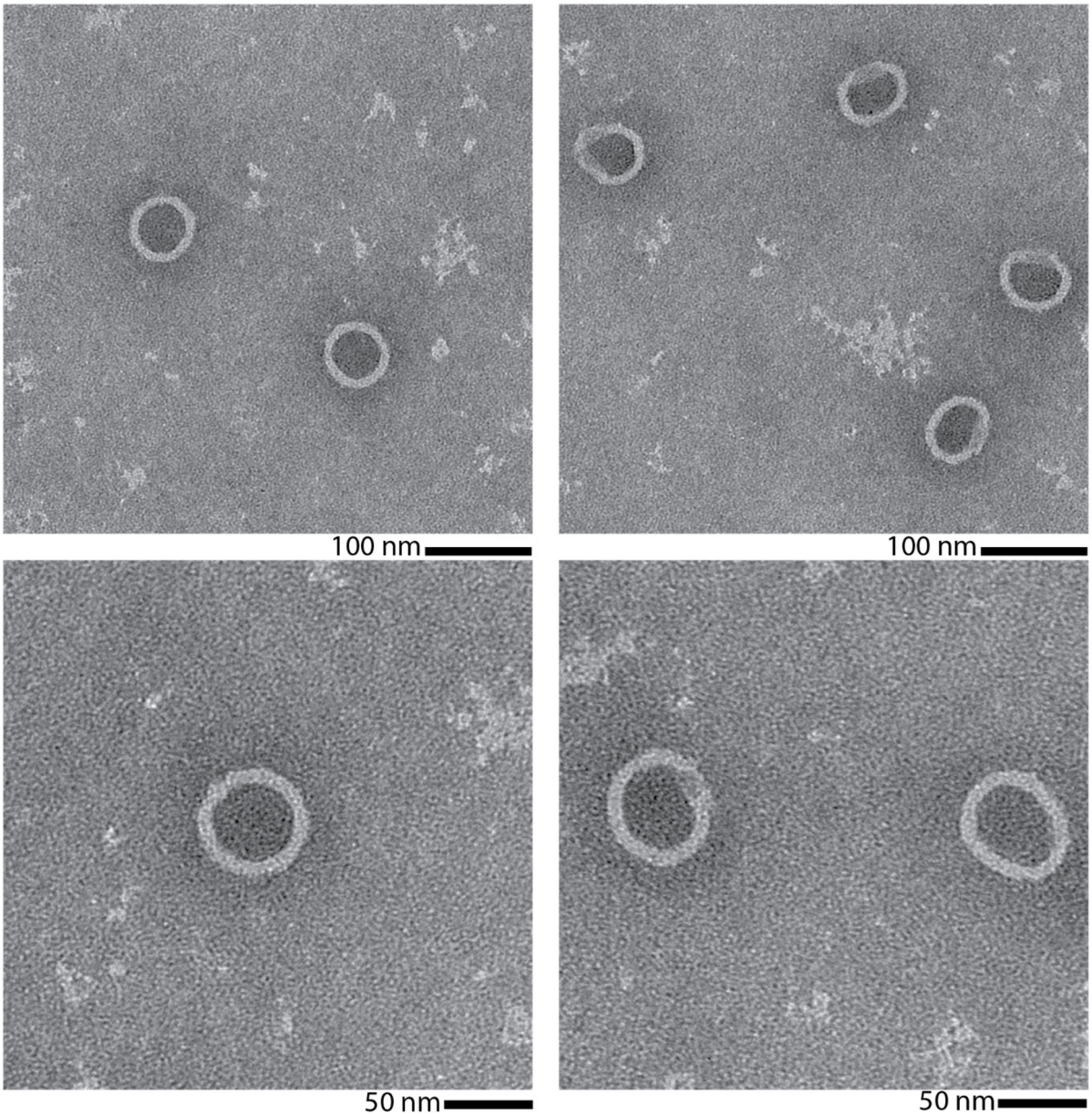

Figure S29. More electron micrographs showing circles with handles that were first hybridized with Cy5-labeled anti-handles and then treated with Cas12a for 30 min. The sample was then gel-purified before viewing under TEM.

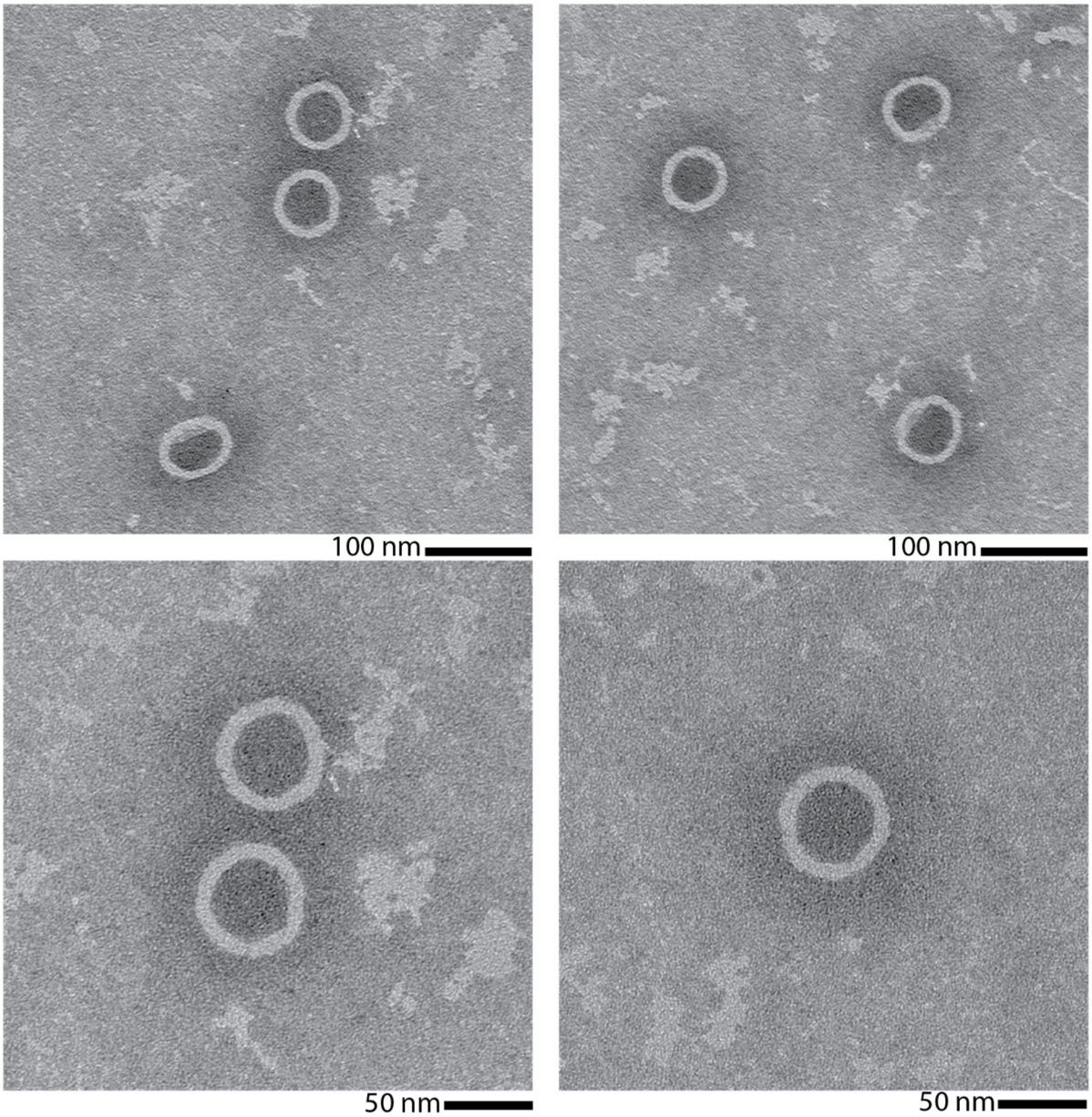

Figure S30. More electron micrographs showing circles. Circles were first treated with Cas12a for 30 min and then gel-purified. Subsequently, the processed circles were incubated with Cy5-labeled anti-handles and gel-purified again before viewing under TEM.

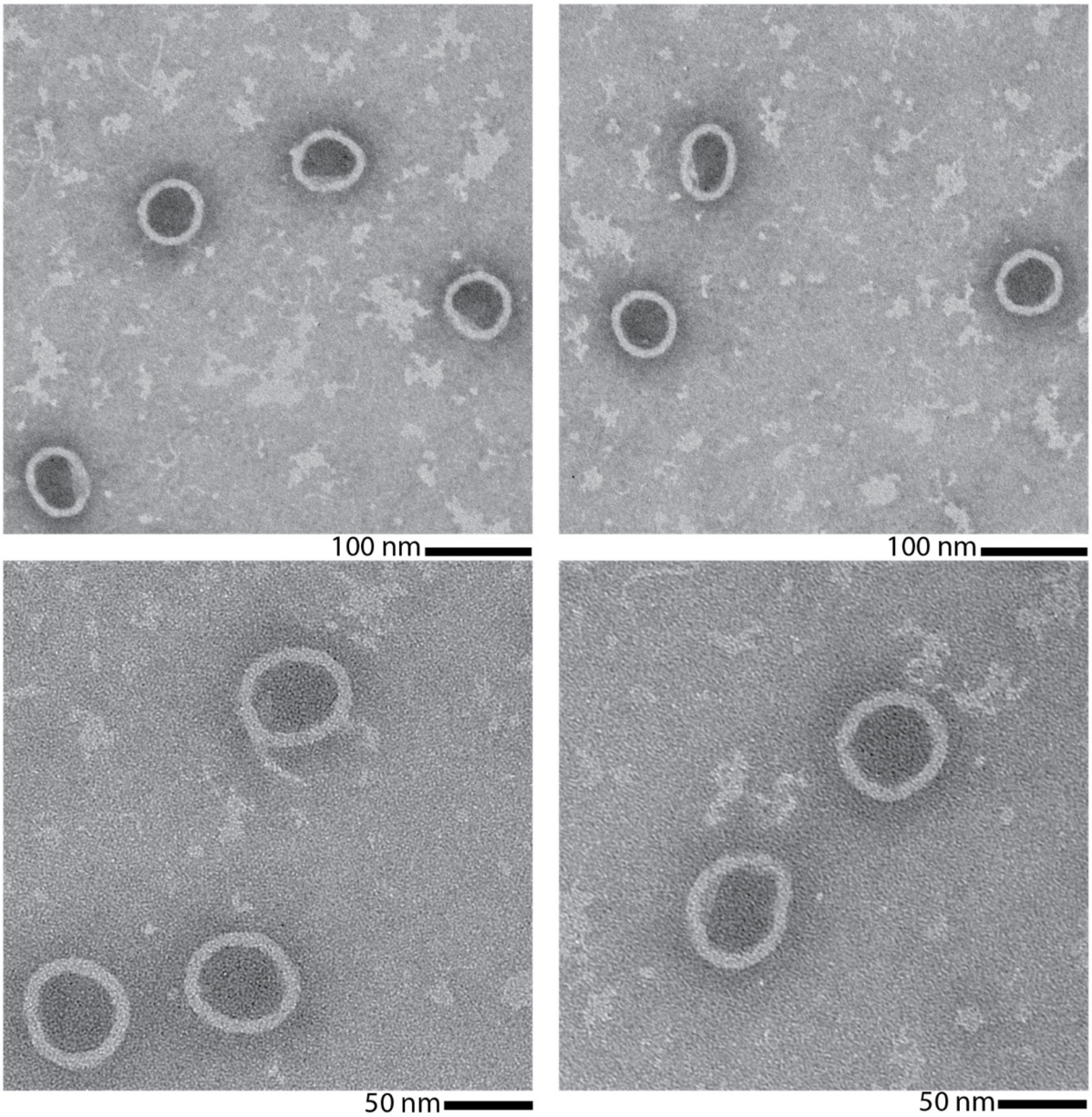

Figure S31. CaDNAno design of the rod thread through three circles. Red: core staples of the rod. Yellow: terminal rod staples with TTTT ends. Orange, green, magenta: core staples of the different circles. Maroon: complementary ssDNA strands to the scaffold tethers between the macrocycle and the shaft. Staple extensions on termini of rod each consists of four thymines to prevent stacking interactions.

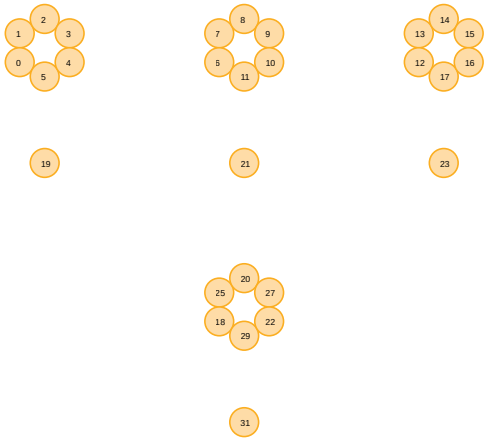

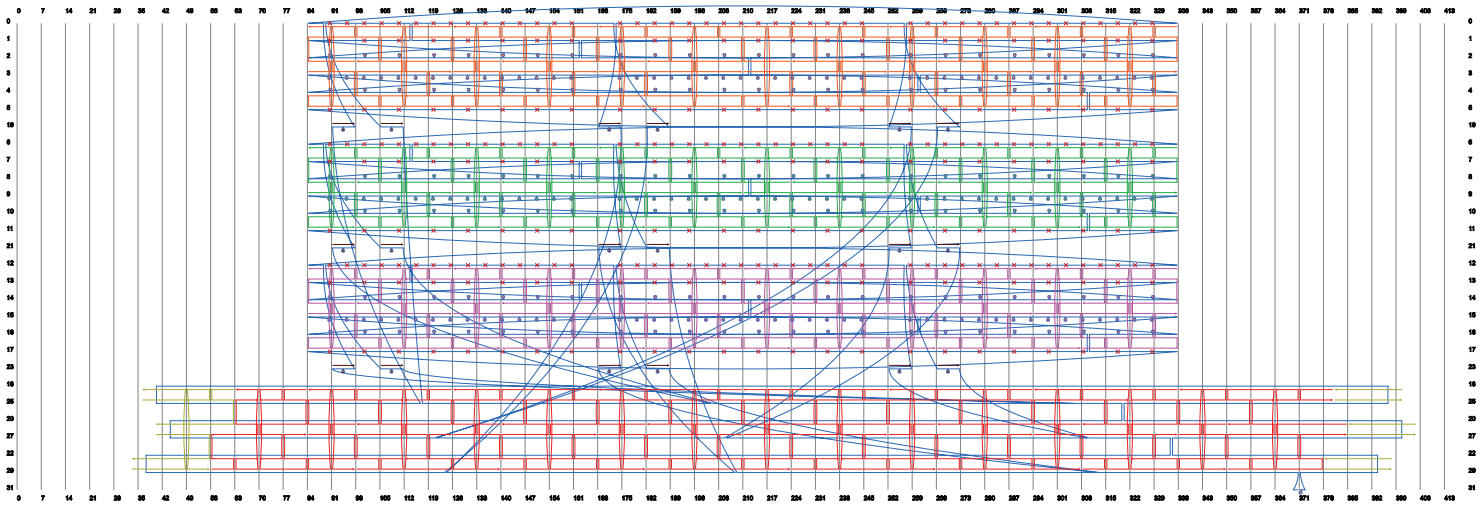

Figure S32. More electron micrographs of gel-purified three-circles-on-a-rod structures.

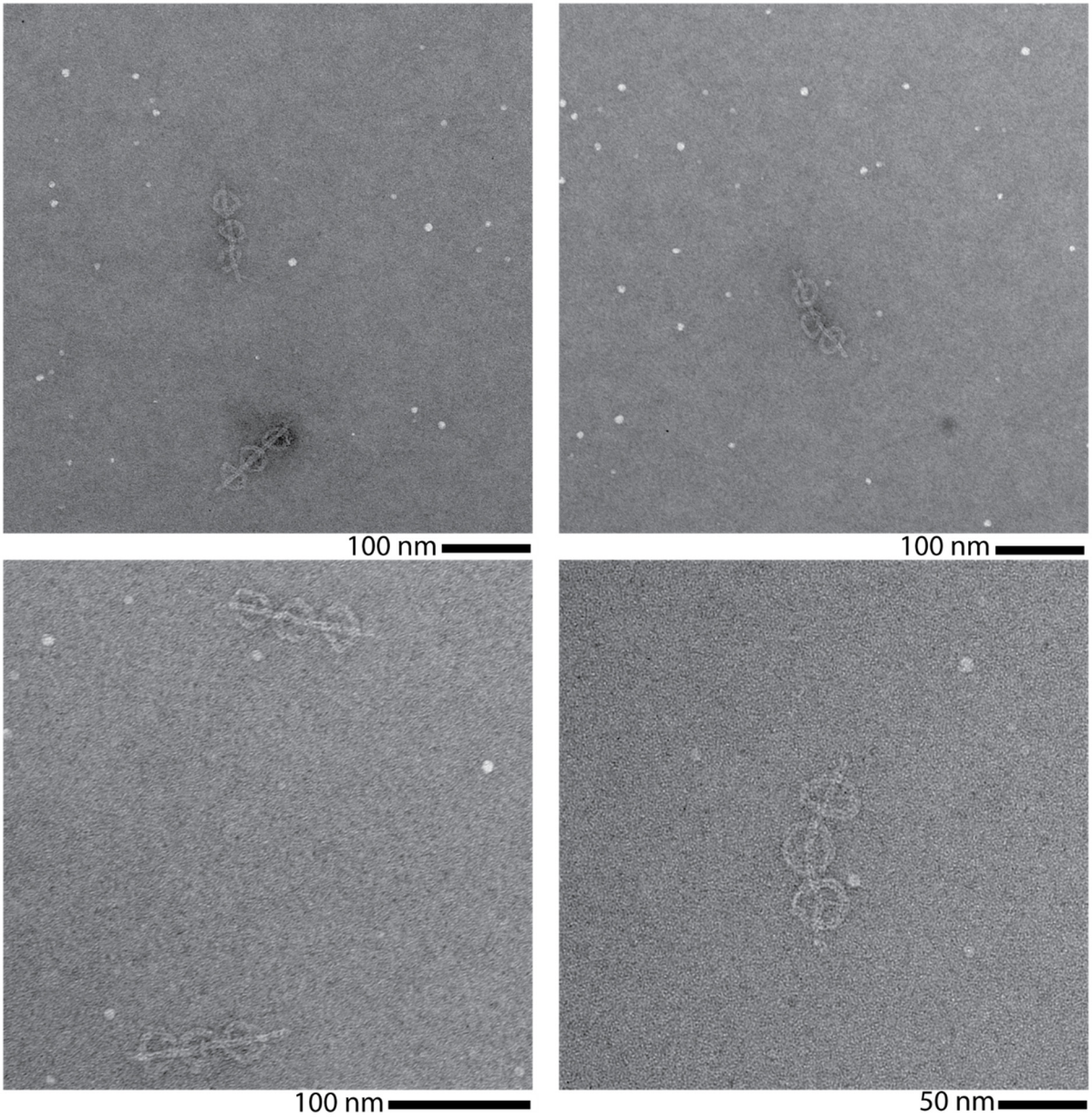

Figure S33. More electron micrographs showing three-circles-on-a-rod structures, gel-purified after 4 hours of Cas12a treatment. Scaffold tethers were not protected *via* pre-hybridization.

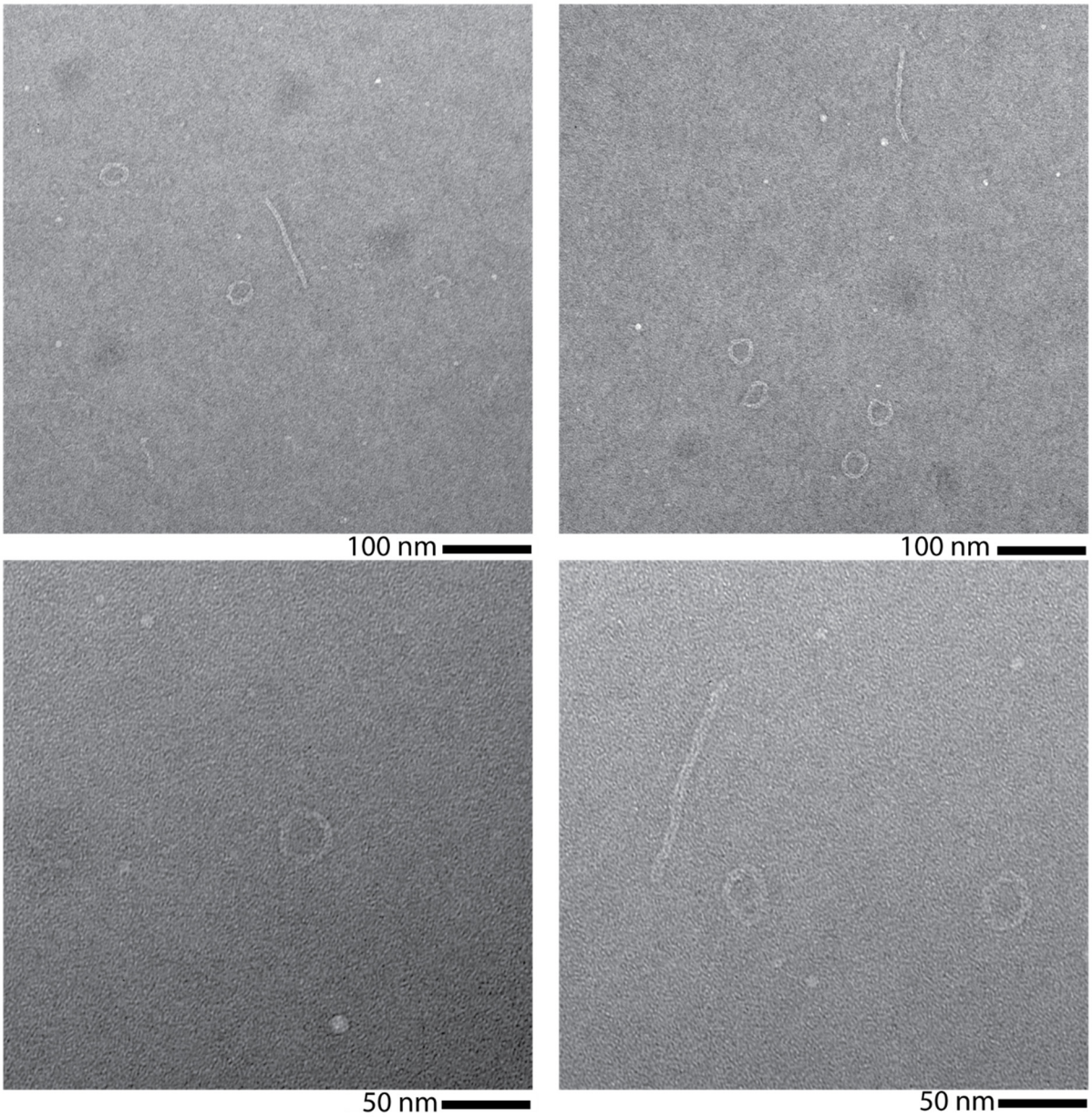

Figure S34. More electron micrographs showing three-circles-on-a-rod structures, gel-purified after 4 hours of Cas12a treatment. All scaffolds tethers were protected *via* pre-hybridization with complementary ssDNA.

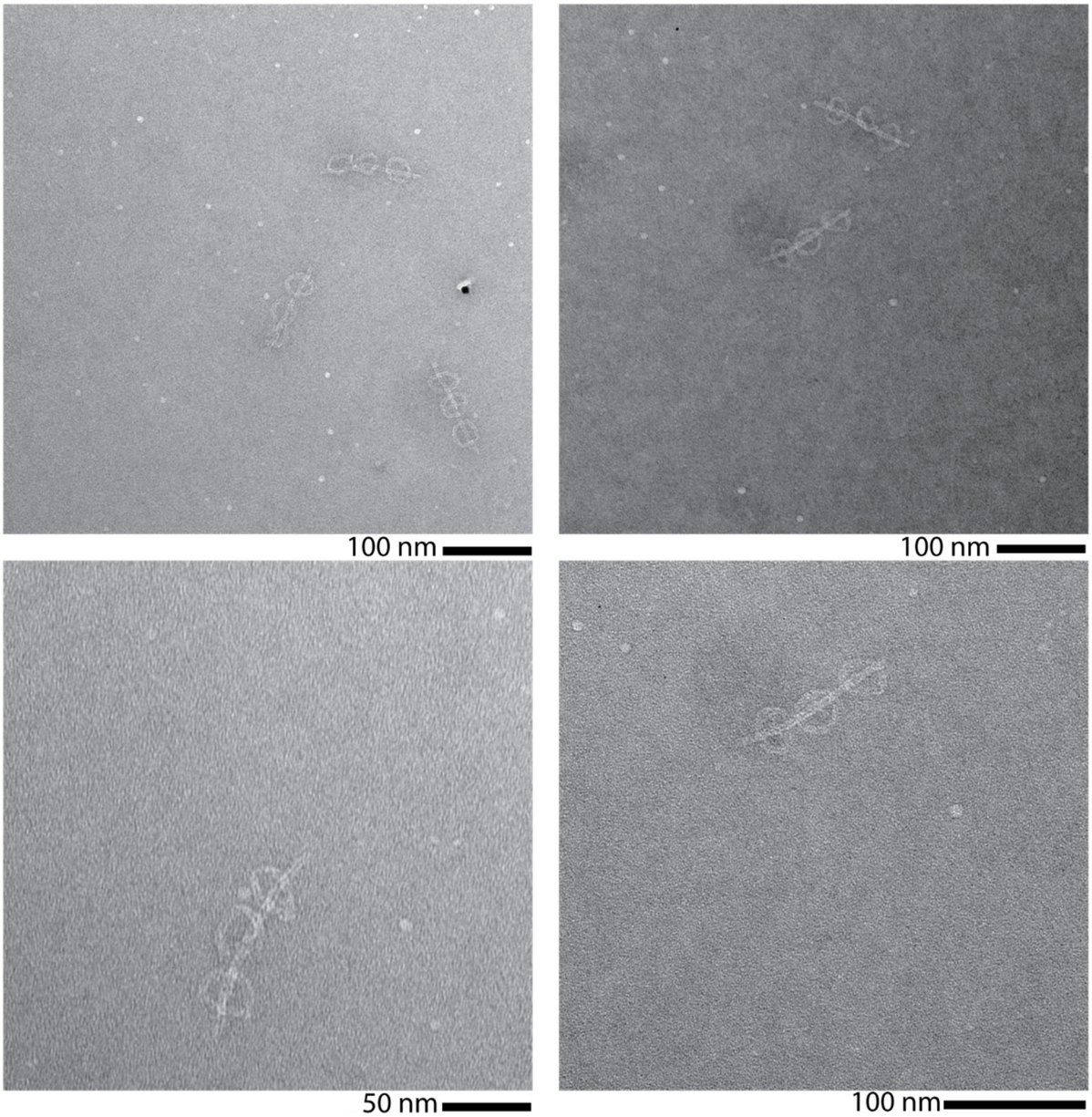

Figure S35. More electron micrographs showing three-circles-on-a-rod structures, gel-purified after 4 hours of treatment by Cas12a. All scaffolds tethers, except those joining the right terminal circle (see **Figure 2c**) to the rod, were protected *via* pre-hybridization with complementary ssDNA, resulting in a rod threading through only two circles after digestion.

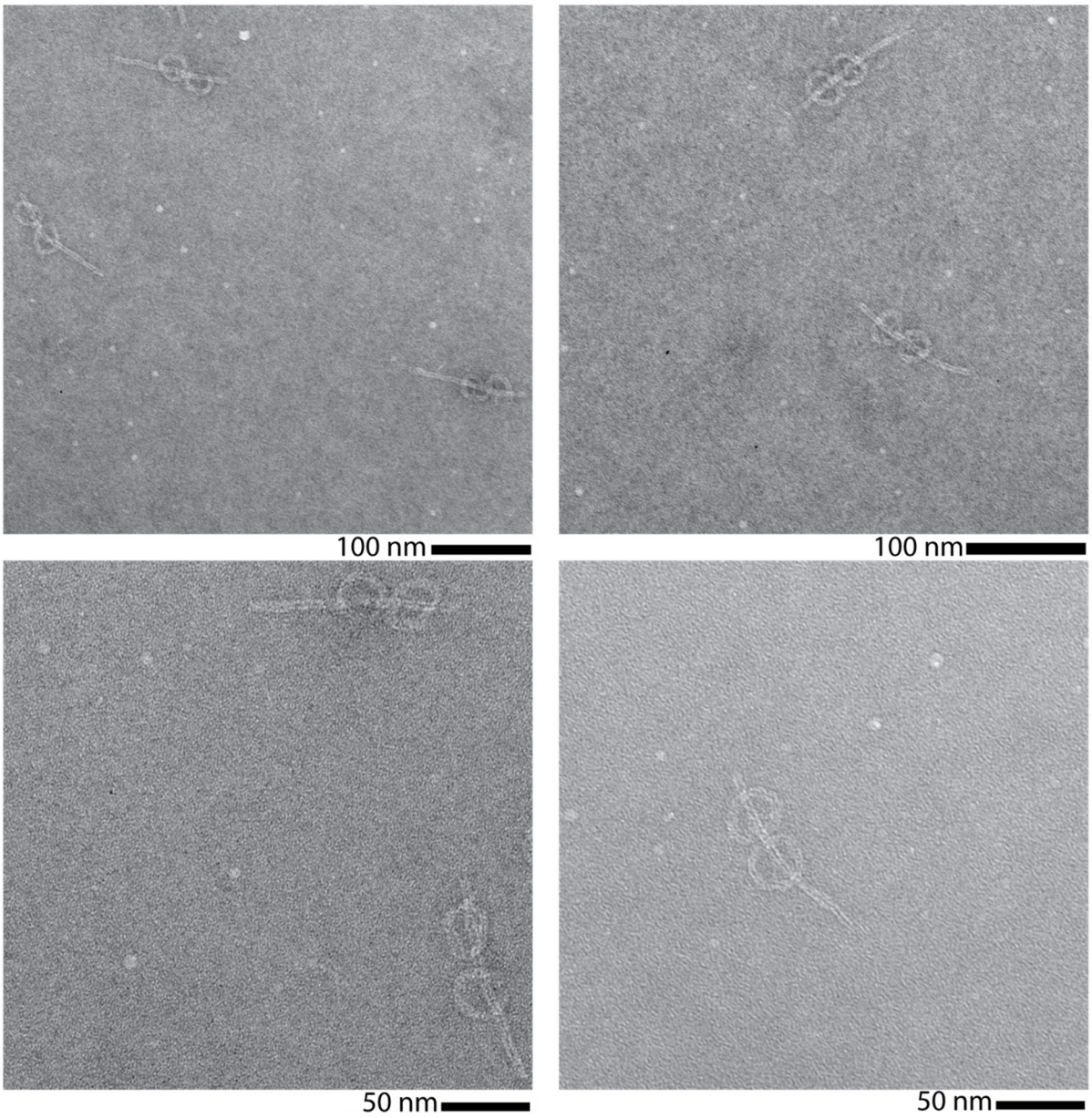

Figure S36. More electron micrographs showing three-circles-on-a-rod structures, gel-purified after 4 hours of Cas12a treatment. All scaffolds tethers, except those joining the middle circle to the rod, were protected *via* pre-hybridization with complementary ssDNA, resulting in a rotaxane after digestion.

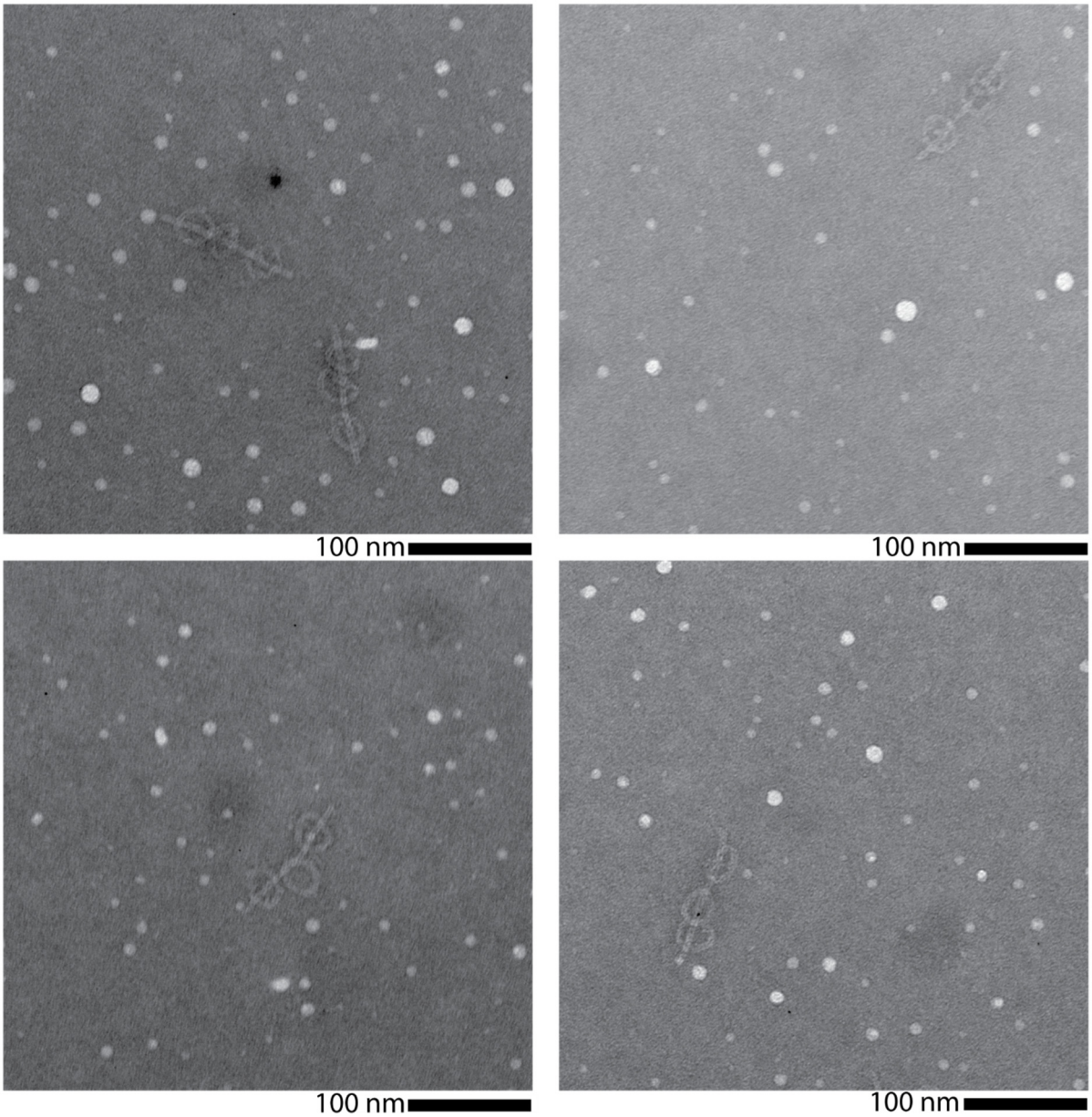

Figure S37. CaDNAno design of the rotaxane. Yellow: core staples of the dumbbell. Green: core staples of the macrocycle. Maroon: complementary ssDNA strands to the scaffold tethers between the macrocycle and the shaft. Staple extensions on termini of dumbbell each consists of four thymines to prevent stacking interactions.

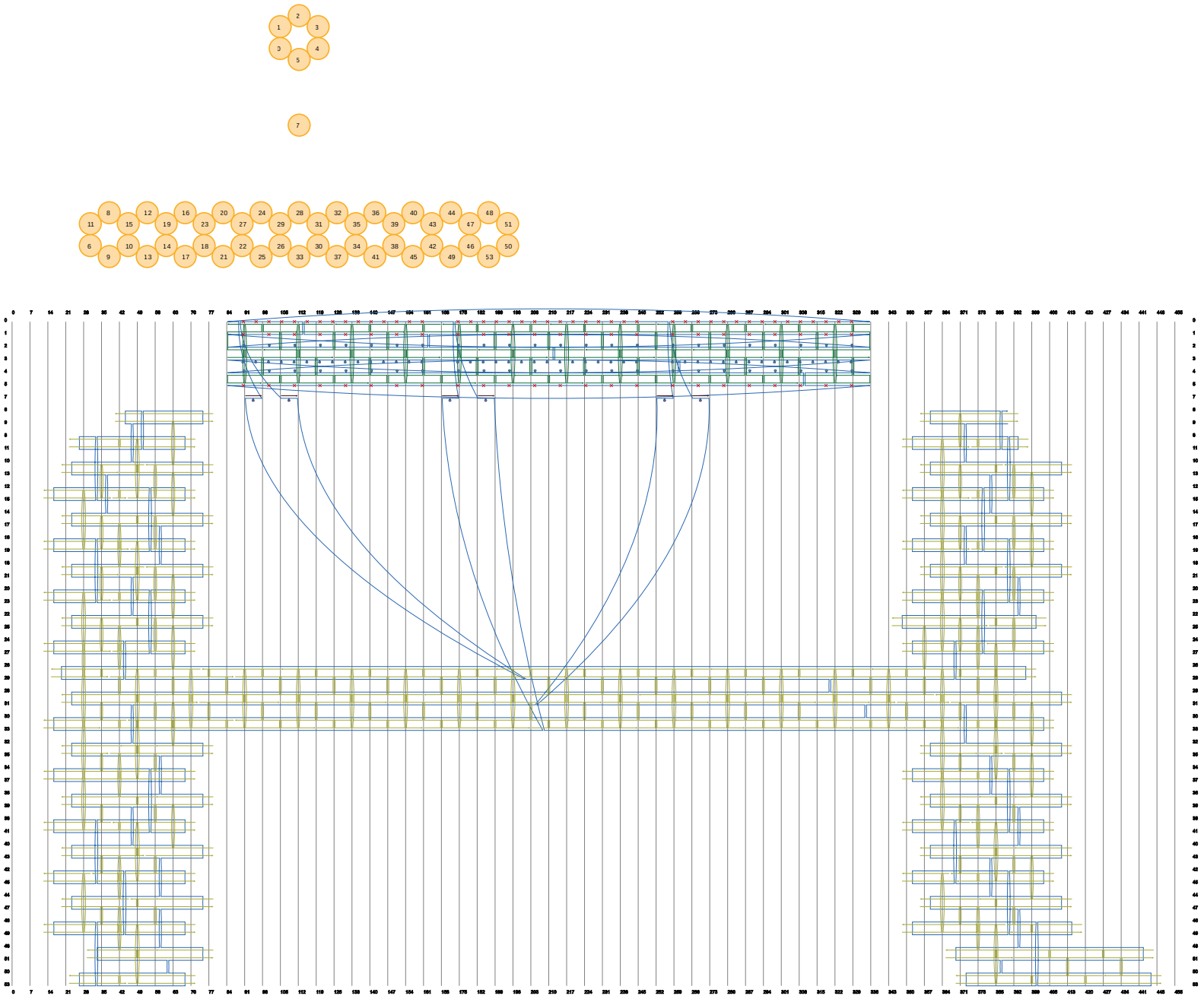

Figure S38. AGE characterizations of the pseudo-rotaxane origami structure after Cas12a treatment. a): trial 1, b): trial 2, and c): trial 3. Average band intensities across trials were used to estimate the yield of stopper-bearing shafts (dumbbells) retaining macrocycles. After normalizing for the different molecular weights of the structures, about 19.89±1.26% of the dumbbells retained macrocycles post Cas12a treatment (upper band in the right lane).

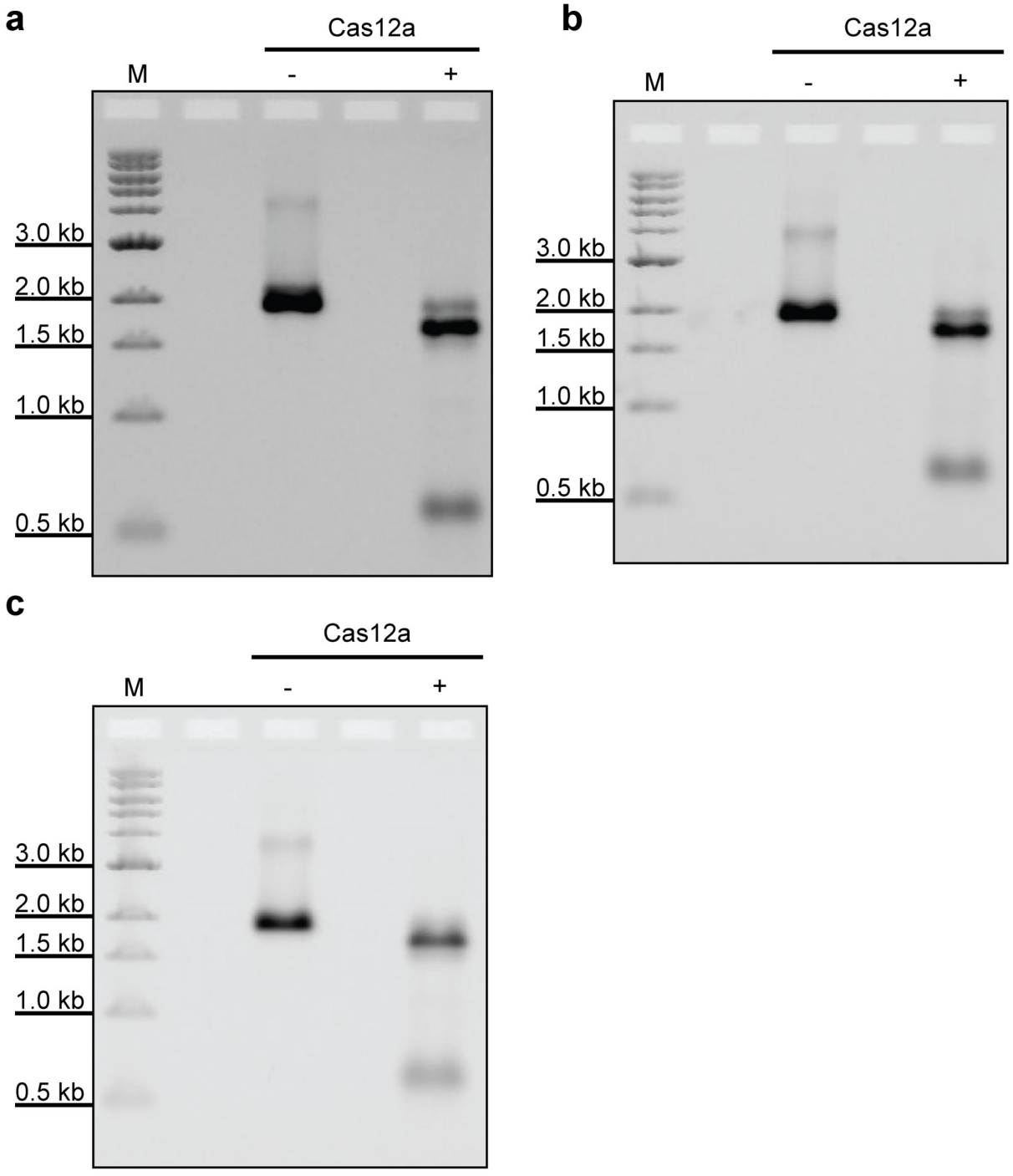

Figure S39. More electron micrographs showing the gel-purified asymmetric pseudo-rotaxane origami structure. Scale bar: 50 nm.

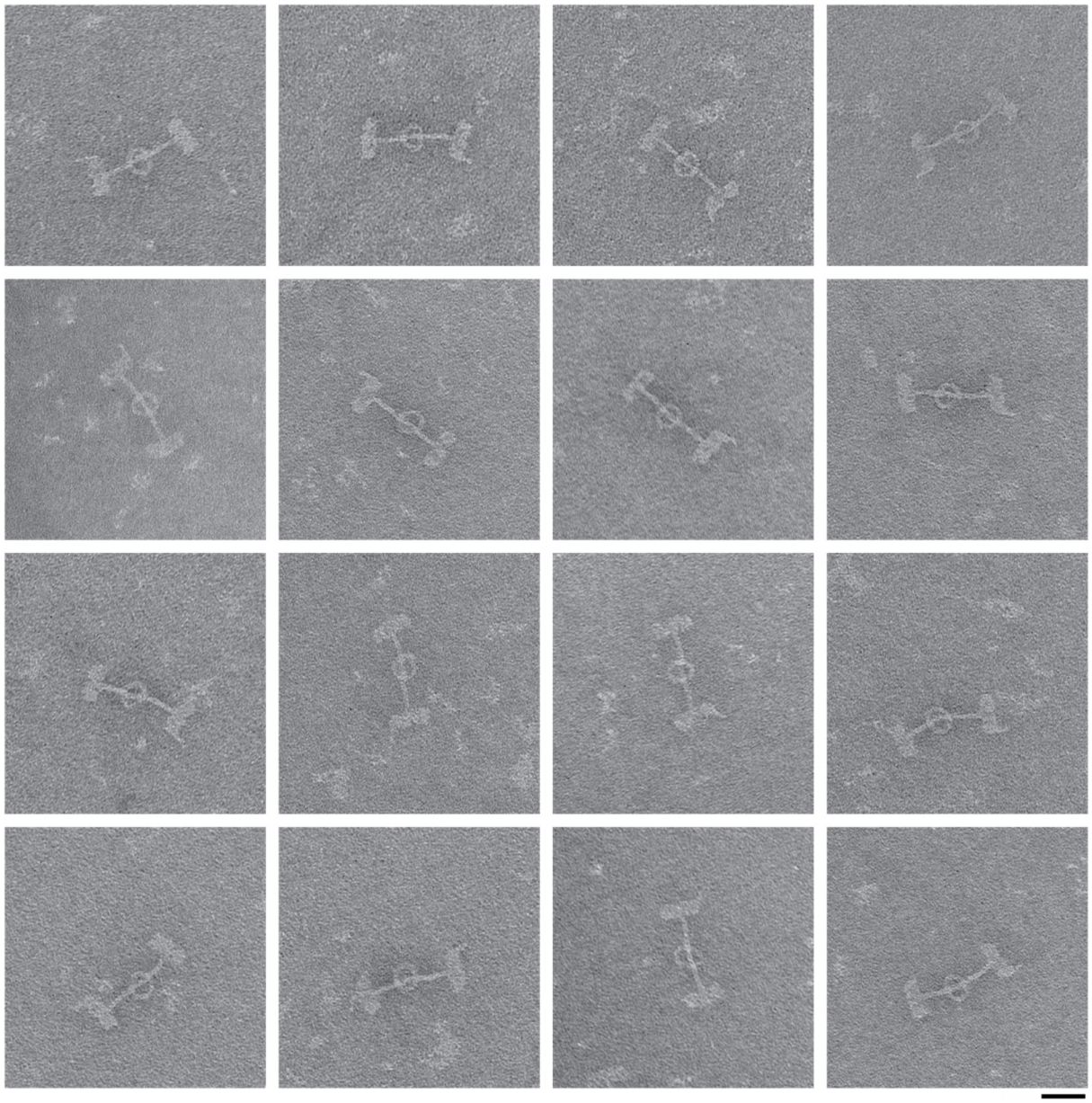

Figure S40. Demonstration of how the position of the macrocycle, ***p***, is determined in ImageJ. Distances are measured using the "Segmented Line" tool and ***p***, is given by distance (AB + AC)/2.

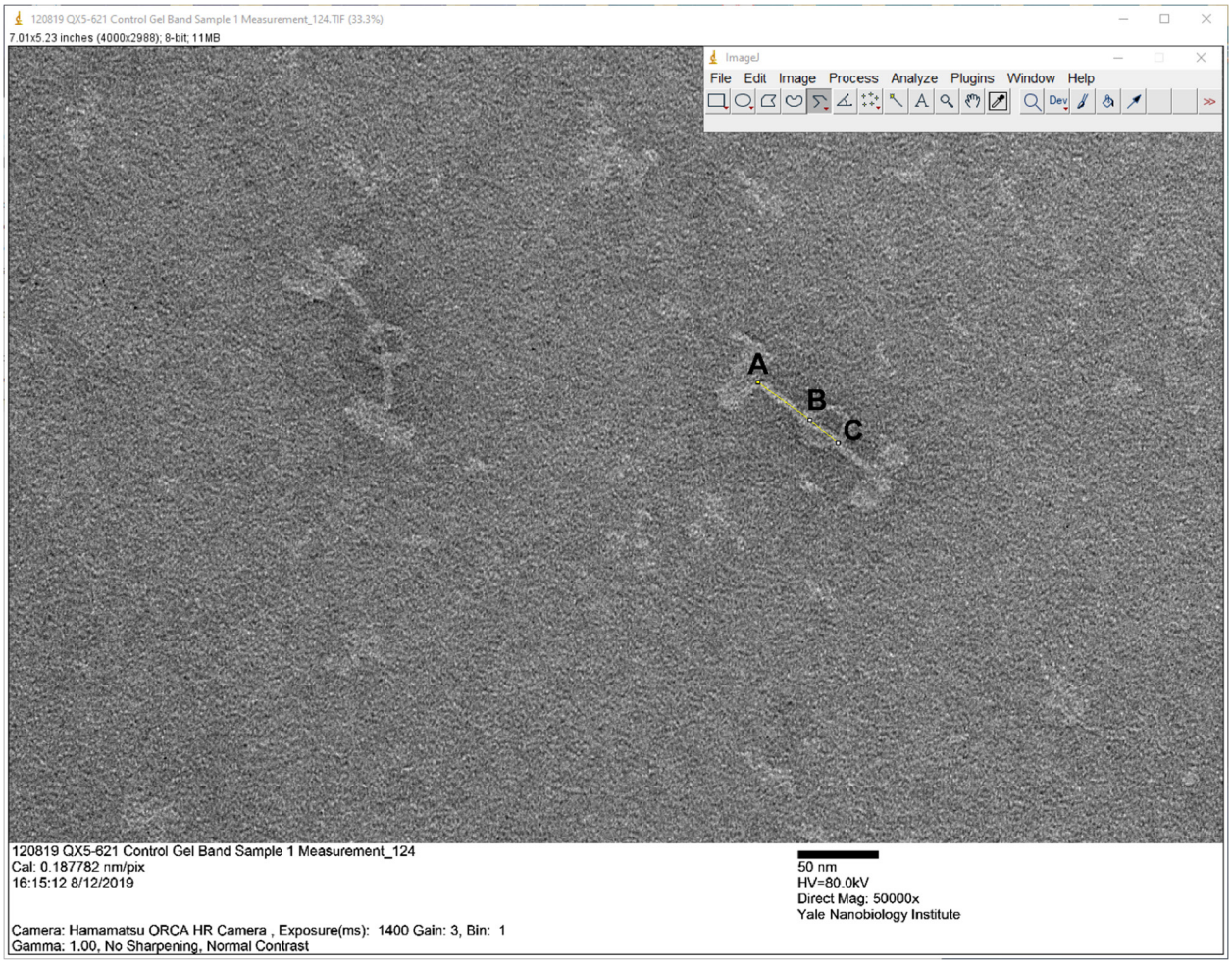

Figure S41. More electron micrographs showing the asymmetric rotaxane origami structures, gel-purified after 4 hours of Cas12a treatment. Scale bar: 50 nm.

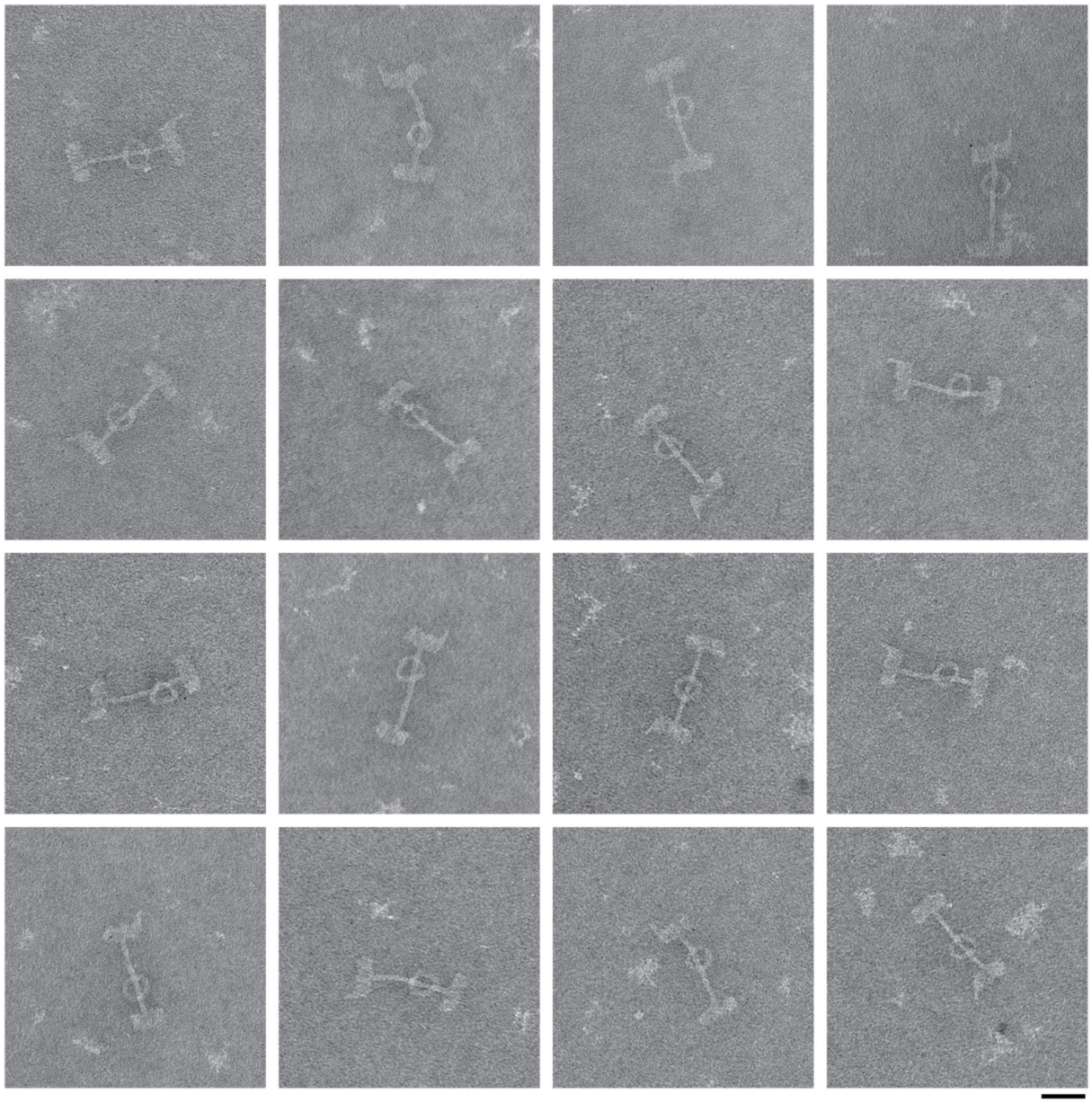

Figure S42. CaDNAno design of the elastic beam. The shorter ssDNA tethers joining the two arms are each stretched at 3.2 pN (Materials and Methods: Elastic Beam Bending Angle Prediction). Red and purple: core staples of the elastic beam. Green: additional staples used to fold the scaffold tethers between the two arms into a 6-helix bundle.

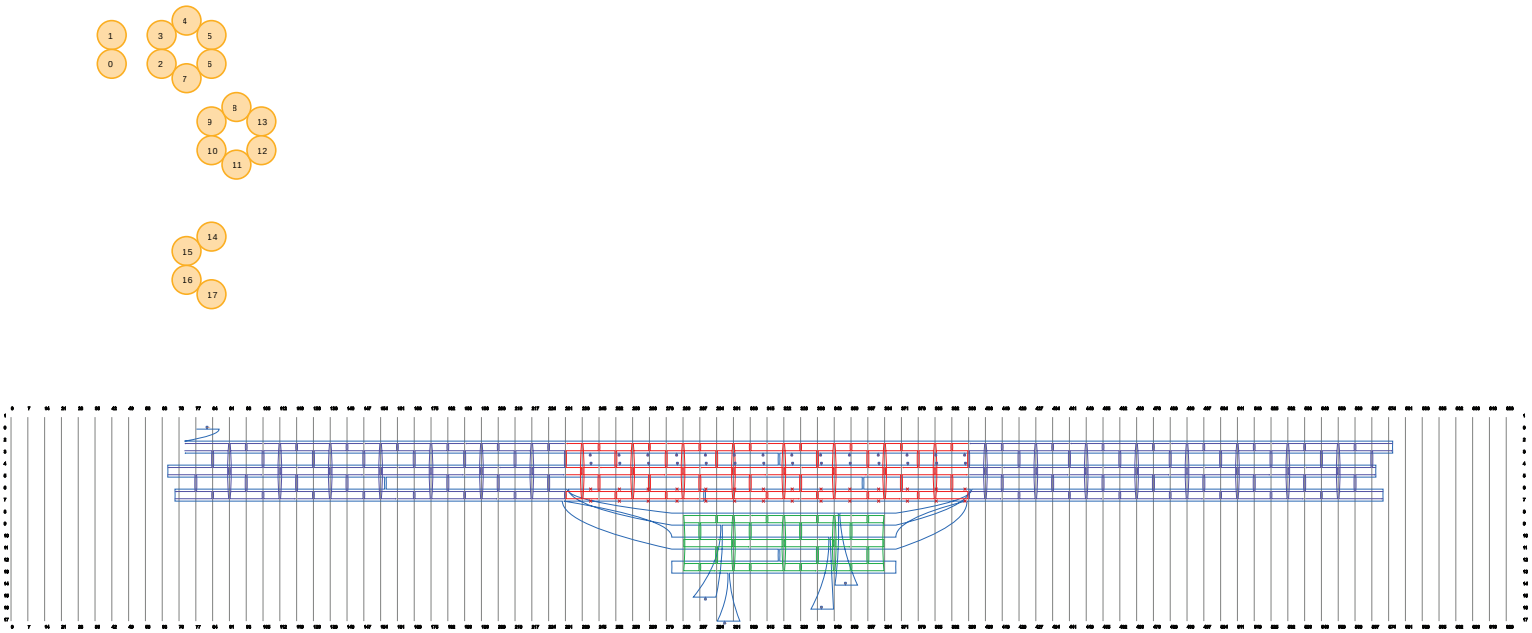

Figure S43. More electron micrographs showing the elastic beam structure. Samples shown were gel-purified. Scale bar: 100 nm.

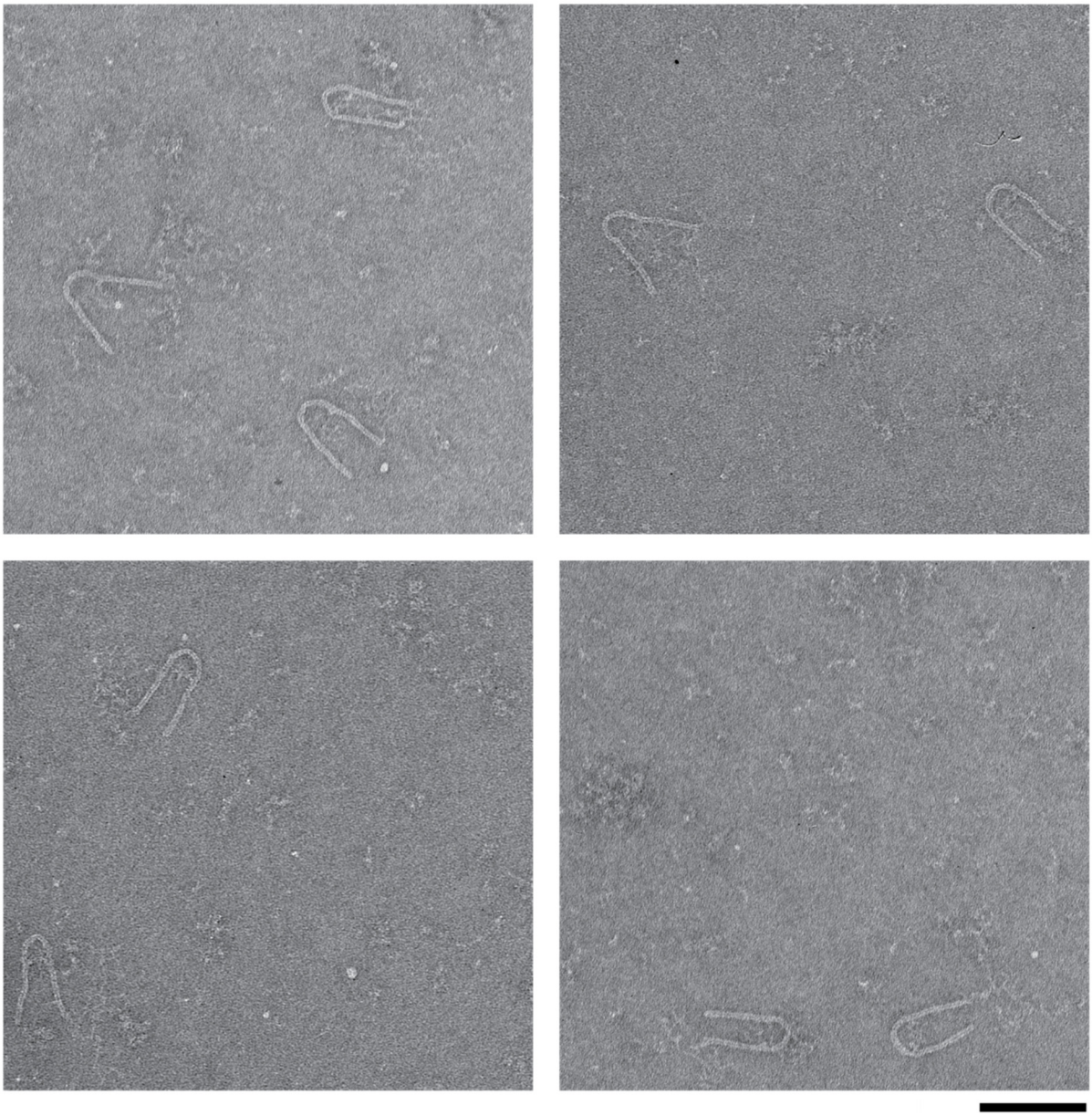

Figure S44. More electron micrographs showing the elastic beam structure. Samples shown were not gel-purified to eliminate the possible effects of purification on bending angles and used for angle quantification. Scale bar: 200 nm.

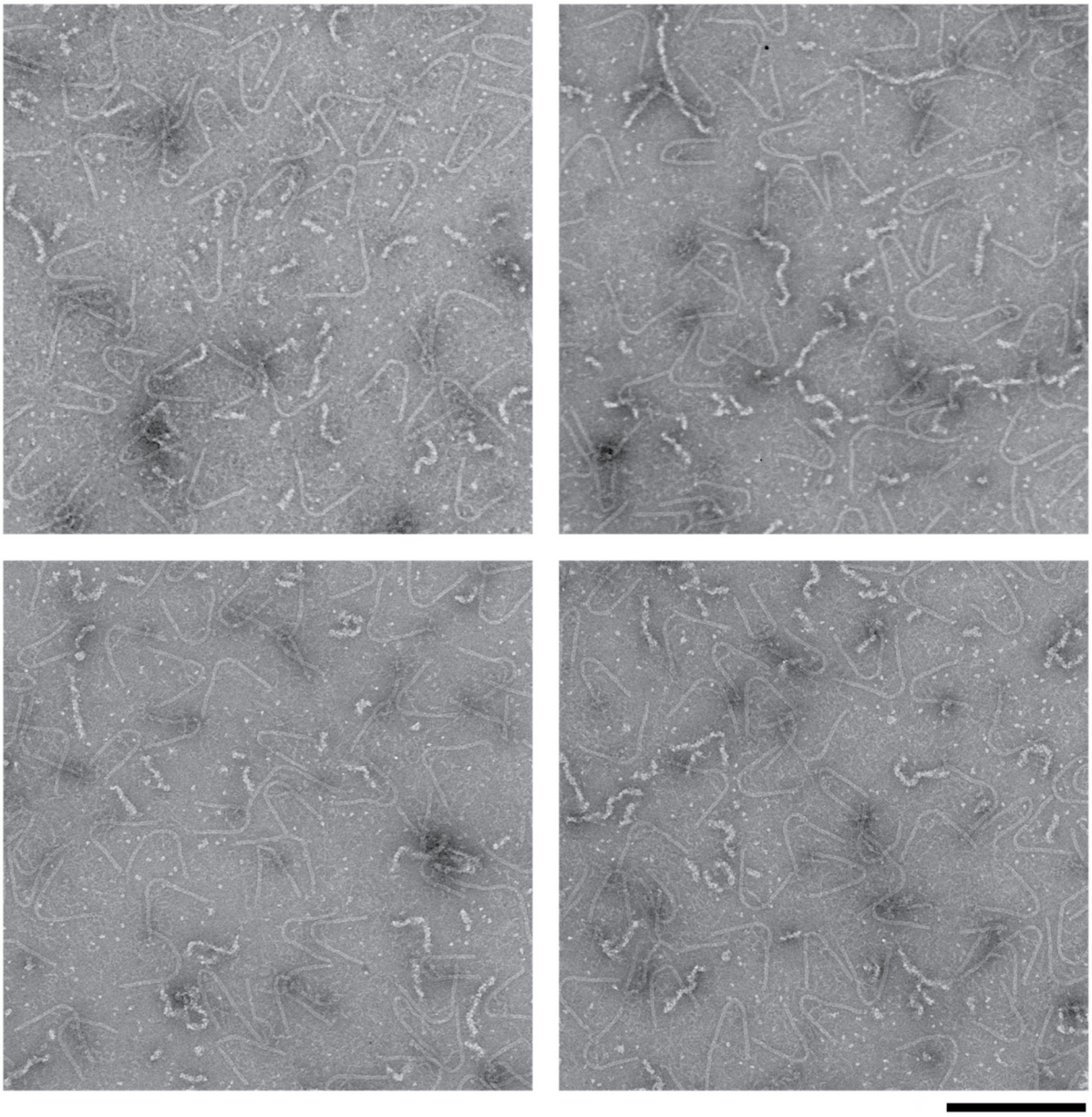

Figure S45. Demonstration of how the bending angles of the elastic beam, θ, is determined in ImageJ. The shapes of the elastic beams are traced using the "Angle" tool and added to the "ROI Manager". Angles of the traces, which should equal to 180°-θ, were then measured.

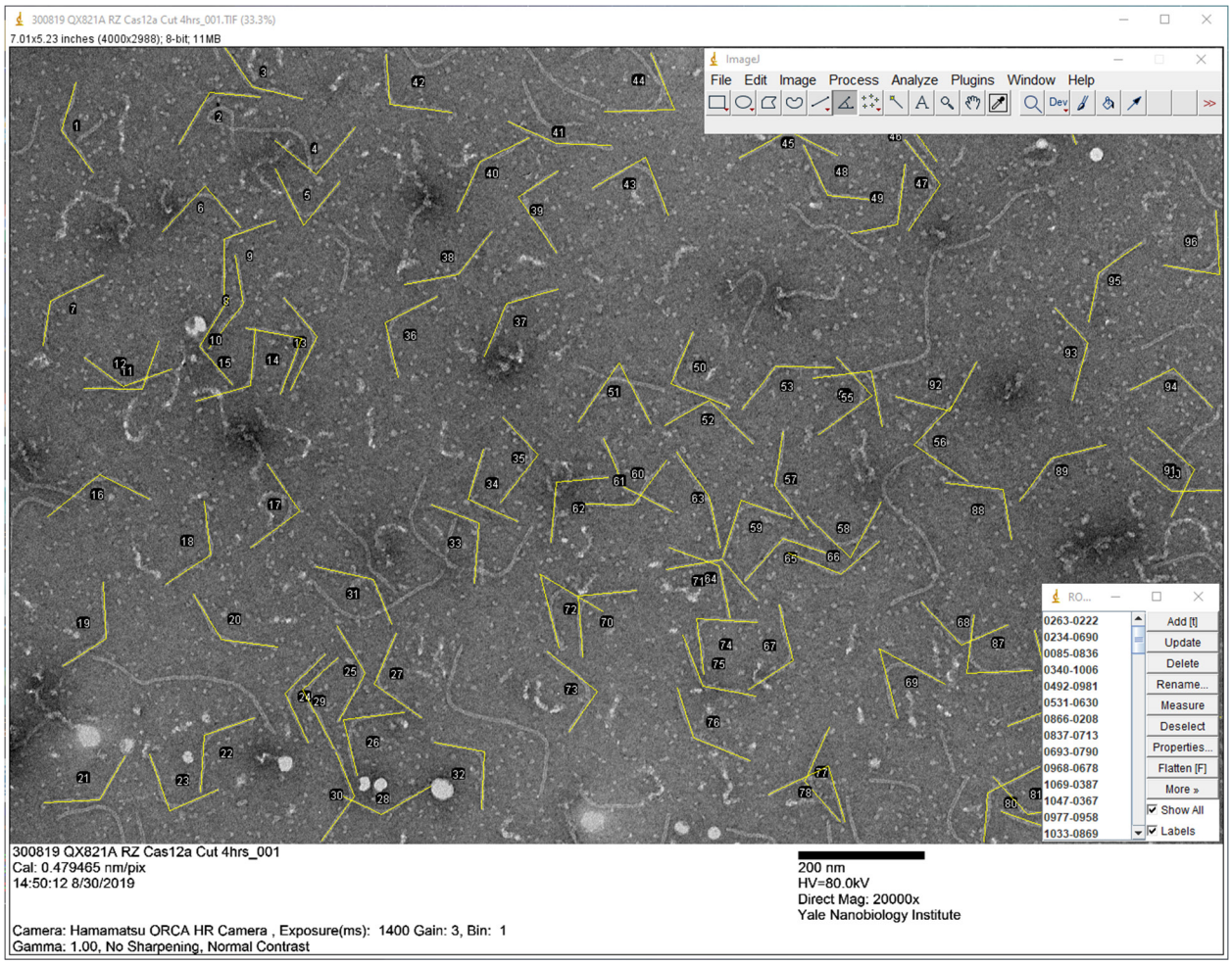

Figure S46. More electron micrographs showing the elastic beam structure after 4 hours of Cas12a digestion. Samples shown were gel-purified. Scale bar: 100 nm.

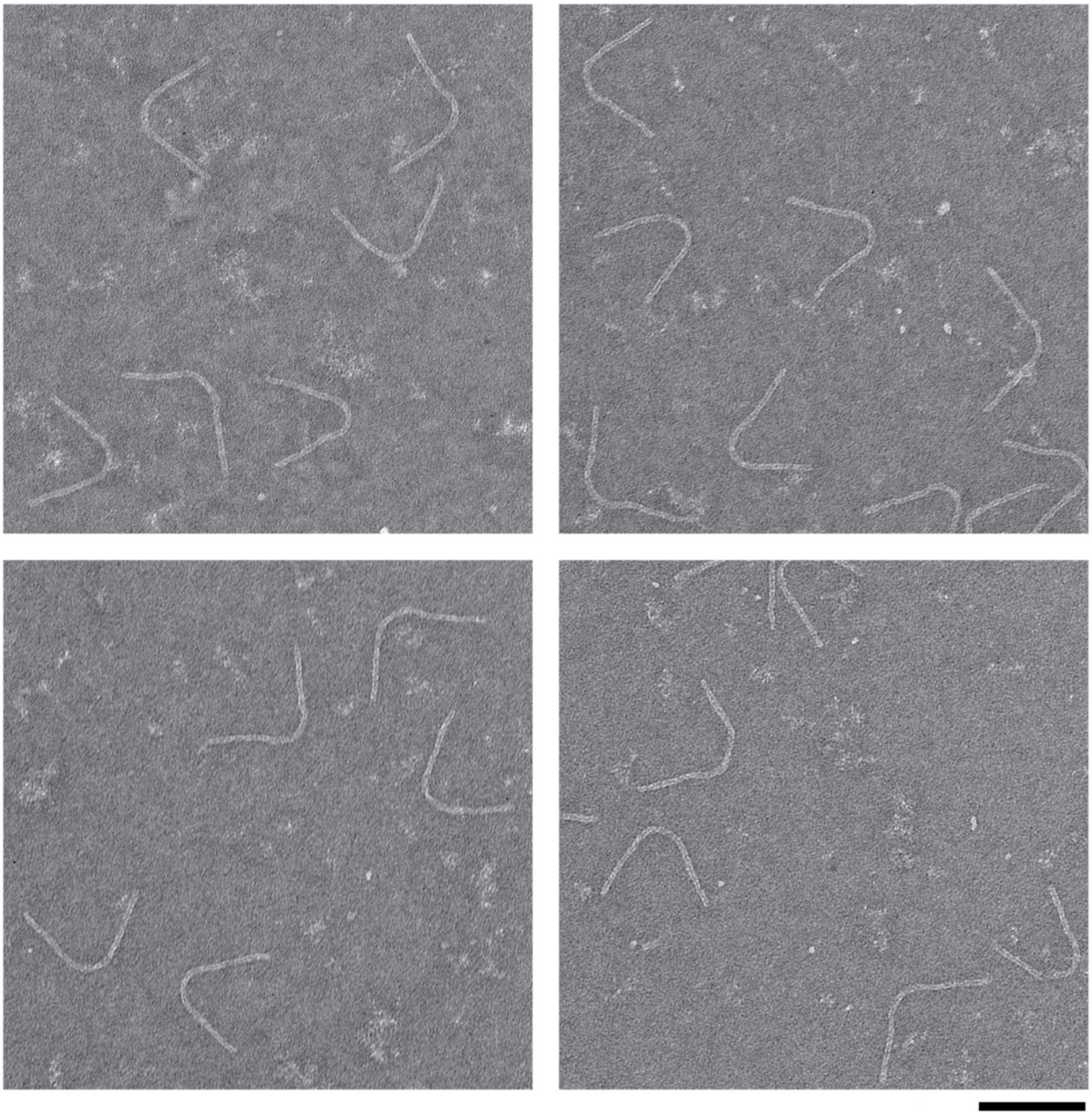

Figure S47. More electron micrographs showing the elastic beam structure after 4 hours of Cas12a digestion. Samples shown were not gel-purified to eliminate the possible effects of purification on bending angles and used for angle quantification. Scale bar: 200 nm.

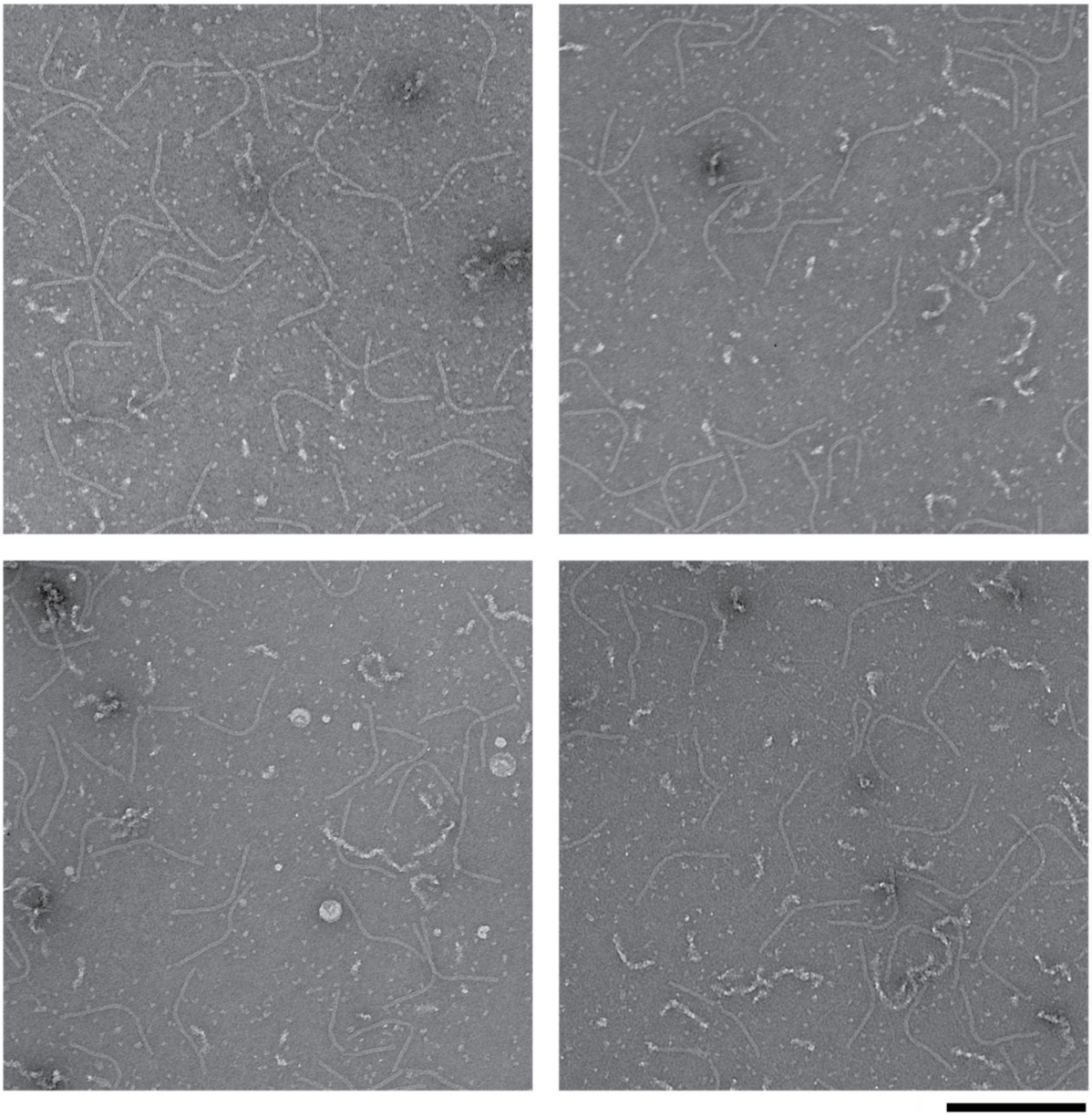

Figure S48. CaDNAno design of the elastic beam without middle scaffold tethers. Red and purple: core staples of the elastic beam.

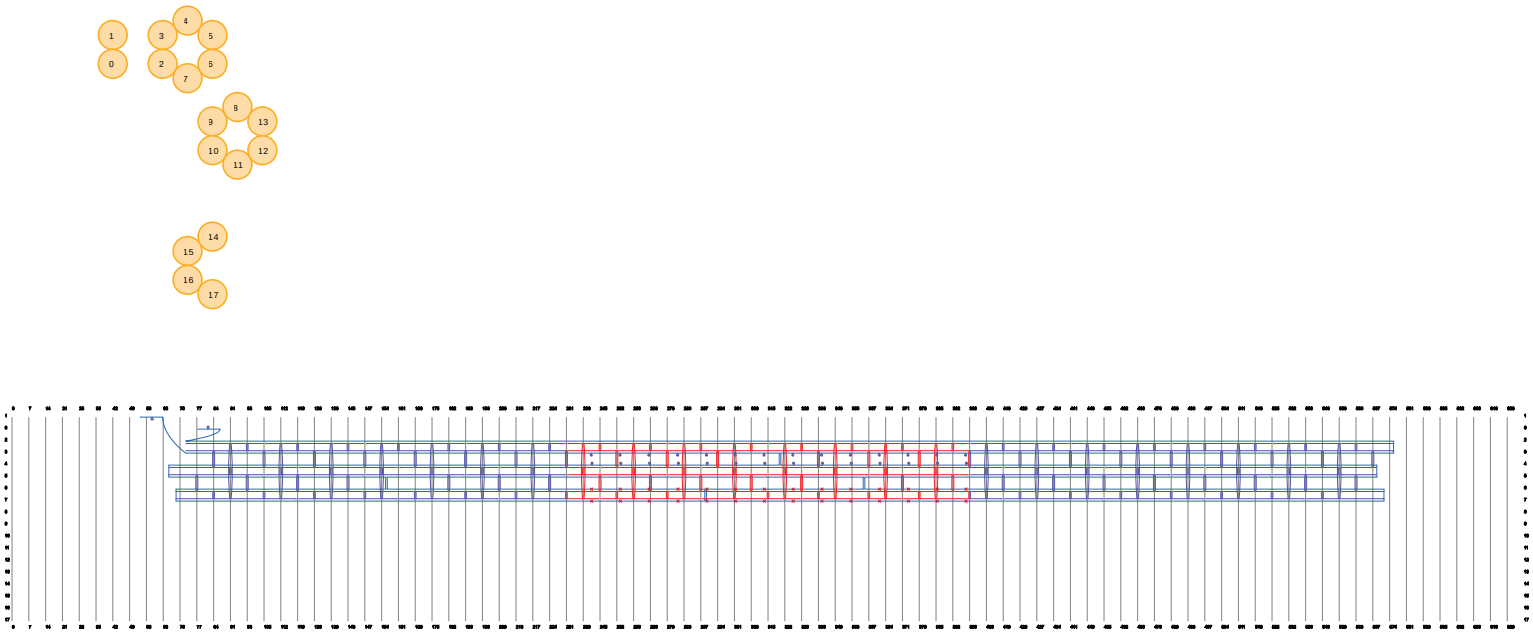

Figure S49. A version of the elastic beam structure lacking scaffold tethers between the arms was constructed and digested by Cas12a. No change in bending angle distribution of the structure was observed after 4 hours of Cas12a treatment. Note that the measured bending angles are in general agreement with ssDNA-tethered elastic beam after Cas12a digestion, both smaller than the predicted angle (~121°). This is likely a result of the untethered arms splaying on TEM surface. (a) Left: AGE characterization of the structures with and without Cas12a treatment. Structures after Cas12a digestion exhibited a faster migration rate because of the removal of an unfolded scaffold loop (Figure S48, top left corner). Right: electron micrographs of the gel-purified structures. Scale bar: 100 nm. (b) Quantification of bending angle distributions with (n = 339) and without (n = 358) Cas12a treatment showed no significant difference, p = 0.51.

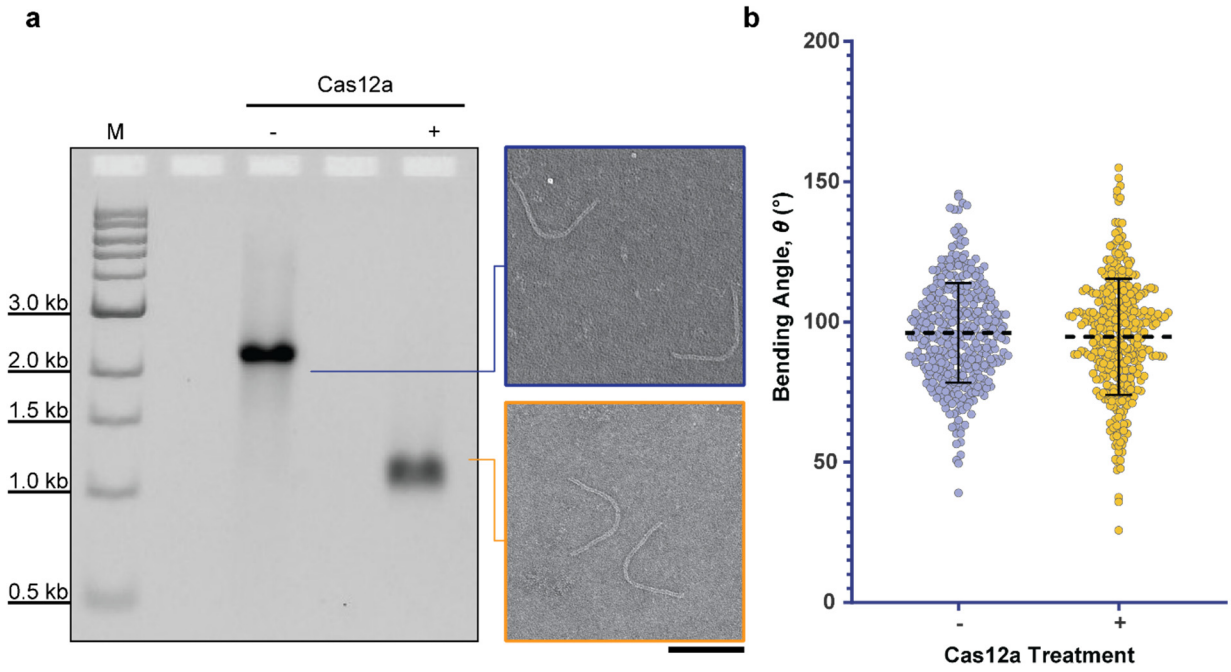

Figure S50. More electron micrographs showing a version of the elastic beam structure without scaffold tethers between the bent arms. Samples shown were gel-purified. Scale bar: 100 nm.

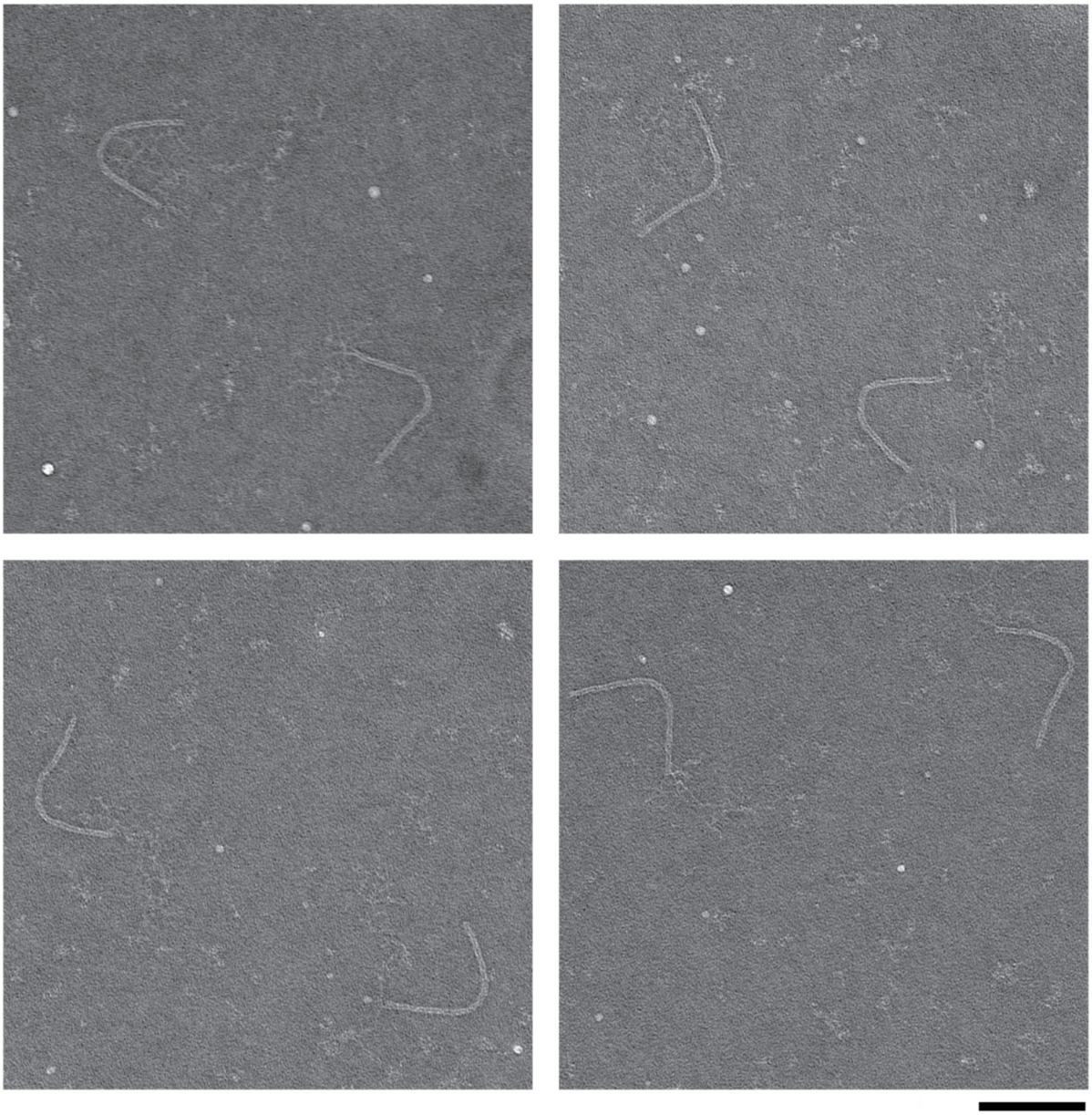

Figure S51. More electron micrographs showing a version of the elastic beam structure without scaffold tethers between the bent arms. Samples shown were not gel-purified to eliminate the possible effects of purification on bending angles and used for angle quantification. Scale bar: 200 nm.

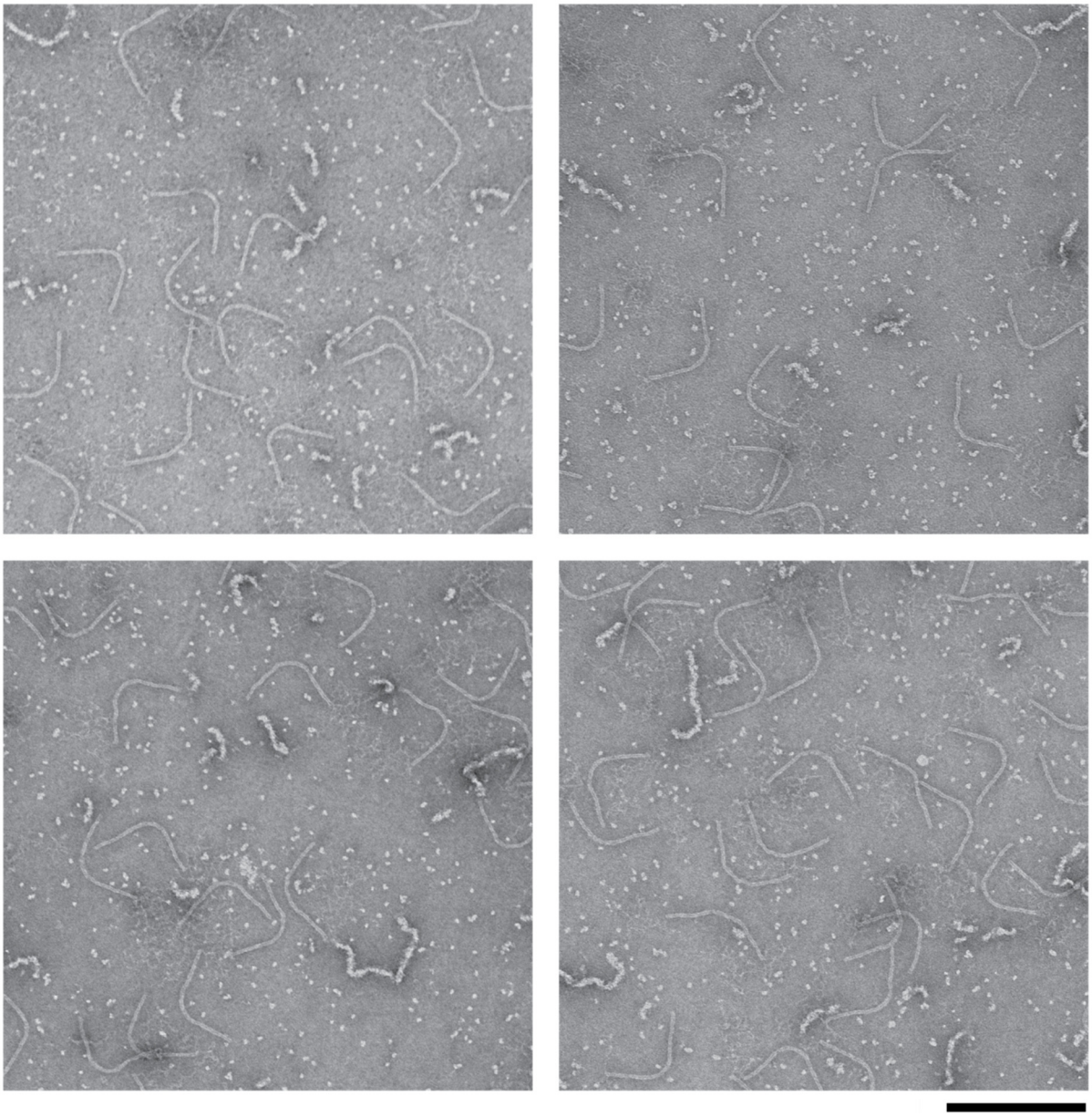

Figure S52. More electron micrographs showing a version of the elastic beam structure without scaffold tethers between the bent arms after 4 hours of Cas12a digestion. Samples shown were gel-purified. Scale bar: 100 nm.

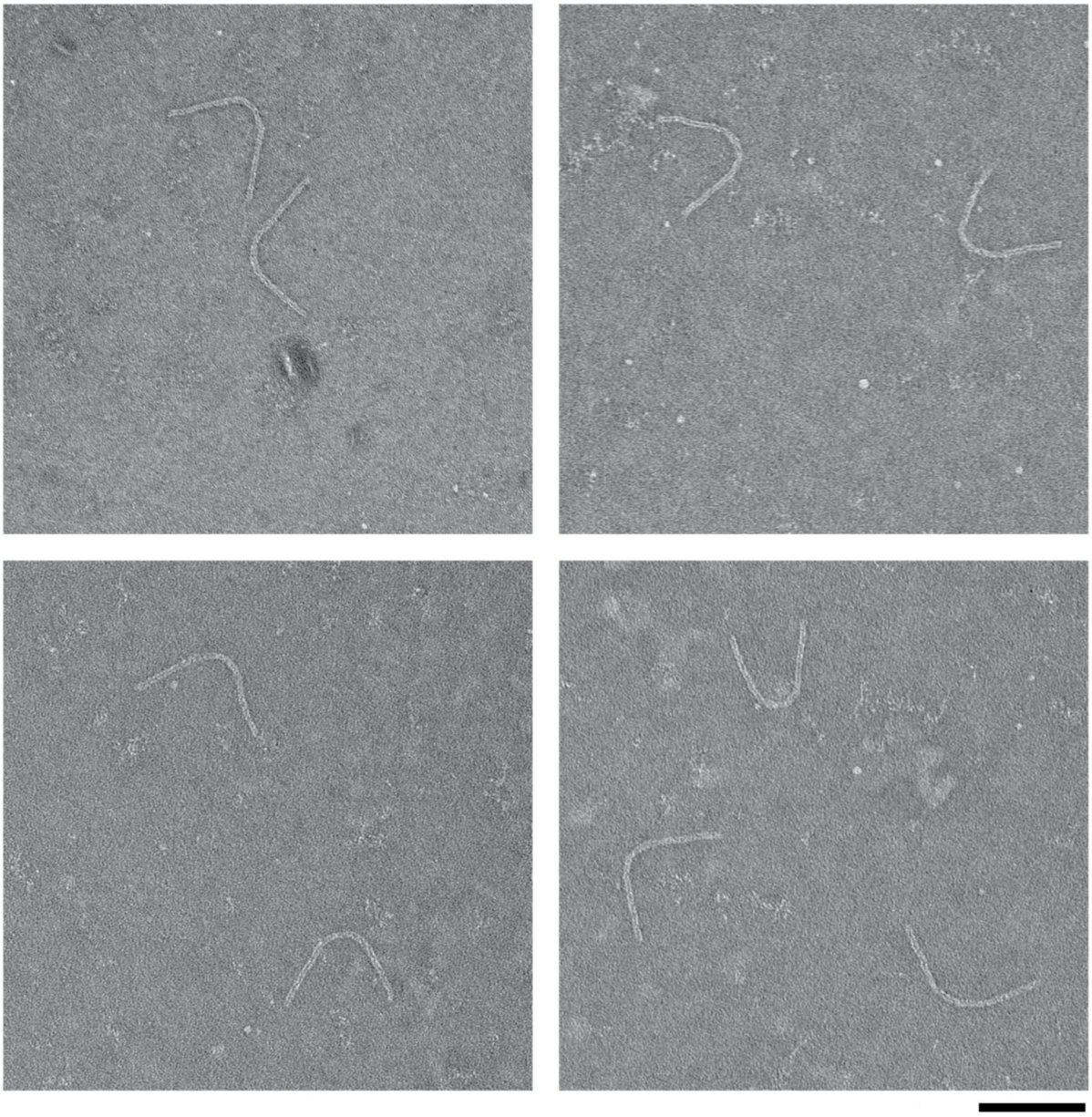

Figure S53. More electron micrographs showing a version of the elastic beam structure without scaffold tethers between the bent arms after 4 hours of Cas12a digestion. Samples shown were not gel-purified to eliminate the possible effects of purification on bending angles and used for angle quantification. Scale bar: 200 nm.

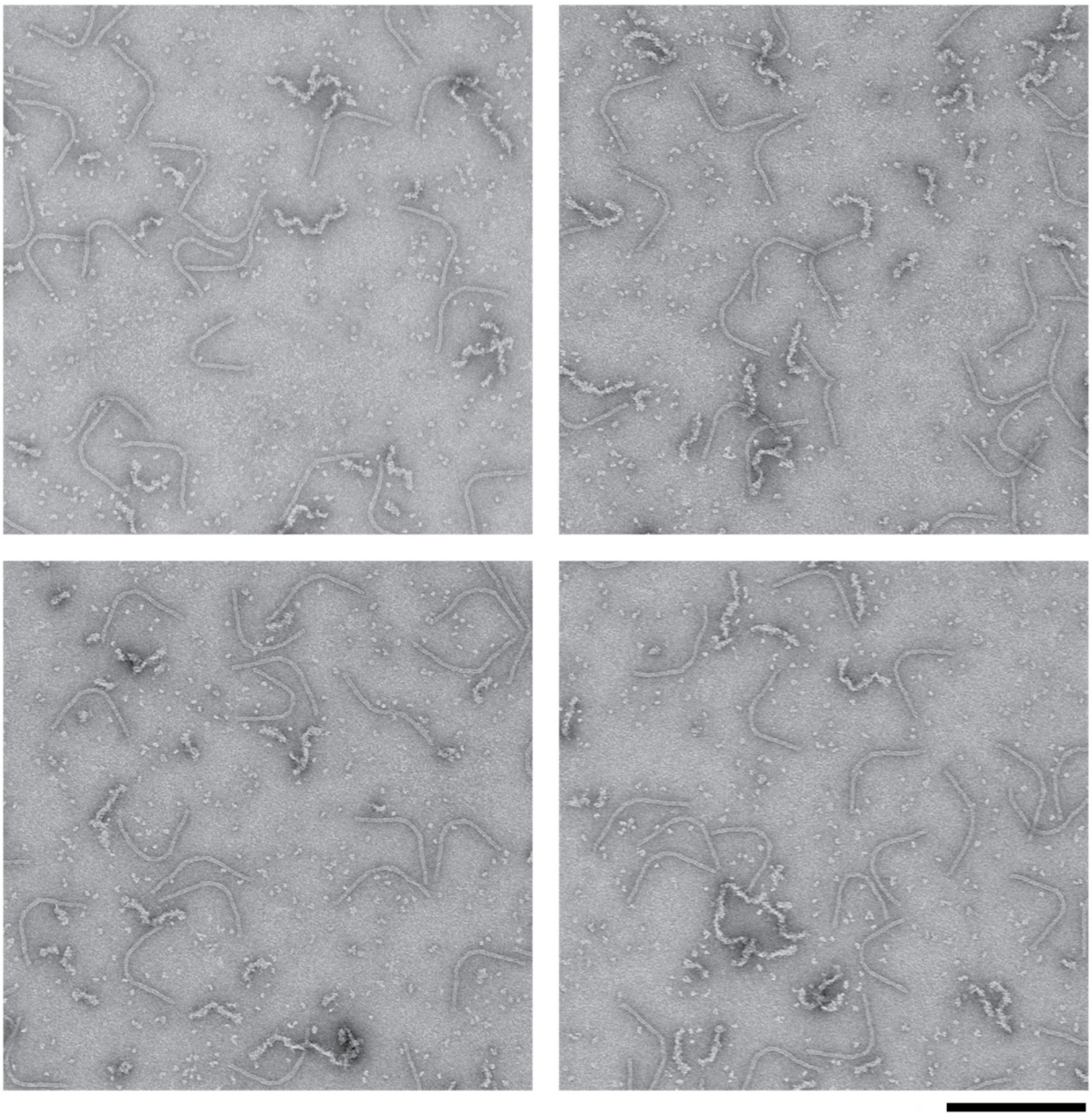

Figure S54. Cas12a digestion of rod-through-square structure[6] under detergent conditions. (a) Schematics of the Cas12a digestion process. The square was initially tethered to the rod *via* four pairs of ssDNA scaffolds. Upon 8 hours of Cas12a digestion, the structure separated into a free square and a naked rod. (b) Left: AGE of Cas12a digested rod-through-square structures under various concentrations of OG (1–5 %). M: 1 kb DNA ladder. Right: electron micrographs showing the untreated rod-through-square structure (top), as well as a free square (middle) and a free rod (bottom) after Cas12a digestion in a reaction buffer containing 5 % OG. Scale bars: 50 nm.

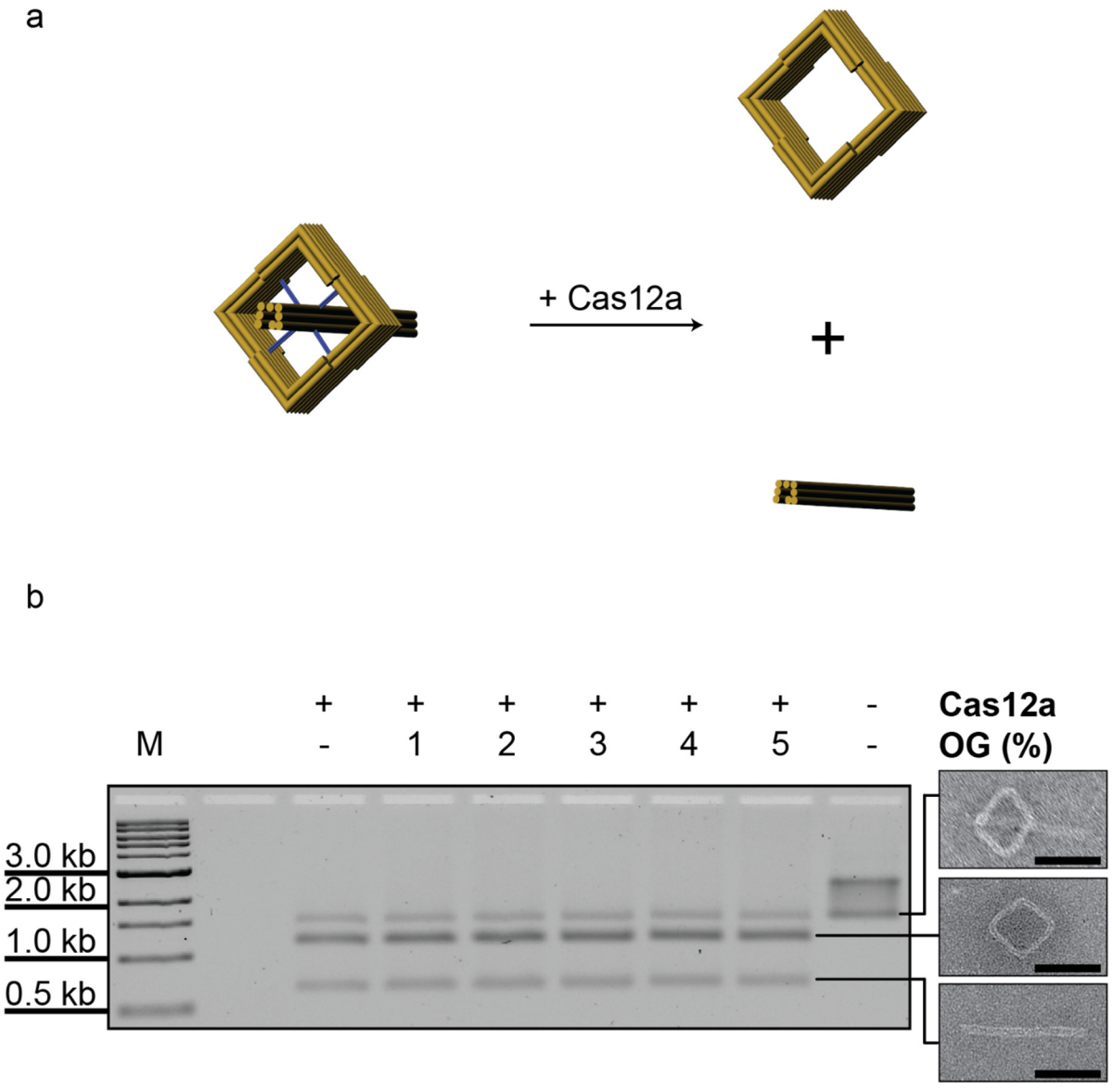

Figure S55. Cas12a digestion of the rod-through-square structure for up to 16 hours. Electron micrographs of the released squares after 16 hours of Cas12a digestion suggest dsDNA damages in the main origami structure. M: 1 kb DNA ladder. Scale bar: 50 nm.

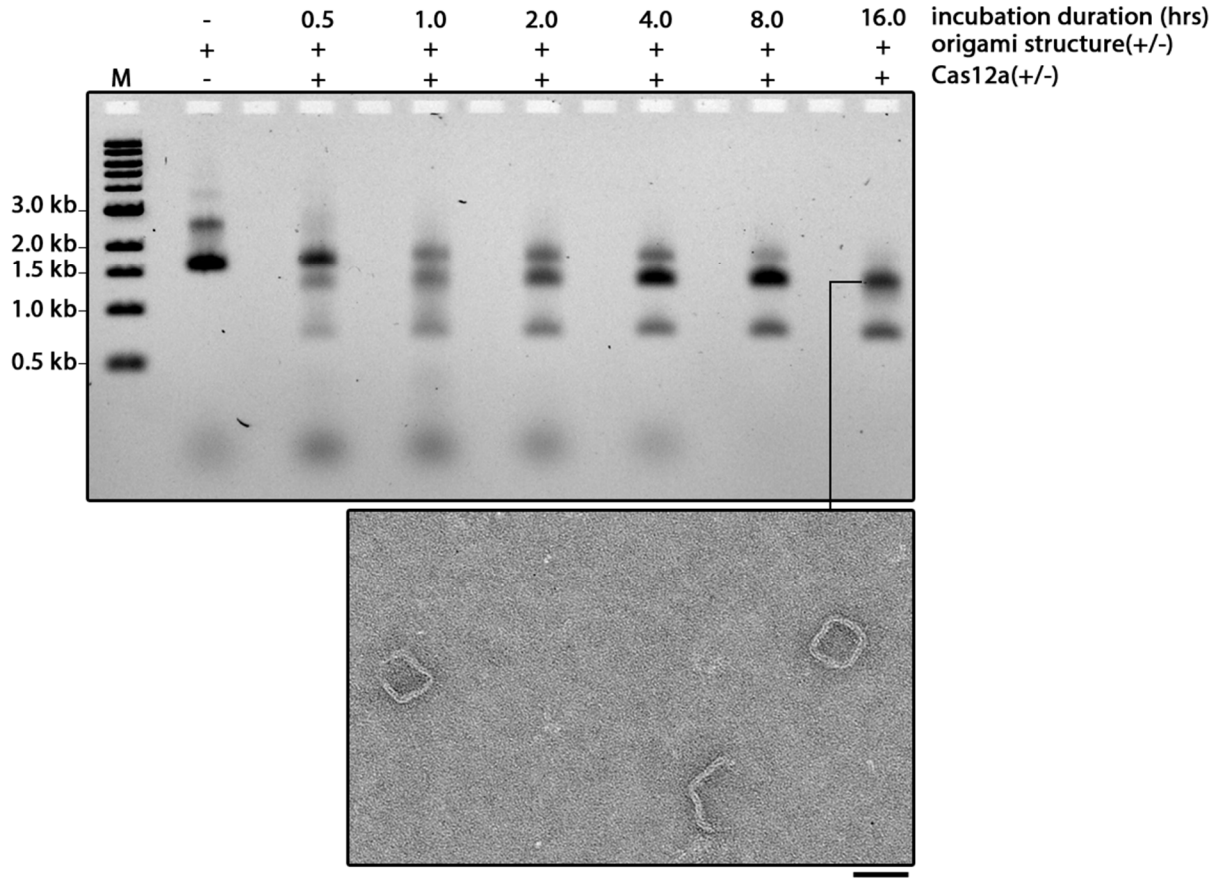

Figure S56. Cas12a digestion of pseudo-rotaxane structure (20 nM) with up to 67 nM of Cas12a for 4 hours. Digestion with 67 nM of Cas12a generated a higher mobility band after AGE, which contains damaged structures. Scale bar: 100 nm.

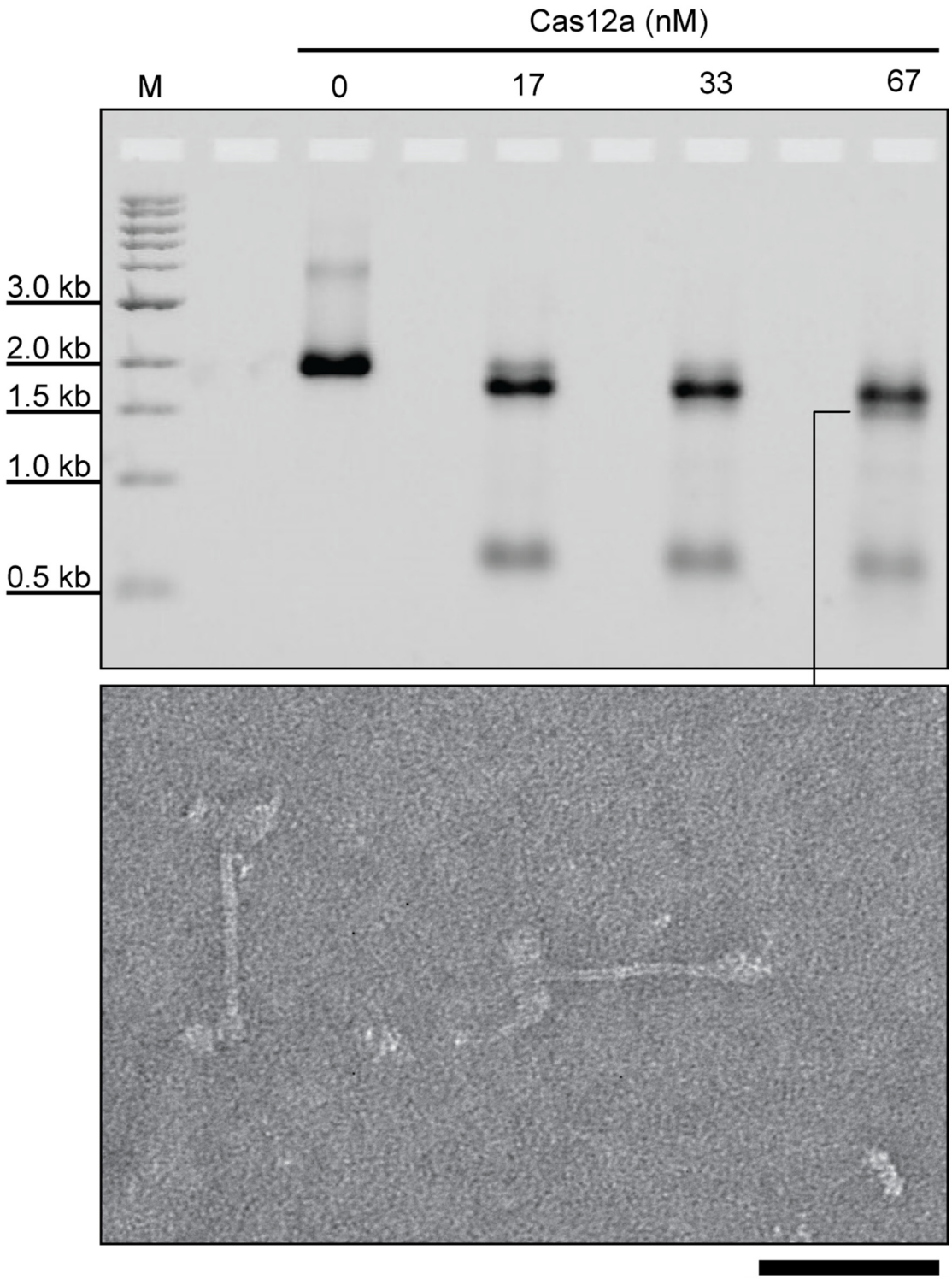

Figure S57. Electron micrographs showing an 'A'-shaped version of the elastic beam structure with scaffold tethers folded into a 6-helix bundle bar (**Figure S42**). This bar is tethered to the arms of the elastic beam *via* 4 ssDNA segments on each end, each 5 nt long. Samples shown were gel-purified. Scale bar: 100 nm.

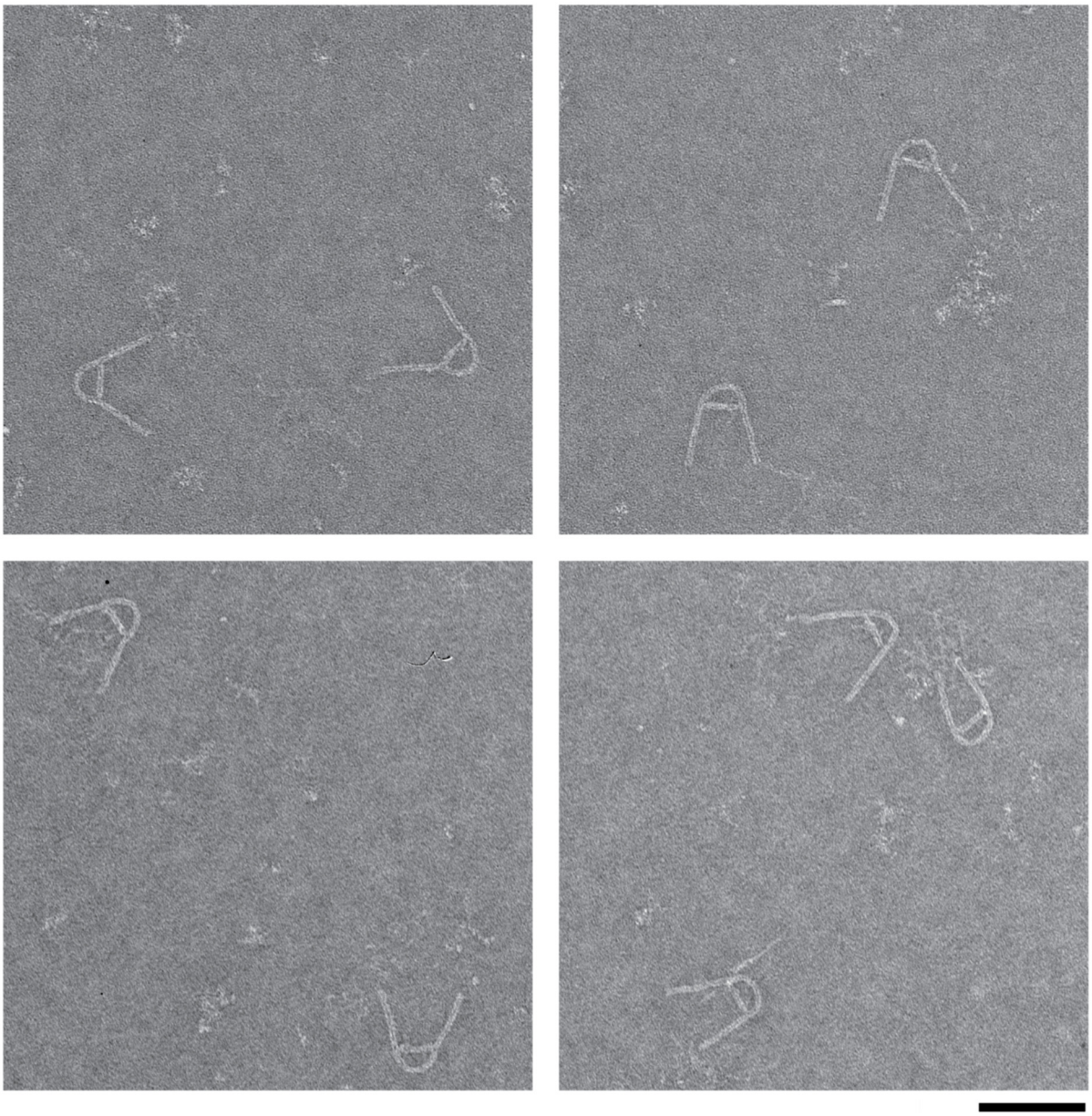

Figure S58. Electron micrographs showing the 'A'-shaped elastic beam (**Figure S42** and **S57**) after 4 hours of Cas12a treatment. Treatment with Cas12a for 4 hours did not release the beam from the elastic beam. Samples shown were gel-purified. Scale bar: 100 nm.

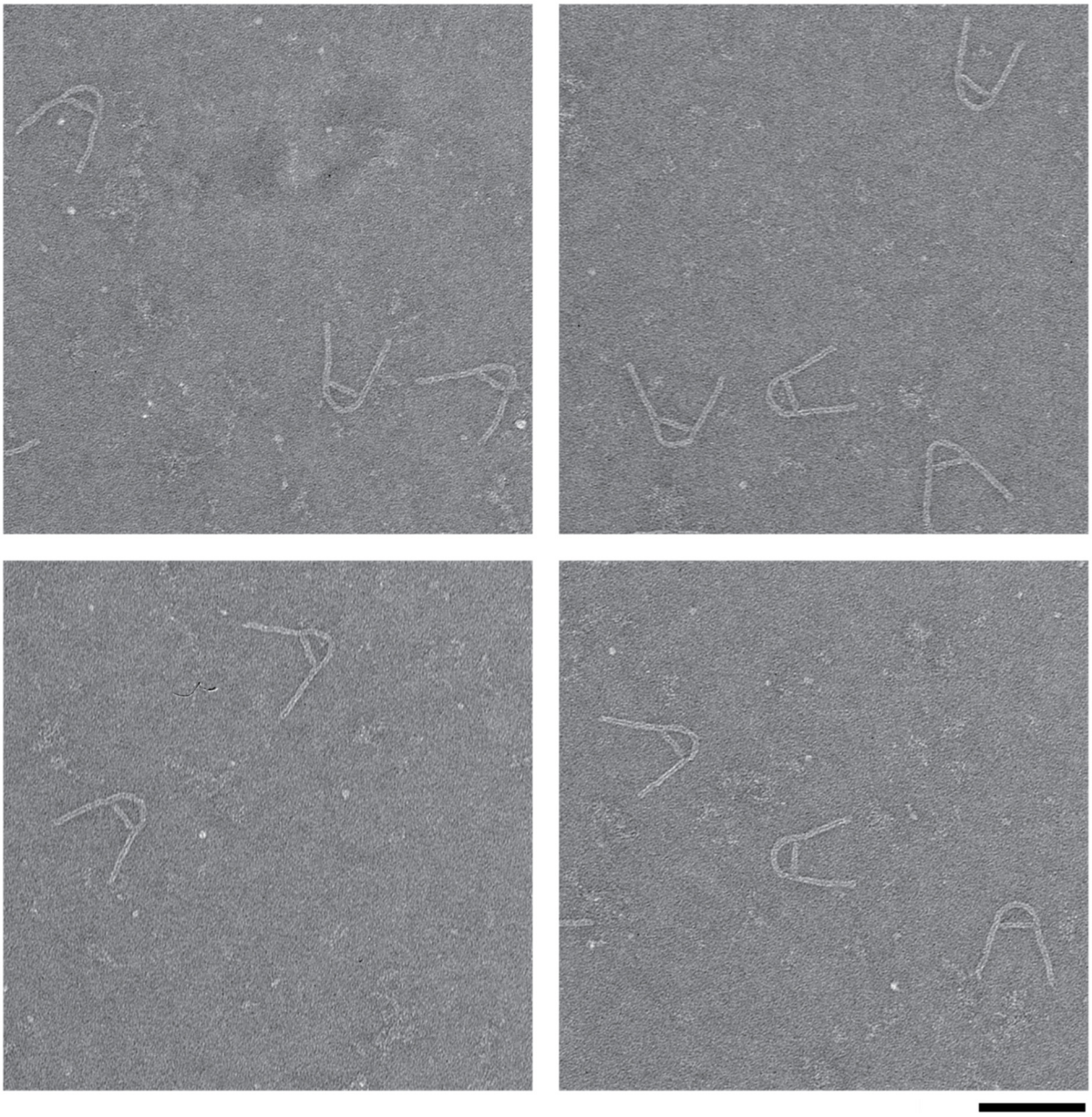

SUPPLEMENTAL TABLES

Table S1. CRISPR-Cas12a Sequences

Sequence Name	Sequence
crRNA (adapted[14])	UAAUUUCUACUAAGUGUAGAUCGUCGCCGUCCAGCUCGACC
DNA for *in vitro* transcription of crRNA (coding strand)	TAATACGACTCACTATAGGGTAATTTCTACTAAGTGTAGATCGTCGCCGTCCAGCTCGACC
DNA for *in vitro* transcription of crRNA (template strand)	GGTCGAGCTGGACGGCGACGATCTACACTTAGTAGAAATTACCCTATAGTGAGTCGTATTA
dsActivator (target strand)	GCCGGGGTGGTGCCCATCCTGGTCGAGCTGGACGGCGACGTAAACGGCCACAAGC
dsActivator (non-target strand)	GCTTGTGGCCGTTTACGTCGCCGTCCAGCTCGACCAGGATGGGCACCACCCCGGC

Table S2. Nuclease volumes and concentrations in nuclease digestion assays.

Structure type	Structure volume (µl)	Nuclease volume (µl)	Total volume (µl)	Final structure concentration (nM)	Final nuclease concentration (nM)
Force clamp	6	9	15	12	15
Semicircle	5	10	15	15	15
Circle with handles	10	9	19	1.58	1.58
Rod with three circles	6	9	15	8	15
Rotaxane with asymmetric stoppers	6	9	15	20	17
Prestressed beams	7.5	7.5	15	16	16
Rod through square	5	10	15	2.5	12.5

Table S3. Deoxyribozyme assay sequences

Sequence Name	Sequence
Deoxyribozyme sequence 1, forward primer	TAAGTTGAAGTGGCTGTACATGGATCCTTATACGGGTACTAG
Deoxyribozyme sequence 1, reverse primer	ATGCTCAACTATGGCTGTACATGAATTCGTAATCATGGTCATAG
BsaI recognition site, forward primer	TAAGTAGGTCTCTGCTGGTCTAGAGTCGACCTG
BsaI recognition site, reverse primer	ATTGTAGGTCTCTGTACCCAGCCACTTCAACTTAATG
Deoxyribozyme sequence 2 with Cy5-probe binding site, forward primer	TAAGTAGGTCTCTGTACTAGCCATGCGTATACGCAGCCATAGTTGAGCATTAAGTTGAAGTGGCTGAGAGACCTACAAT
Deoxyribozyme sequence 2 with Cy5-probe binding site, reverse primer	ATTGTAGGTCTCTCAGCCACTTCAACTTAATGCTCAACTATGGCTGCGTATACGCATGGCTAGTACAGAGACCTACTTA
Free two-deoxyribozymes sequence	TTCATGTACAGCCATAGTTGAGCATTAAGTTGAAGTGGCTGGGTACTAGCCATGCGTATACGCAGCCATAGTTGAGCATTAAGTTGAAGTGGCTG
Cy5-labeled ssDNA probe	/5Cy5/CGTATACGCATGGCTAGTACC

REFERENCES

(1) Douglas, S. M.; Marblestone, A. H.; Teerapittayanon, S.; Vazquez, A.; Church, G. M.; Shih, W. M. Rapid Prototyping of 3D DNA-Origami Shapes with CaDNAno. *Nucleic Acids Res.* **2009**, *37* (15), 5001–5006. https://doi.org/10.1093/nar/gkp436.

(2) Douglas, S. M.; Dietz, H.; Liedl, T.; Hogberg, B.; Graf, F.; Shih, W. M. Self-Assembly of DNA into Nanoscale Three-Dimensional Shapes. *Nature* **2009**, *459* (7245), 414–418. https://doi.org/10.1038/nature08016.

(3) Douglas, S. M.; Chou, J. J.; Shih, W. M. DNA-Nanotube-Induced Alignment of Membrane Proteins for NMR Structure Determination. *Proc. Natl. Acad. Sci. U. S. A.* **2007**, *104* (16), 6644–6648. https://doi.org/10.1073/pnas.0700930104.

(4) Bellot, G.; McClintock, M. A.; Chou, J. J.; Shih, W. M. DNA Nanotubes for NMR Structure Determination of Membrane Proteins. *Nat. Protoc.* **2013**, *8* (4), 755–770. https://doi.org/10.1038/nprot.2013.037.

(5) Nickels, P. C.; Wünsch, B.; Holzmeister, P.; Bae, W.; Kneer, L. M.; Grohmann, D.; Tinnefeld, P.; Liedl, T. Molecular Force Spectroscopy with a DNA Origami–Based Nanoscopic Force Clamp. *Science* **2016**, *354* (6310), 305–307. https://doi.org/10.1126/science.aah5974.

(6) Powell, J. T.; Akhuetie-Oni, B. O.; Zhang, Z.; Lin, C. DNA Origami Rotaxanes: Tailored Synthesis and Controlled Structure Switching. *Angew. Chem. Int. Ed.* **2016**, *55* (38), 11412–11416. https://doi.org/10.1002/anie.201604621.

(7) Lin, C.; Perrault, S. D.; Kwak, M.; Graf, F.; Shih, W. M. Purification of DNA-Origami Nanostructures by Rate-Zonal Centrifugation. *Nucleic Acids Res.* **2013**, *41* (2), e40–e40. https://doi.org/10.1093/nar/gks1070.

(8) Liedl, T.; Högberg, B.; Tytell, J.; Ingber, D. E.; Shih, W. M. Self-Assembly of 3D Prestressed Tensegrity Structures from DNA. *Nat. Nanotechnol.* **2010**, *5* (7), 520–524. https://doi.org/10.1038/nnano.2010.107.

(9) Zhou, L.; Marras, A. E.; Su, H.-J.; Castro, C. E. DNA Origami Compliant Nanostructures with Tunable Mechanical Properties. *ACS Nano* **2014**, *8* (1), 27–34. https://doi.org/10.1021/nn405408g.

(10) Dietz, H.; Douglas, S. M.; Shih, W. M. Folding DNA into Twisted and Curved Nanoscale Shapes. *Science* **2009**, *325* (5941), 725–730. https://doi.org/10.1126/science.1174251.

(11) Virtanen, P.; Gommers, R.; Oliphant, T. E.; Haberland, M.; Reddy, T.; Cournapeau, D.; Burovski, E.; Peterson, P.; Weckesser, W.; Bright, J.; et al. SciPy 1.0--Fundamental Algorithms for Scientific Computing in Python. *ArXiv190710121 Phys.* **2019**.

(12) Marko, J. F.; Siggia, E. D. Stretching DNA. *Macromolecules* **1995**, *28* (26), 8759–8770. https://doi.org/10.1021/ma00130a008.

(13) Schneider, C. A.; Rasband, W. S.; Eliceiri, K. W. NIH Image to ImageJ: 25 Years of Image Analysis. *Nat. Methods* **2012**, *9* (7), 671–675. https://doi.org/10.1038/nmeth.2089.

(14) Chen, J. S.; Ma, E.; Harrington, L. B.; Costa, M. D.; Tian, X.; Palefsky, J. M.; Doudna, J. A. CRISPR-Cas12a Target Binding Unleashes Indiscriminate Single-Stranded DNase Activity. *Science* **2018**, eaar6245. https://doi.org/10.1126/science.aar6245.